UPPSALA
UNIVERSITET

Digital Comprehensive Summaries of Uppsala Dissertations from the Faculty of Science and Technology 706

Atomistic Spin Dynamics, Theory and Applications

JOHAN HELLSVIK

ACTA
UNIVERSITATIS
UPSALIENSIS
UPPSALA
2010

ISSN 1651-6214
ISBN 978-91-554-7921-3
urn:nbn:se:uu:diva-120103

Dissertation presented at Uppsala University to be publicly examined in Polhemsalen, Ångström laboratory, Lägerhyddsvägen 1, Uppsala, Friday, December 3, 2010 at 10:15 for the degree of Doctor of Philosophy. The examination will be conducted in English.

Abstract
Hellsvik, J. 2010. Atomistic Spin Dynamics, Theory and Applications. Acta Universitatis Upsaliensis. *Digital Comprehensive Summaries of Uppsala Dissertations from the Faculty of Science and Technology* 706. 108 pp. Uppsala. ISBN 978-91-554-7921-3.

The topic of this Thesis is magnetization dynamics on atomic length scales. A computational scheme, Atomistic Spin Dynamics, based on density functional theory, the adiabatic approximation and the atomic moment approximation is presented. Simulations are performed for chemically disordered systems, antiferromagnets and ferrimagnets and also systems with reduced dimensionality

The autocorrelation function of the archetypical spin glass alloy CuMn is sampled in simulations following a quenching protocol. The aging regime can be clearly identified and the dependence of the relaxation on the damping parameter is investigated. The time evolution of pair correlation and autocorrelation functions has been studied in simulations of the dilute magnetic semiconductor GaMnAs. The dynamics reveal a substantial short ranged magnetic order even at temperatures at or above the ordering temperature. The dynamics for different concentrations of As antisites are discussed.

Antiferromagnets offer opportunities for ultrafast switching, this is studied in simulations of an artificial antiferromagnet. For the right conditions, the cooperative effect of applied field torque and and the torque from the other sublattice enables very fast switching. The dynamics of bcc Fe precessing in a strong uniaxial anisotropy are investigated. It is demonstrated that the magnetization can shrink substantially due to a spin wave instability. The dynamics of a two-component model ferrimagnet at finite temperature are investigated. At temperatures where the magnetic system is close to the magnetic and angular momentum compensations points of the ferrimagnet, the relaxation in a uniaxial easy exis anisotropy resembles results in recent experiments on ferrimagnetic resonance.

The different cases of uniaxial or colossal magnetic anisotropy in nanowires at different temperatures are compared. The magnon softening in a ferromagnetic monolayer is investigated, giving results that compare well with recent experiments. The effect of lattice relaxation can be treated in first principles calculations. Subsequent simulations captures the softening of magnons caused by reduced dimensionality and temperature.

Keywords: ab initio calculations, spin dynamics, magnetization, magnetic switching, diluted magnetic semiconductors, spin glasses, ferromagnetic relaxation, ferrimagnets, antiferromagnets

Johan Hellsvik, Department of Physics and Astronomy, Materials Theory, Box 516, Uppsala University, SE-751 20 Uppsala, Sweden.

ISSN 1651-6214
ISBN 978-91-554-7921-3
urn:nbn:se:uu:diva-120103 (http://urn.kb.se/resolve?urn=urn:nbn:se:uu:diva-120103)

To my parents, Inga and Lars

List of Papers

This thesis is based on the following papers, which are referred to in the text by their Roman numerals.

I **A method for atomistic spin dynamics simulations: implementation and examples.**
B. Skubic, J. Hellsvik, L. Nordström, and O. Eriksson
Journal of Physics: Condensed Matter **20**, 315203 (2008)

II **Dynamics of diluted magnetic semiconductors from atomistic spin-dynamics simulations: Mn-doped GaAs.**
J. Hellsvik, B. Skubic, L. Nordström, B. Sanyal, P. Nordblad, P. Svedlindh, and O. Eriksson
Physical Review B **78**, 144419 (2008)

III **Atomistic spin dynamics of the Cu-Mn spin-glass alloy.**
B. Skubic, O. E. Peil, J. Hellsvik, P. Nordblad, L. Nordström, and O. Eriksson
Physical Review B **79**, 024411 (2009)

IV **Atomistic Spin Dynamics simulations on Mn-doped GaAs and CuMn.**
J. Hellsvik
Journal of Physics: Conference Series **200**, 072040 (2010) (Proceedings of the International Conference on Magnetism, 27-31 July 2009, Karlsruhe, Germany)

V **Simulation of a spin-wave instability from atomistic spin dynamics.**
J. Hellsvik, B. Skubic, L. Nordström, and O. Eriksson
Physical Review B, **79**, 184426 (2009)

VI **Ultrafast switching in a synthetic antiferromagnetic random-access memory device.**
A. Bergman, B. Skubic, J. Hellsvik, L. Nordström, A. Delin, and O. Eriksson
Submitted

VII **Magnon softening in a ferromagnetic monolayer: A first-principles spin dynamics study.**
A. Bergman, A. Taroni, L. Bergqvist, J. Hellsvik, B. Hjörvarsson, and O. Eriksson
Physical Review B **81**, 144416 (2010)

VIII **Atomistic spin dynamics of atomic Pt wires.**
A. Bergman, J. Hellsvik, and A. Delin
In manuscript

Contents

1. Introduction

This Thesis is a theoretical treatment of magnetization dynamics on atomic length scales. The study is semiclassical in the regard that parameters are extracted from quantum mechanical calculations and mapped onto a classical Hamiltonian, describing the magnetic interactions coarse grained over the size of atoms. The equations of motion for this Hamiltonian are non-linear and coupled. Algebraic solutions are possible for only a limited set of geometries and interactions. To proceed further numerical simulations are an invaluable tool to take on where algebraic treatment becomes cumbersome or impossible.

Maxwell's equations for the electromagnetic fields [1] are the basis on which many aspects of electricity and magnetism can be understood. Maxwell theory explains the induced voltage of a generator, the propagation of light and radio waves and that magnetic field lines always close. Augmented with material specific constitutive relations they are the framework within many aspects of magnetism in solids can be described. In a classical theory the magnetization is expressed as a vectorfield. Its thermal equilibrium properties can be described by Brown's equations [2] which are derived from a generalised Gibbs free energy. The solutions of the Brown's equations constitute metastable states reflecting that the Gibbs free energy has many local minima. A metastable state is defined as a state where the magnetization in each point is parallel to an effective magnetic field. The effective field is defined as the functional derivative of the Gibbs free energy with regard to the magnetization. When the local magnetization in a point of space is not parallel with the effective effective field the magnetization is not anymore in equilibrium and will evolve in time.

Landau and Lifshitz postulated [3] an equation for gyroscopic magnetic dynamics where the local magnetization precess around the local effective magnetic field. The Landau-Lifshitz (LL) equation has become a very important tool for exploring magnetization dynamics of small particles, thin fims, and nano-stripes [4]. In numerical simulations of the LL equation the magnetization density is discretised into cells or finite elements that are small enough compared to the length scales over which the magnetization changes direction. Depending on the problem at hand, the spatial resolution in a solution of the micromagnetic problem can range from a few nanometers up to micrometers. Simulations of magnetization dynamics can be motivated, not only by scientific curiosity, but also as the simulations can be used to investigate

the behaviour of components used for magnetic storage media and play an important role in the design and specifications of new devices.

Magnetization that exist in solids can only be understood from quantum mechanics. This is expressed in the Bohr van-Leeuven theorem [2] that proves that a pure classical theory cannot lead to ferro- or paramagnetism. The reason is that in a classical theory the electrons will not interact with a magnetic field, or in other words, the susceptibility will be zero. On the microscopic level magnetization is typically expressed in units of Bohr magnetons $\mu_{\mathrm{B}} = \frac{\hbar e}{2mc}$. Magnetization in a solid is carried mainly by electron magnetic moments that are associated with orbital angular momentum $\mathbf{l}$ and spin angular momentum $\mathbf{s}$ through the gyromagnetic ratio $\gamma_l = g_l \frac{\mu_{\mathrm{B}}}{\hbar}$. The electron g-factor takes the value $g_s \approx 2$ for spin angular momentum and $g_l = 1$ for orbital angular momentum. The total magnetic moment $\mu = \mu_s + \mu_l$ for an electron can be expressed as

$$\mu = -(\gamma_s \mathbf{s} + \gamma_l \mathbf{l}) \tag{1.1}$$

$$= -\frac{\mu_{\mathrm{B}}}{\hbar}(2\mathbf{s} + \mathbf{l}). \tag{1.2}$$

Also the nuclei carry angular momentum and magnetic moment but these must usually not be taken into account in theories of ferromagnetism and electronic spin dynamics. As a consequence of the postulates of quantum mechanics, the electronic spins will precess in an applied magnetic field. This can be seen by calculating the Heisenberg equation of motion $\frac{d\hat{A}}{dt} = \frac{i}{\hbar}[\hat{A}, \mathscr{H}]$ for the spin angular momentum operator and the Hamiltonian. This will be done in Chapter 3 for the single-particle Kohn-Sham Hamiltonian used in density functional theory. By integrating the magnetization density over the volumes of atoms, an equation of motion for the atomic magnetic moments, similar in form to the micromagnetic Landau-Lifshitz equation, is obtained.

The physics of the solid state is a very rich field with a long tradition. The theoretical framework that has been, and continue to be, worked out, aim to describe various aspects of a solid such as the mechanical properties, crystalline phases, electrical and optical properties, presence of magnetism and more. In order to understand and analyse different properties of a class of solids, it is important to identify and try to model the essential mechanisms that give rise to a certain behaviour. Most, if not all, of the microscopic interactions that govern chemical and solid state physics have been known since the early days of quantum mechanics. The macroscopic and mesoscopic behaviour of a solid emerge as the combined interaction of a very large number of particles, even in a small piece of matter. A theory of solids therefore always needs to, in one way or the other, approach the many-body problem. A large number of techniques are at hand and the interested reader is referred to classical textbooks on general solid state physics [5, 6], on equilibrium statistical physics [7], and to the recent textbook on electronic structure methods written by Martin [8]. The concept of emergent behaviour and the importance

of symmetry breaking mechanisms in the theory of condensed matter are discussed in the lectures of Anderson [9] and Coleman [10].

Experiments are crucial in guiding the development of theory. It is of course possible, within a purely theoretical context, to prove a freshly proposed model or theory to be inconsistent or in contradiction with more established results. The models used in solid state physics always rely on some approximations and assumptions. It is most often the case that the restrictions on applicability of the model cannot be known beforehand by solely theoretical considerations, but need to be carefully investigated in comparison with experimental results. To demonstrate the merits and accuracy of a theory, it is therefore very important that the model shows qualitative and quantitative correspondence to measurements. A good theory can suggest new experiments to be ventured, and have predictive capability on the outcome of these experiments. A model is also characterised by how it compares with results from other theory that relies on fewer approximations and assumptions.

Numerical simulations, often for systems with many degrees of freedom, can be viewed as a class of experiments in their own right. The difference to traditional experimental techniques is that here the experiments are performed in the computers, instead of on the table in the laboratory. Numerical simulation techniques are of increasing importance for research in all fields of physics, in the other natural sciences, in medicine, social sciences and economy sciences. Simulation techniques are sometimes discussed as the third leg of science, on par with the traditional pillars of theory and experiment.

Modern solid state theory often merges efforts to model some property or behaviour of a class of solids with materials specific calculations from first principles. The materials specific calculations can give not only quantitative information but also shine light on which mechanisms, out of a few possible ones, are the more important ones to account for a certain behaviour. In the discipline of magnetism of solids, this approach has proven very useful in research on how magnetism is mediated in diluted magnetic semiconductors [11, 12, 13] and how magnetic ordering can give rise to ferroelectric polarization in multiferroic materials [14, 15, 16].

The present Thesis is an example of a two-step approach for investigations on magnetization dynamics. First principles density functional theory calculations for the electronic structure of a magnetic solid are used to extract quantitive information on the size of the atomic magnetic moments and how they interact. The results are mapped onto a parametrized Hamiltonian, for which the corresponding equation of motion is investigated in Langevin dynamics simulations. Figure 1.1 show a snapshot from an atomistic spin dynamics simulation of GaAs doped with 5% Mn and no As antisites. At temperature $T = 100$ K, the magnetization averaged over the magnetic moments in the simulation cell is $\sim 65\%$ of the saturated magnetization at $T = 0$ K. The magnetic moments are strongly correlated over short distances.

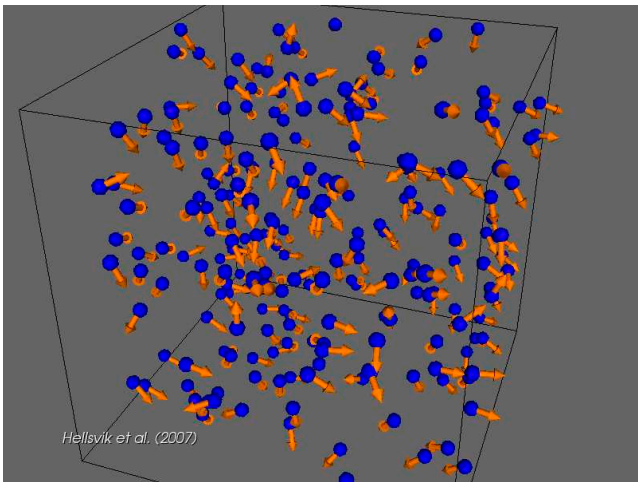

Figure 1.1: Snapshot from an atomistic spin dynamics simulation of GaAs doped with 5% Mn and no As antisites. The blue spheres show Mn atoms that randomly have substituted Ga atoms in the GaAs zincblende structure. The arrows show the direction of the atomic magnetic moments. At temperature $T = 100$ K, the magnetization averaged over the magnetic moments in the simulation cell is $\sim 65\%$ of the saturated magnetization at $T = 0$ K. The magnetic moments are strongly correlated over short distances.

The theoretical foundations for the approach is well established, but as will be developed throughout the Thesis, there are also many examples of where the method would need to be further developed to be applicable. In a wider scope the Thesis connects to ongoing developments in time-dependent density functional theory, nonequilibrium statistical mechanics, simultaneous molecular and spin dynamics and magnetooptic and optomagnetic mechanisms.

The outline of the Thesis is as follows: Magnetism in solids is discussed in Chapter 2. The Atomistic Spin Dynamics method is developed in Chapter 3, followed by observation on the Landau-Lifshitz equation in Chapter 4. Details on how the method can be implemented as a software for numerical simulations and some examples are given in Chapter 5. Chapter 6 introduces Papers I-VIII. Atomic units are used in Chapter 3. SI-units are used in all other chapters. The wording “magnetic field” refers to the electromagnetic B-field throughout all the Thesis.

2. Magnetism in solids

Only a few elements are ferromagnetically ordered in the solid state. The density matrix of the electrons can be spin-polarised, but if the polarisation direction varies over space the solid does not necessarily possess a net magnetic moment. This can be contrasted with the abundance of elements that are magnetic as free atoms or in small molecules. In atoms a net magnetic moment arises due to incomplete filling of the electron shells. The Pauli principle expresses that two fermions cannot occupy the same state. Electrons are fermions and the filling of electron shells in an atom can be understood as a strive to minimise the ground state energy and at the same time respect the Pauli principle. For most elements Hund's rules [17] neatly expresses the order into which the electron shells are filled and how the orbital and angular momenta are coupled [1]

In solids the situation is qualitatively different than in atoms and molecules. The electrons low in energy close to the atomic core remain in atomic-like shells whereas electrons further out hybridise with electrons from neighbouring atoms, taking part in chemical bonding. In metals, the outer electrons are itinerant (highly mobile) and they hop in the lattice sharing their time between different atoms. In magnetic 3d-transition metals, the largest contribution to the magnetization comes from the spin-polarisation of the itinerant 3d-electrons. The nature of ferromagnetism can be distinctly different in other metals, as for instance the rare earth 4f metals. The textbook of Chikazumi [17] covers important aspects of ferromagnetism and ferromagnetic compounds. For an advanced level description of the theory of magnetism, the monograph of Yosida [19] is suggested reading.

That the ground state is ferromagnetic can in density functional theory calculations be understood from a generalised Stoner criterion where the Stoner exchange constant I is calculated as an integral over the exchange-correlation and N is the density of states at the Fermi energy. If the product IN is larger than 1, then the ferromagnetic state is stable. The monograph of Kübler [20], with emphasises on the theory of on itinerant electrons magnetism, describes how magnetization in the solid state can be investigated in the framework of density functional theory.

[1] The breakdown of Hund's rules in certain situations is a topic of active research. A new set of rules, the Katt's rules [18], has recently been proposed as a complement to Hund's rules.

2.1 FM ordering at zero and finite temperatures

In the $T = 0$ K ground state of an ideal ferromagnet, there exist a global direction of the magnetization vector field over distances larger than the range of the interatomic exchange interactions. The explanation for the ferromagnetic ordering is the interatomic exchange interaction, a quantum mechanical interaction with no classical counterpart, that favours parallel alignment of the spins of neighbouring atoms. The long range magnetic ordering motivates the definition of the ferromagnetic order parameter as the average of the local magnetic moments over a finite volume extending over lengths long in comparison to the exchange interactions. Over even longer length scales, the magnetostatic interaction, which is solenoidal in nature, and of classical origin, will make the magnetization depart from a global direction. The boundary conditions for the electromagnetic fields in the interface of the magnetic sample and its environment combine with the magnetostatic interaction in the interior of the sample to make it energetically favourable for the magnetic to have a (degenerate) multi domain ground state [2].

At finite temperature, transversal and longitudinal fluctuations of the magnetization lower the magnetic moment. This is associated with an energy penalty where the magnetic sample increases its internal energy in terms of exchange energy, magnetostatic energy and magnetocrystalline energy. The distribution function for the energies of individual atomic moments follow Boltzmann statistics [7]. With increasing temperature, the magnetization eventually reaches the Curie temperature where the magnetization goes to zero. This is most of the time a second order phase transition for the ferromagnetic order parameter. There are some compounds, e.g. Fe_2P, where the magnetization abruptly crops to zero at a first order phase transition. The transversal fluctuations are spin waves where the local magnetic moments have constant magnitudes but directions prescribing a spiral ordering (of helical or cycloidal form). The wave vectors of the fluctuations are restricted by the space group symmetries of the lattice. For shorter wave lengths, the transversal spin waves increase the exchange energy, but contribute less to the magnetostatic energy. In the limit of long wave length, the penalty in exchange energy is negligible but the magnetostatic contribution to the internal energy becomes of importance. The crystal structure determines not only the cut off in wave vector but also the number of spin wave modes. If the crystal has one atom in the unit cell, there is typically only one mode. With n atoms in the chemical unit cell the ferromagnet will possess n spin wave modes manifested in experiments as n spin wave dispersion relations[2]. The longitudinal fluctuations can be Stoner single-electron excitations. Longitudinal fluctuations of the magnetization can

[2]The chemical and magnetic unit cells are equivalent for ferromagnets in the ground state. There can be up to three spin wave modes per atom in the unit cells. Of these modes, the two transversal modes are often degenerate and the longitudinal mode too high in energy to get excited.

also arise as superpositions of transversal spin waves, resulting in spin density waves. The Stoner excitations are high in energy which is associated with short decay times. The transversal fluctuations can for large wave vectors have energies of the order of the exchange splitting energy between the electron bands. In materials where this condition is fulfilled, the spin waves can decay into Stoner fluctuations. The decay of Stoner excitations can also be in form of subsequent spin flips.

2.2 Collinear and noncollinear AFM ordering

In the case that some or all of the exchange interactions favour antiparallel spins, the material can have a different ground state than the ferromagnetic one. Antiferromagnetic ordering is sometimes used as an umbrella for all types of longe range magnetic orderings that are not ferromagnetic ordering. A more narrow definition of antiferromagnetism covers only collinear ground states where the magnetic moments pairwise cancel each other. Incomplete cancellation of the magnetic moments leave a net magnetic moment resulting in ferrimagnetic ordering. Among the noncollinear orderings, there are orderings where the ground state is in a spin spiral configuration. The periodicity of the spin spiral can coincide with an integer multiple (commensurate spin-spiral) or a fractional multiple (incommensurate spin-spiral) of the lattice constant(s) of the chemical unit cell. Spin spiral ground states can arise as a consequence of frustration of isotropic exchange interactions [21]. Relativistic anisotropic exchange interaction, known as the Dzyaloshinskii-Moriya interaction [22, 23] can perturb otherwise collinear antiferromagnetic configurations to have finite canting angles yielding a net ferromagnetic moment [21]. Spin spiral and weak ferromagnetic ordering are of importance, not only because of their intricate orderings in themselves. But, also as these orderings breaks the inversions symmetry of the crystal [21]. A broken inversion symmetry allows for electric polarisation which in the case of multiferroic materials coexists with magnetic ordering [14, 24, 21].

In modelling of the collinear and noncollinear antiferromagnetic orderings, the primary variables can be taken to be the sublattice magnetization defined as an average over all magnetic moments belonging to one sublattice [25]. The sublattice description is useful for modelling of magnetization dynamics, such as in the theory of antiferromagnetic [26] and ferrimagnetic resonance [27]. The temperature dependence of the sublattice magnetizations can here be taken directly from experimental values or from Monte Carlo simulations [7, 28] of a parametrized spin Hamiltonian. The dynamics can be modelled in terms of coupled Landau-Lifshitz equations for the sublattice magnetization vectors. That this approach is not always applicable is discussed in Papers V,VI.

2.3 Experimental techniques

The physicist who wants to investigate magnetization and magnetization dynamics in experiments has a wide range of experimental techniques to choose from. The different techniques have their respective merits and shortcomings. There is no single technique that allows for simultaneous insight in all aspects of what goes on in a magnetic solid. Among the specifications that are relevant are the spatial resolution, the resolution in the time and frequency domain and element specificity. There are different probes that are good for bulk measurements and for surface measurements.

The magnetic state, of the whole sample or a small part of it, can be read off by measuring the magnetic stray field out from the sample. For precise measurements superconducting quantum interference devices are often used. Another technique is to read the magnetic state by measuring the resistivity, either directly in the sample or in a probe that is magnetized by the stray field from the sample. The latter is the working principle of readheads in harddrives. As the harddisk rotates under the readhead, the lower part of the readhead device aligns with the magnetization in a domain, that represents one bit of information in the harddisk. The signal is read out as a current, the strength of which depends on the magnetization in lower part of the readhead through the giant magnetoresistive effect [29, 30] or the tunnelling magnetoresistive effect [31].

One of the more fundamental experiments is the hysteresis measurement [17]. The protocol for a hysteresis measurement is as follows: starting from a demagnetized state, an applied field drives the magnetization from low values up to its saturation value, M_s. As the field is decreased a finite magnetization remain also when the field has been decreased all the way to zero. This magnetization is called the remanent magnetization. Increasing the field, this time in the antiparallel direction, the magnetization will eventually be zero. The strength of the field for which this occur is called the coercive field. Increasing the field still more, saturation of the magnetization is reached, this time in the direction antiparallel to the first saturated state. Sweeping the field from $-H_s$ to H_s closes the hysteresis loop. The presence of a hysteresis loop which enclose a finite area distinguish the ferromagnetic state from the paramagnetic state and indicates that energy is dissipated each time the hysteresis loop is traversed. The area of the loop represents how much energy is dissipated from the magnetic system to the electrons and to the lattice. The mechanisms for how energy and angular momentum can transfer from the magnetic system to the electrons and the lattice are important both for micromagnetic as well as for atomistic spin dynamics and will be discussed in Chapter 3.

There are numerous techniques that use photons in the form of light or x-rays to investigate the magnetization of a sample. The techniques rely on magnetooptic phenomena, the mechanisms of which can be understood in terms of the scattering mechanisms of photons incident on a magnetic material. Ex-

amples of magnetooptic phenomena are the magnetooptical Kerr rotation [32] where the polarisation of incoming light is rotated to give the reflected light a different polarisation or the related Faraday rotation in transmission. The Kerr and Faraday rotations are often probed with laser pulses. Higher energetic photons in the soft or hard x-ray regime can probe the element specific magnetization in x-ray magnetic dichroism measurements. Synchrotrons can be used to produce coherent, short and bandwidth tuned x-ray pulses.

If rotating a magnetic sample to have a finite angle to an applied static magnetic field, the magnetization will precess in a spiral motion to eventually align with the axis of the applied field. In ferromagnetic resonance (FMR) experiments [5], the magnetic sample is also exerted to an alternating electromagnetic field in the gigahertz regime. The ac-field feeds energy and angular momentum to the magnetization, with the intensity of the absorption dependent on the frequency of the driving field and the material and geometric properties of the sample [33]. With the magnetocrystalline anisotropy energy and the exchange interaction known from other measurements [17], and the form factor for the magnetostatic demagnetizion field tabulated for many geometries [33], FMR provides a mean to measure the strength of the damping mechanisms acting in the precessing magnetic system. The resonance peak in the absorption, plotted as a function of the driving frequency of the AC-field, will broaden with increasing strength of the damping. The hysteresis protocol indicate the presence of damping, FMR allows for it to be measured. Magnetic resonance measurements can also be performed on antiferromagnets [26] and ferrimagnets [27]. The theory here is more evolved and the experiments can be more difficult to perform as the frequencies involved here are even higher than in the FMR case. Magnetization resonance can alternatively be probed with laser light or coherent x-rays. The response can here be in the form of magnetooptical Faraday rotation or x-ray magnetic circular dichroism (XMCD). In combined FMR and XMCD measurements, Bailey *et al* [34], could get element-specific information on the ferromagnetic resonances of $Ni_{81}Fe_{19}$ permalloy. The experiment of Stanciu *et al.* [35] is an example of how one can use the resonance conditions for magnetic resonance in analysis also of experiments where there was no driving ac-field.

Neutron scattering in magnetic compounds is an important technique for characterisation of the magnetic ground state and the excitation spectra [36]. The energy and the wavelengths of the incoming neutrons can be changed, to some degree independently of each other, which enable the energy and wavelength dependent excitation spectra of the magnetization to be measured. This information can be condensed into the dynamic structure factor $S(\mathbf{q}, \omega)$. For complicated magnetic compounds with competing interactions, a series of measurements at different temperatures and sample composition can be used to draw phase diagrams for the magnetic configurations dependent on composition and temperature.

3. Spin dynamics from first principles

In this chapter the equations of motion (EOM) for atomistic spin dynamics (ASD) will be worked out. The description closely follows the book of Kübler [20], one of the pioneers of first principles calculations on magnetic compound with noncollinear ground state orderings [37]. An overview on modern electronic structure methods is given in the monograph by Martin [8]. A review on calculation techniques for noncollinear magnets was written by Sandratskii [38]. Important components for a first principles treatment of magnetism at finite temperature were worked out by Gyorffy *et al.* [39].

Atomic units $m_e = 1/2$, $\hbar = 1$, and $e^2 = 1$ will be used throughout this chapter.

3.1 Dynamics in the time or frequency domain

Spin dynamics from first principles is a relatively young development. In two papers from the mid 1990's, Antropov *et al.* [40, 41] developed in detail how the time evolution of the magnetization at finite temperatures can be calculated within density functional theory (DFT), a popular method for electronic structure calculation which will be introduced in this chapter. The scheme was very extensive and included treatment of systems with substantial orbital contribution to the magnetization and opened up for simultaneous spin and molecular dynamics. Example calculations were done for γ-Fe, a crystalline phase of iron known for its complicated magnetic structure. Stocks *et al.* [42] realised the importance of constraining fields in self-consistent field computations on spin dynamics of noncollinear magnetic systems, which later enabled them to [43] to calculate the magnetic ground state configuration of a finite Co chain along a Pt(111) surface.

To extend the Landau-Lifshitz equation to the case of finite temperatures Brown [44] and Kubo and Hashitsume [45] used Langevin dynamics and obtained stochastic differential equations aimed to describe the dynamics of a magnetic nanoparticle [44] or a single classical spin [45]. It was proposed [41] that Langevin dynamics can be used to model finite temperature also within a scheme for spin dynamics from first principles. The technique was used in calculations of the paramagnetic state of Fe and Ni [46]. Langevin dynamics is also what is used in the calculations presented in this Thesis.

The computational effort for self consistent field spin dynamics simulations is very large. For that reason different schemes to parametrize the magnetic degrees of freedom have been proposed. Fähnle et al. proposed a scheme [47] to parametrize the magnetic degrees of freedom in a spin cluster expansion, inspired by the methods for cluster expansion used in alloy theory [48]. A parametrization from electronic structure calculations to a magnetic Hamiltonian containing Heisenberg interactions was used to calculate the spin wave spectra in bcc Fe in the paramagnetic state [49]. Here the standard classical Heisenberg Hamiltonian was extended to include exchange interactions for four coordinations shells of neighbouring atoms instead of only between the nearest neighbours.

Calculations on spin dynamics often aim to investigate the evolution in time of a magnetic system. Alternatively, concentrating on the frequency domain, one can aim to calculate the spin wave spectra. The spectra is represented by the dynamic structure factor $S(\mathbf{q},\omega)$, or in dispersion relations $\omega = \omega(\mathbf{q})$ extracted from $S(\mathbf{q},\omega)$. Halilov *et al.* [50, 51] made calculations for the 3d metals Fe, Ni and Co and arrived at magnon dispersion relations that showed good correspondence with experimental data. Investigated was also how the magnetic moment would shrink from its maximum value when the atomic moments were forced into a spin spiral configuration.

Central to both Antropov and Halilovs work were the adiabatic approximation and the atomic moment approximation. The method for atomistic spin dynamic that has been used in the calculations presented in this Thesis rely on both these approximations and a parametratization of the magnetic interactions to an effective Hamiltonian for the magnetic degrees of freedom. There are also methods to investigate spin dynamics from first principles without incorporating the approximations above. These approaches have been used primarily in calculations of the spin waves spectra. Working within the adiabatic approximation but without coarsegraining the magnetization to be collinear within atomic cells Niu *et al.* [52, 53] used Berry phases terms to calculate expression for the spin wave spectra. Using linear response DFT it is possible also to do without the adiabatic approximation in calculations of $S(\mathbf{q},\omega)$. This is important for systems where the transversal fluctuations, for high $\mathbf{k}$-vectors have energies that enter the Stoner continuum. Savrasov developed a technique [54] based on the Sternheimer method and successfully calculated the spectra for paramagnetic bcc Cr. Linear response was later used in calculations of $S(\mathbf{q},\omega$ for different (half-)Heusler alloys with up to three magnetic atoms in the chemical unit cell [55] and in calculations for the antiferromagnetic phase of the superconducting material $CaFe_2As_2$ [56]. The linear response calculations for systems with more than one magnetic atom in the chemical unit cell is substantially more involved than the ones corresponding to only one magnetic atom.

3.2 The many-body problem

To solve the full many-body problem, is despite the present computing capabilities, not feasible for anything but small systems. In quantum chemistry the Dirac equation can be solved for atoms and also molecules by exact diagonalization and quantum Monte Carlo methods. The time-dependent problem can for small systems be treated by direct integration of the time-dependent Dirac- or Schrödinger equation. In a crystalline solid, even when exploiting the space group symmetries inherited in the lattice structure, the number of unknowns remains too large for a direct solution. Effective low-energy model Hamiltonian has therefore been and continues to be very important in solid state and condensed matter physics. Investigations of model Hamiltonians are arguably important as they give insight into the general behaviour of individual interactions in different situation such as different temperature and different dimensionality of the solid. In the theory of magnetism, N-vector models such as the quantum mechanical or classical Heisenberg, the XY and the Ising models [7] have generated a large amount of work, often of a more theoretical nature but still with immediate relevance for many magnetic materials. The Heisenberg model(s) corresponds to isotropic magnets, whereas the XY-model and the Ising model represent the limits of strong in-plane or uniaxial anisotropy respectively. For some magnetic systems, for example colossal magnetoresistance materials, Hamiltonians containing both classical terms and quantum mechanical operators are very useful [57]. An important example of a different kind of Hamiltonian is the Anderson model [58] which is important in the theory of how magnetic impurities affect otherwise nonmagnetic metals.

If the question at hand is to learn more about the properties for a specific solid (or class of solids), electronic structure calculations from first principle can give quantitative information that often compare very well with experimental values. A hallmark of a good theory is that it not only shows good correspondence with experimental data already at hand but also have predictive power for the outcomes of experiments not yet performed. In materials science, electronic structure calculations can for example suggest which new materials it can be worth to synthesise, if a certain property is sought after.

A natural development has been the emergence of two-step procedures where parameters are calculated in first principles electronic structure calculations to be used in effective Hamiltonians, typically in the same form as model Hamiltonians. Such procedures can be used in investigations of the properties of a system at finite temperatures.

3.3 Spin-polarized density functional theory

The development that enabled first principle calculations in solid state physics with large but reasonable computational effort was the emergence of density

functional theory. Hohenberg and Kohn [59] formulated a theorem that reduces the N-particle problem to the simplified one of finding the ground state electronic density. The electron density is a function of only 3 variables which can be compared with the many-body wave function that is a function of $3N$ ordinary coordinates and also spin indices. To find the ground state electron density the Kohn-Sham (KS) [60] equation, a Schrödinger like equation, is solved. The KS equation is the basis for the vast majority of calculations on the electronic structure of solids.

In density functional theory we assume that we can determine single particle functions with which the density matrix can be expressed as a sum over occupied single particle states. In the simplest case allowing for magnetization the wave functions are 2-component Pauli spinors $\Psi_{i\alpha}(\mathbf{r},\mathbf{t})$ where the spin index α takes the values 1 and 2. The density matrix is then expressed as a 2×2 matrix

$$\rho(\mathbf{r},t)=\sum_{i=1}^{N}\begin{pmatrix}\Psi_{i1}(\mathbf{r},\mathbf{t})\Psi_{i1}^{*}(\mathbf{r},\mathbf{t}) & \Psi_{i1}(\mathbf{r},\mathbf{t})\Psi_{i2}^{*}(\mathbf{r},\mathbf{t})\\ \Psi_{i2}(\mathbf{r},\mathbf{t})\Psi_{i1}^{*}(\mathbf{r},\mathbf{t}) & \Psi_{i2}(\mathbf{r},\mathbf{t})\Psi_{i2}^{*}(\mathbf{r},\mathbf{t})\end{pmatrix}. \tag{3.1}$$

The particle density and the magnetization density are calculated as traces of the density matrix,

$$n(\mathbf{r},t) = \mathrm{Tr}[\rho(\mathbf{r},t)], \tag{3.2}$$
$$\mathbf{m}(\mathbf{r},t) = \mathrm{Tr}[\hat{\sigma}\rho(\mathbf{r},t)], \tag{3.3}$$

where $\hat{\sigma}$ is a vector of Pauli matrices. Reciprocally the density matrix can be expressed in terms of $n(\mathbf{r},t)$ and $\mathbf{m}(\mathbf{r},t)$ as

$$\rho(\mathbf{r},t)=\frac{1}{2}\left[n(\mathbf{r},t)\mathbf{1}+\mathbf{m}(\mathbf{r},t)\cdot\hat{\sigma}\right]. \tag{3.4}$$

The Kohn-Sham equation in TD-SDFT is a Schrödinger-type equation,

$$i\frac{\partial\Psi_{i\alpha}(\mathbf{r},t)}{\partial t}=\sum_{\beta=1}^{2}\left[-\nabla^2\delta_{\alpha\beta}+v_{\alpha\beta}^{\mathrm{eff}}(\mathbf{r})\right]\Psi_{i\beta}(\mathbf{r},t), \tag{3.5}$$

with the effective potential,

$$\begin{aligned}v_{\alpha\beta}^{\mathrm{eff}}(\mathbf{r},t) &= v^{\mathrm{ext}}(\mathbf{r},t)+2\int d\mathbf{r}'\,\frac{n(\mathbf{r}',t)}{|\mathbf{r}-\mathbf{r}'|}\delta_{\alpha\beta}+v_{\alpha\beta}^{\mathrm{xc}}(\mathbf{r},t)\\ &\quad+([\mathbf{B}^{\mathrm{ext}}(\mathbf{r},t)+\mathbf{B}^{\mathrm{con}}(\mathbf{r},t)]\cdot\hat{\sigma})_{\alpha\beta}.\end{aligned} \tag{3.6}$$

Here $v^{\mathrm{ext}}(\mathbf{r},t)$ is the Coulomb potential from the atomic nuclei, $2\int d\mathbf{r}'\,\frac{n(\mathbf{r}',t)}{|\mathbf{r}-\mathbf{r}'|}$, is the Hartree potential, and $v_{\alpha\beta}^{\mathrm{xc}}(\mathbf{r})=\frac{\delta E_{\mathrm{xc}}[n(\mathbf{r},t)]}{\delta n(\mathbf{r},t)}$ is the exchange correlation (xc) potential. $\mathbf{B}^{\mathrm{ext}}(\mathbf{r},t)$ is an external magnetic field and $\mathbf{B}^{\mathrm{con}}(\mathbf{r},t)$ is an op-

tional constraining magnetic field. The role of the constraining field will be discussed later.

If a global quantisation direction exist in the system, as is the case for a ferromagnet and a collinear antiferromagnet, all terms that go into the KS equations can be made diagonal. This allows for the equation to be separated into one equation for the spin up electrons and one equation for the spin down electrons. The case of noncollinear magnetism, where no global quantisation direction exist, is for many reasons more complicated. One reason is that many of the standard parametrizations for the generalised gradient approximations to the exchange-correlation are applicable only for the case that the density matrix is diagonal [20]. In order to proceed local coordinate systems are defined by a unitary transformation of the density matrix,

$$\sum_{\alpha\beta} U_{i\alpha}(\theta(\mathbf{r}),\phi(\mathbf{r}))n_{\alpha\beta}(\mathbf{r})U^{\dagger}_{\beta j}(\theta(\mathbf{r}),\phi(\mathbf{r})) = \delta_{ij}n_i(\mathbf{r}), \tag{3.7}$$

where $(U_{\alpha\beta})$ is a spin-half rotation matrix,

$$U_{\alpha\beta}(\theta(\mathbf{r}),\phi(\mathbf{r})) = \begin{pmatrix} \exp(i\frac{\phi}{2})\cos(\frac{\theta}{2}) & \exp(-i\frac{\phi}{2})\sin(\frac{\theta}{2}) \\ -\exp(i\frac{\phi}{2})\sin(\frac{\theta}{2}) & \exp(-i\frac{\phi}{2})\cos(\frac{\theta}{2}) \end{pmatrix}. \tag{3.8}$$

The transformation can in principle be made in every point $\mathbf{r}$ of space. What has been commonly used is to partition space into regions for which it is assumed that the magnetization density is reasonably collinear. The partition can be into arbitrary shaped disjunct regions Ω_ν centred around a lattice site ν and spanning all space Ω. The partition can also be into overlapping spheres, which comes natural in implementations of the KS equation where the tight-binding linear muffin-tin orbital (TB-LMTO) [61, 62] or the Korringa-Kohn-Rostoker (KKR) [63] formalism are used in combination with the atomic sphere approximation (ASA) for the potential. Regardless of how the partitioning of space is done, an atomic magnetic moment can be defined for each lattice site ν as the integral of the magnetization density over the region Ω_ν,

$$\mathbf{m}_\nu = \int_{\Omega_\nu} \mathbf{m}(\mathbf{r})\, d\mathbf{r}. \tag{3.9}$$

Also the density matrix itself can be averaged over the atomic cell Ω_ν,

$$n^{\nu}_{\alpha\beta} = \int_{\Omega_\nu} n_{\alpha\beta}(\mathbf{r})\, d\mathbf{r}. \tag{3.10}$$

The rotation matrix $U(\theta_\nu,\phi_\nu)$ for each cell ν can be calculated from the averaged elements of the density matrix,

$$\tan\phi = -\frac{Im(n_{12})}{Re(n_{12})}, \tag{3.11}$$

$$\tan\theta = \frac{2\sqrt{(Re(n_{12}))^2+(Im(n_{12}))^2}}{(n_{11}-n_{22})}. \tag{3.12}$$

The rotation of the density matrix allows for the xc-potential to be calculated as a linear combination of the xc-potential for the spin-up and the spin-down density,

$$\begin{aligned} v^{\rm xc}_{\alpha\beta}(\mathbf{r},t) &= \frac{\delta E_{\rm xc}[n_{ba}(\mathbf{r},t)]}{\delta n_{\alpha\beta}(\mathbf{r},t)} = \sum_{i=1}^{2}\frac{\delta E_{\rm xc}[n(\mathbf{r},t)]}{\delta n_i(\mathbf{r},t)}\frac{\delta n_i(\mathbf{r},t)}{\delta n_{\beta\alpha}(\mathbf{r},t)} \\ &= \sum_{i=1}^{2}\frac{\delta E_{\rm xc}[n(\mathbf{r},t)]}{\delta n_i(\mathbf{r},t)}U(\theta_\nu,\phi_\nu)_{i\beta}U(\theta_\nu,\phi_\nu)^\dagger_{\alpha i}. \end{aligned} \tag{3.13}$$

The effective potential can now be written as a sum,

$$(v^{\rm eff}_{\alpha\beta}(\mathbf{r},t)) = v_0(\mathbf{r},t)\delta_{\alpha\beta} + (\mathbf{B}^{\rm eff}(\mathbf{r},t)\cdot\hat{\sigma})_{\alpha\beta}, \tag{3.14}$$

of a diagonal, nonmagnetic potential,

$$v_0(\mathbf{r},t) = v^{\rm ext}(\mathbf{r},t) + 2\int d\mathbf{r}'\,\frac{n(\mathbf{r}',t)}{|\mathbf{r}-\mathbf{r}'|} + v^{\rm xc}_0(\mathbf{r},t), \tag{3.15}$$

$$v^{\rm xc}_0(\mathbf{r},t) = \frac{1}{2}\left(\frac{\delta E_{\rm xc}[n(\mathbf{r},t)]}{\delta n_1(\mathbf{r},t)} + \frac{\delta E_{\rm xc}[n(\mathbf{r},t)]}{\delta n_2(\mathbf{r},t)}\right), \tag{3.16}$$

and a magnetic potential,

$$\begin{aligned} (\hat{\sigma}\cdot\mathbf{B}^{\rm eff}(\mathbf{r},t))_{\alpha\beta} &= (\hat{\sigma}\cdot\mathbf{B}^{\rm ext}(\mathbf{r},t)_{\alpha\beta} + \mathbf{B}^{\rm con}(\mathbf{r},t))_{\alpha\beta} \\ &\quad + \Delta v(\mathbf{r},t)U^\dagger(\theta_\nu,\phi_\nu)_{i\alpha}\sigma_z U(\theta_\nu,\phi_\nu)_{\beta i} \end{aligned} \tag{3.17}$$

$$\Delta v(\mathbf{r},t) = \frac{1}{2}\left(\frac{\delta E_{\rm xc}[n(\mathbf{r},t)]}{\delta n_1(\mathbf{r},t)} - \frac{\delta E_{\rm xc}[n(\mathbf{r},t)]}{\delta n_2(\mathbf{r},t)}\right). \tag{3.18}$$

The resulting KS equation with the Hamiltonian split into a kinetic term, a scalar potential, and a magnetic potential is written

$$i\frac{\partial\Psi_{i\alpha}(\mathbf{r},t)}{\partial t} = \sum_{\beta=1}^{2}\left[-\nabla^2\delta_{\alpha\beta} + v_0(\mathbf{r},t)\delta_{\alpha\beta} + (\hat{\sigma}\cdot\mathbf{B}^{\rm eff}(\mathbf{r},t))_{\alpha\beta}\right]\Psi_{i\beta}(\mathbf{r},t). \tag{3.19}$$

3.4 The adiabatic approximation

This is still a time-dependent Schrödinger-like equation, requiring a parametrization of the exchange correlation potentials for the time-dependent case. Whereas there are well established parametrization of the exchange and correlation potentials for time-independent DFT, the development of potentials for time dependent DFT has not come that far. The step taken to avoid the complications with solving a time-dependent KS equation is the adiabatic approximation that enables a separation of slower and faster degrees of freedom. The slower developing variables are regarded as frozen on time scales on which the faster degrees of freedom evolve. The most well known example of the adiabatic approximation is the Born-Oppenheimer approximation [64, 6] separating the time scale for electronic and ionic motion in a crystal or molecule. The Born-Oppenheimer approximation relies on the difference in mass of heavy ions and light electrons.

In the case of noncollinear magnetism, the slow variables are the local directions of the magnetization. The fast moving variables are the electron density. The magnetization density fluctuates rapidly due to scattering of itinerant electrons, which for 3d-transition metals are the main carriers of magnetic moment. Averaging over the typical scattering time is an important step in the atomic moment approximation [39, 41]. In contrast to the Born-Oppenheimer approximation there is no large mass governing the slower evolution of the magnetization directions and the adiabatic approximation cannot be as rigorously justified as when separating electronic and ionic motion. The adiabatic approximation is here plausible as the energies of transversal excitations of the magnetization are of the the order of meV:s as compared with the energy scale of the electronic structure of eV:s. Of relevance is here the bandwidth of the spin-polarized electrons and also the exchange splitting of energy between the spin up and spin down bands. For the example of the 3d metal Fe, Co and Ni, one can observe that the exchange splitting of Fe and Co are of the order of 1 eV but only around 300 meV for Ni [20]. It also no surprise that the construction of atomic moments work out better for Fe and Co than for Ni.

Given that the adiabatic approximation is applicable to the magnetic system at hand, the task to solve the time-dependent KS is traded for the task to solve a regular time-independent KS equation,

$$\varepsilon_i \Psi_{i\alpha}(\mathbf{r},t) = \sum_{\beta=1}^{2} \left[-\nabla^2 \delta_{\alpha\beta} + v_0(\mathbf{r})_{\alpha\beta} + (\mathbf{B}^{\mathrm{eff}}(\mathbf{r},t)\cdot\hat{\boldsymbol{\sigma}})_{\alpha\beta} \right] \Psi_{i\beta}(\mathbf{r},t), \quad (3.20)$$

for the electronic structure with prescribed directions for the local magnetization direction. The solution for the electronic density then serves as a potential for the effective magnetic fields that will act as a torque on the magnetization.

3.5 EOM for local magnetization directions

The equation of motion for the slow variables, or the directions of the atomic magnetic moments, can be derived by evaluating the commutator between the spin operator and the KS Hamiltonian. The equation will contain a term involving spin currents $J(\mathbf{r},t)$. The operator for the spin current is defined as an outer product of the vector of Pauli matrices and the current $\hat{\mathbf{j}}(\mathbf{r},t)$ and written

$$J^{KS}(\mathbf{r},t) = \sum_i^N \langle \Phi | \sigma \otimes \mathbf{j}_i(\mathbf{r},t) | \Phi \rangle, \tag{3.21}$$

where the current operator is,

$$\hat{\mathbf{j}}(\mathbf{r},t) = \frac{1}{i}\sum_i^N \nabla_i \delta(\mathbf{r}-\mathbf{r}_i) + \delta(\mathbf{r}-\mathbf{r}_i)\nabla_i. \tag{3.22}$$

The commutator of the KS Hamiltonian and the spin operator are evaluated term by term. In the absence of relativistic effects the spin operator $\hat{s} = \frac{\hbar}{2}\hat{\sigma}$ commutes with the effective scalar potential [65]. The commutator with the magnetic field potential gives the precession term and the commutator with the kinetic energy gives a term involving spin currents. The final result is written

$$i\left[\sum_{\beta=1}^{2} -\nabla^2\delta_{\alpha\beta} + v_0(\mathbf{r})_{\alpha\beta} + (\mathbf{B}^{\text{eff}}(\mathbf{r},t)\cdot\hat{\sigma})_{\alpha\beta}\ ,\ \hat{s}\right] = -\nabla\cdot J^{KS}(\mathbf{r},t) + \frac{q}{2mc}\hat{s}(\mathbf{r},t)\times\mathbf{B}^{\text{eff}}(\mathbf{r},t). \tag{3.23}$$

Taking the expectation values with the KS wave functions one arrives to a continuity equation for the spin density,

$$\frac{d\mathbf{s}(\mathbf{r},t)}{dt} + \nabla\cdot J(\mathbf{r},t) = 2\mathbf{s}(\mathbf{r},t)\times\mathbf{B}^{\text{eff}}(\mathbf{r},t). \tag{3.24}$$

The tensorial divergence of the spin current term can be discarded for systems with negligible spin currents such as insulators. The action of the spin currents on the magnetization is the mechanism behind the spin-transfer-torque [66] effect that have received much attention since the seminal work of Slonzewskci [67] and Berger [68]. The mechanism is also important as it contributes to the relaxation of the magnetization. If we omit the current term and integrate over the atomic cells we arrive to an equation of motion for the atomic magnetic moments,

$$\frac{d\mathbf{m}_\nu}{dt} = -\gamma\mathbf{m}_\nu\times\mathbf{B}^{\text{eff}}(\mathbf{r},t). \tag{3.25}$$

The sign here has changed as the magnetic moment associated with spin angular momentum is pointing in the negative direction.

3.6 Constraining fields

A general noncollinear magnetic configuration does not constitute a ground state within DFT. The iteration of Eq. 3.20 towards self consistency for the electronic structure would by itself drift towards the ground state, e.g. a collinear ferromagnetic state. To prevent this, constraining fields can be included. The technique to tackle this problem is to use constrained DFT as developed by Dederichs *et al.* [69]. Lagrangian multipliers are introduced to constrain some quantity, such as the particle number within the muffin-tin or the size of the magnetic moment. For self consistent field ASD the directions of the atomic magnetic moments should be fixed during the calculation of the electronic structure. This can be achieved by addition of a constraint

$$\int_{\Omega_\nu} \mathbf{m}(\mathbf{r},t) \times \mathbf{e}_\nu^{\mathrm{con}}\, d\mathbf{r} = 0. \tag{3.26}$$

The cross product form of the constraint ensures that the atomic magnetic moment has no components normal to the direction of the prescribed magnetization direction $\mathbf{e}_\nu^{\mathrm{con}}$. An important observation was done by Stocks *et al.* [42]. They realised that the magnetic field that is used to constrain the direction of the magnetic moment can be used to construct the effective field that give the correct precession torque on the local magnetic moment, a torque that is needed to perform SCF spin dynamics simulations. The technique has been used to investigate the canted magnetism of a finite Co chain along a Pt(111) surface step edge [43]. In this study the aim was to calculate the magnetic ground state configuration. For this it is actually possible to use the effective field for a damping motion (see section 3.10.1) only, and to exclude the precession term in the equation of motion.

3.7 Self consistent field spin dynamics

The calculation of the evolution of the magnetization and charge densities from a time t to $t+\Delta t$ is hence a two-step procedure. The first step is to solve the KS equation until self-consistency is obtained with constrained moment directions. The second step is to evolve the magnetization according to the equation of motions for the slow degrees of freedom in a time interval Δt. With the new directions for the atomic magnetic moments, the KS equation is solved anew. This procedure is then repeated. The bottleneck of this procedure is that the electronic structure calculation is very time consuming. The computational effort for most schemes to solve the KS equation scales badly with the number of atoms in the simulation cell (quadratically or worse). The magnetization configurations of interest can span over distances much larger than the chemical unit cell. This has as consequence that even a single sequence of iterations to self consistency for the electronic structure with prescribed mag-

netic moment directions can be computationally demanding. What has been more common, and is the method used for the results presented in this Thesis, is to parametrize the total energy as a function of the magnetic degrees of freedom.

3.8 The magnetic Hamiltonian

Its quantum mechanical origin apart, the parametrized magnetic Hamiltonian that will be described in the following paragraphs is purely classical as it does not contain any quantum mechanical operators. The terms of the Hamiltonian contain single or double sums over atom indices *i*. The presentation below is limited to the case where the coupling constants J_{ij} are independent of the atomic coordinates and the magnetic configuration. That is, the validity of the Hamiltonian is restricted to problems where magnetostriction/exchange striction is not of primary importance and the exchange interactions do not change too much when the (local) magnetic configuration is changed. The parametrized magnetic Hamiltonian consists of the following terms

$$\mathscr{H} = \mathscr{H}_{\text{iex}} + \mathscr{H}_{\text{ma}} + \mathscr{H}_{\text{dd}} + \mathscr{H}_{\text{ext}}. \tag{3.27}$$

The first term represents interatomic exchange interactions. The second term represents onsite magnetocrystalline anisotropy energy. Magnetostatic dipole-dipole-interaction is expressed in the third term. The fourth and final term is the Zeeman energy. As will be developed below, the decomposition of the magnetic Hamiltonian is not entirely unique.

At the heart of atomistic spin dynamics is the isotropic Heisenberg exchange interaction. Compared to other contributions to the internal energy it is much stronger. One of the consequences is that it is mainly the Heisenberg exchange that governs the the temperature dependence of the magnetic system. A Heisenberg Hamiltonian expressing the exchange interaction between atoms *i* and *j* is, to first order (bilinear in $\mathbf{m}_i \cdot \mathbf{m}_j$) written as

$$\mathscr{H}_{\text{heis}} = -\frac{1}{2}\sum_{i \neq j} J_{ij}\mathbf{m}_i \cdot \mathbf{m}_j, \tag{3.28}$$

where $\mathbf{m_i}$ is the classical atomic magnetic moment and J_{ij} is the exchange integral. Higher order terms $J_{ij}^{(n)}(\mathbf{m}_i \cdot \mathbf{m}_j)^n$ can also be included. The minus sign in Eq. 3.28 above indicate that the exchange integral is defined so that a positive value correspond to ferromagnetic coupling and a negative value to antiferromagnetic coupling.

The presence of onsite magnetocrystalline anisotropy energy is a relativistic effect that arise through spin-orbit coupling. The magnetocrystalline anisotropy energy can be expressed as a series expansion of the angles of the

magnetic moment to the crystallographic axes [5],

$$\mathscr{H}_{\mathrm{ma}} = \sum_i K_i(\mathbf{m}_i). \tag{3.29}$$

The symmetry of the crystal determines the functional forms of these series expansions [2]. For a uniaxial anisotropy the dominant contribution is of the form,

$$\mathscr{H}_{\mathrm{ma}} = \sum_i K_{1,i}(\mathbf{m}_i \cdot \mathbf{e}_K)^2, \tag{3.30}$$

where $\mathbf{e}_K$ is the direction of the anisotropy axis and K the strength of the anisotropy energy. A negative value of K corresponds to easy axis anisotropy, a positive value to easy plane anisotropy.

In addition to the well known Heisenberg exchange interaction, also other type of interatomic exchange interactions are possible. Symmetry considerations restrict what contributions are allowed in various crystal structures. In an expansion including terms up to second order the most general [70] spin-spin exchange interaction can be written

$$\mathscr{H}_{\mathrm{iex}} = -\frac{1}{2}\sum_{ij} \mathbf{m}_i \mathscr{J}_{ij} \mathbf{m}_j. \tag{3.31}$$

The matrices $\mathscr{J}_{ij}$, linking the magnetic moment $\mathbf{m}_i$ with the atomic moment $\mathbf{m}_j$, are 3×3 matrices $\mathscr{J}_{ij}^{rs}$ where the r,s indicies run over x,y,z. When interchanging the atomic indicies i,j the matrices are transposed, $\mathscr{J}_{ij} = \mathscr{J}_{ji}^t$. The matrices $\mathscr{J}_{ij}$ can be written as a sum of three terms,

$$\mathscr{J}_{ij} = J_{ij}\mathbf{1} + \mathscr{J}_{ij}^S + \mathscr{J}_{ij}^A, \tag{3.32}$$

where $\mathbf{1}$ is the unit matrix and

$$\begin{aligned} J_{ij} &= \frac{1}{3}\mathrm{Tr}(\mathscr{J}_{ij}) \\ \mathscr{J}_{ij}^S &= \frac{1}{2}(\mathscr{J}_{ij} + \mathscr{J}_{ij}^t) - J_{ij}\mathbf{1} \\ \mathscr{J}_{ij}^A &= \frac{1}{2}(\mathscr{J}_{ij} - \mathscr{J}_{ij}^t) \end{aligned} \tag{3.33}$$

The J_{ij} terms constitute isotropic exchange interactions and correspond to Heisenberg exchange. The $\mathscr{J}_{ij}^S$ terms are symmetric anisotropic exchange interactions. These are also named pseudodipolar exchange interactions as they have angular dependence similar to the magnetostatic dipole-dipole-interaction [25]. The $\mathscr{J}_{ij}^A$ terms are antisymmetric anisotropic exchange interations and correspond to the Dzyaloshinskii-Moriya interaction. Both anisotropic terms are traceless. The interatomic exchange

interaction can also be written on the form

$$\mathscr{H}_{\rm iex} = -\frac{1}{2}\sum_{i\neq j}\left\{J_{ij}\mathbf{m}_i\cdot\mathbf{m}_j + \mathbf{m}_i\mathscr{J}_{ij}^{S}\mathbf{m}_j + \mathbf{D}_{ij}\cdot(\mathbf{m}_i\times\mathbf{m}_j)\right\}. \tag{3.34}$$

Here the Dzyaloshinskii-Moriya vector $\mathbf{D}_{ij}$ with elements

$$\begin{aligned} D_{ij}^{x} &= \frac{1}{2}(\mathscr{J}_{ij}^{yz} - \mathscr{J}_{ij}^{zy}), \\ D_{ij}^{y} &= \frac{1}{2}(\mathscr{J}_{ij}^{xz} - \mathscr{J}_{ij}^{zx}), \\ D_{ij}^{z} &= \frac{1}{2}(\mathscr{J}_{ij}^{xy} - \mathscr{J}_{ij}^{yx}). \end{aligned} \tag{3.35}$$

has been introduced. The sum in Eq. 3.31 above runs over $i = j$. The sum in Eq. 3.34 is over $i \neq j$ which is possible if we have transferred the onsite anisotropy interactions $\mathbf{m}_i\mathscr{J}_{ij}^{A}\mathbf{m}_i$ to the term $\sum_i K(\hat{\mathbf{m}}_i)$ for the onsite magnetocrystalline anisotropy energy. This is one example of that the decomposition of the magnetic Hamiltonian is not unique. The third term, with implicit summation over μ and ν,

$$\mathscr{H}_{\rm dd} = -\frac{1}{2}\sum_{i\neq j} Q_{ij}^{\mu\nu} m_i^{\mu} m_j^{\nu}, \tag{3.36}$$

represents dipolar interactions. Here μ and ν are coordinate indices and the quadrupole $Q_{ij}^{\mu\nu}$ is given by

$$Q_{ij}^{\mu\nu} = \frac{\mu_0}{4\pi}(3R_{ij}^{\mu}R_{ij}^{\nu} - \delta_{\mu\nu}R_{ij}^{2})R_{ij}^{-5}, \tag{3.37}$$

where R_{ij} is the distance between atomic moments i and j. Dipolar interactions are long ranged and important for the long wave length excitations [2]. The interaction can be neglected in studies of short wave length excitations. For finite systems, dipolar interactions lead to a shape anisotropy, in the form of form factors that describe the demagnetization field [2]. The last term of Eq. (3.27),

$$\mathscr{H}_{\rm ext} = -\mathbf{B}_{\rm ext}\cdot\sum_i \mathbf{m}_i, \tag{3.38}$$

is the Zeeman term and describes the interaction of the magnetic system with an external magnetic field. The magnetic field can in general depend both on space and time. For small structures, an alternating applied electromagnetic field, can be approximated to be spatially uniform over the sample. For short wavelengths this approximation can be violated which e.g. complicates the theory of ferromagnetic resonance.

The contributions to the magnetic Hamiltonian sum up to a rather lengthy expression, which is stated here for later reference,

$$\begin{aligned}\mathscr{H}_{\text{magn}} &= -\frac{1}{2}\sum_{i\neq j}\left\{J_{ij}\mathbf{m}_i\cdot\mathbf{m}_j+\mathbf{m}_i\mathscr{J}_{ij}^{S}\mathbf{m}_j+\mathbf{D}_{ij}\cdot(\mathbf{m}_i\times\mathbf{m}_j)\right\}+\sum_i K_i(\mathbf{m}_i)\\ &\quad -\frac{\mu_0}{8\pi}\sum_{i\neq j}\frac{3(\mathbf{R}_{ij}\cdot\mathbf{m}_i)(\mathbf{R}_{ij}\cdot\mathbf{m}_j)-R_{ij}^2(\mathbf{m}_i\cdot\mathbf{m}_j)}{R_{ij}^{-5}}-\mathbf{B}_{\text{ext}}\cdot\sum_i\mathbf{m}_i.\end{aligned} \tag{3.39}$$

Often only a subset of the terms of the Hamiltonian is used in a specific atomistic spin dynamics study. The sample geometry and the symmetry of the crystal structure are important factors that can restrict which interactions can take finite values and gives a hint on whetherthey will be large or not. More precise quantitative information on the strength of interactions cannot be provided by symmetry and geometry considerations alone but must be calculated or obtained from experiments. The isotropic interatomic exchange interaction is typically much stronger than the other energies in the Hamiltonian. Nevertheless, small but finite contributions in form of anisotropy or Dzyaloshinskii-Moriya energies can influence the magnet ground configuration. An example of this can be seen in Figs. 3.1 and 3.2 where the magnetic ground state configurations for a monolayer of iron on tungsten, Fe/W(110), are shown. The calculation of the Heisenberg interatomic exchange interactions is described in Paper VII. In Fig. 3.1, only Heisenberg (isotropic) interatomic exchange is present. The balance of ferromagnetic and antiferromagnetic exchange interaction makes a spin spiral configuration energetically favourable. By adding a small uniaxial anisotropy, the balance is changed and a ferromagnetic ground state has the lowest energy, as shown in Fig. 3.2. In calculations of the spin wave spectra (See Paper VII), a small anisotropy was used in addition to the Heisenberg exchange parameters. In experiments, Fe/W(110) has a ferromagnetic groundstate. As demonstrated by Udvardi *et al.* [71], the Dzyaloshinskii-Moriya interaction can cause a chiral asymmetry of the spin-wave spectra. This is an example on that a small but finite contribution to the magnetic Hamiltonian can change not only the ground state, but also the properties of excitations.

It is also possible to go in the other direction and if necessary include even more general terms. Higher order terms can be included in the expansion of the interatomic exchange energy. The restriction to have the size of the magnetic moments fixed can be revoked. The applied magnetic field can in numerical simulations have in principle arbitrary form. In reality there are geometric restrictions for coils and other components that, governed by Maxwell's equations, radiate an electromagnetic field when an alternating or direct current flows through them. The mechanism for an effective applied magnetic field can also be optomagnetic interactions, as e.g. the inverse Faraday effect [72].

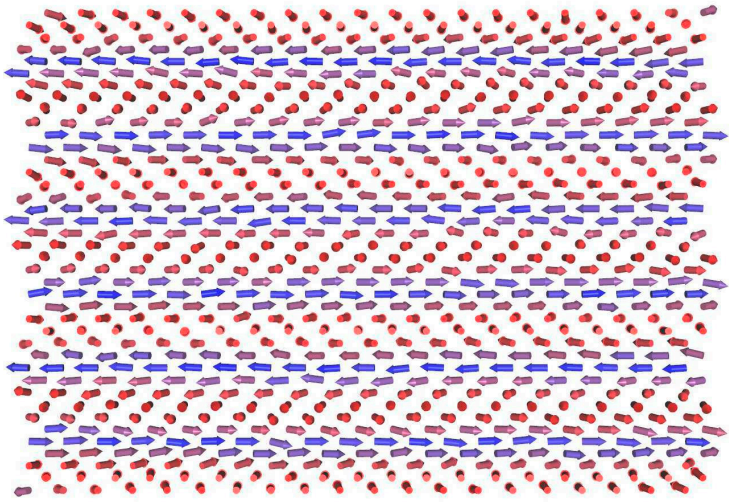

Figure 3.1: The magnetic ground state configuration for a monolayer of iron on tungsten, Fe/W(110). With only isotropic interatomic exchange parameters in the magnetic Hamiltonian, the ground state is a spin spiral.

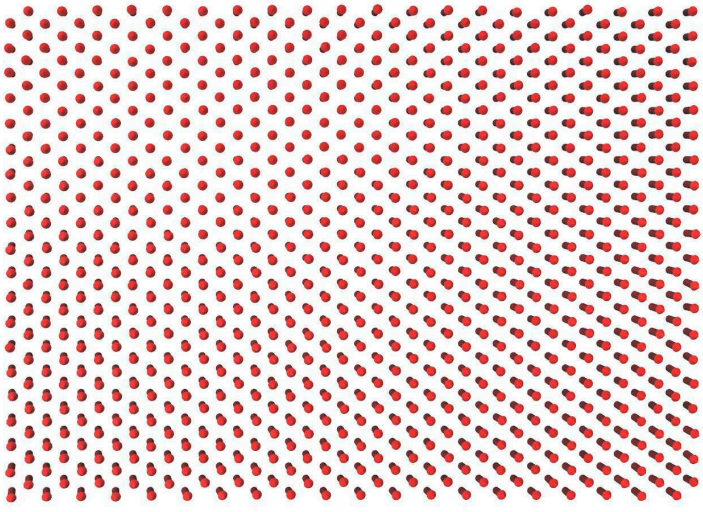

Figure 3.2: The magnetic ground state configuration for a monolayer of iron on tungsten, Fe/W(110). The same isotropic interatomic exchange parameters as in Fig. 3.1. Here is present also a small magnetocrystalline anisotropy with a hard out of plane axis. The anisotropy energy is small in comparison with the interatomic exchange parameters, but large enough to tip the balance and make a ferromagnetic groundstate favourable.

3.9 Calculation of interactions

The parametrization to a Heisenberg Hamiltonian can be performed within an electronic structure calculation in several ways. Using a supercell, with two or more repetitions of the chemical unit cell, it is possible to do a set of total energy calculations for different magnetic configurations imposed with constraining fields. Nearest and next nearest neighbour interactions can be obtained in this way, but the technique is not practical to capture more long ranged exchange interactions. Liechtenstein *et al.* [73] derived a method based on the Andersen force theorem [74]. The method, which will be referred to as the Liechtenstein formula, contains an expression for the intersite exchange interactions J_{ij},

$$J_{ij} = \frac{\mathrm{Im}}{4\pi} \int_{-\infty}^{E_F} d\varepsilon \, \mathrm{Tr}[\delta_i^M(\varepsilon) \bar{g}_{ij}^{M,M\uparrow}(\varepsilon) \delta_j^M(\varepsilon) \bar{g}_{ji}^{M,M\downarrow}(\varepsilon)], \tag{3.40}$$

where J_{ij} is the pair exchange interaction between atoms i and j. The trace, Tr, runs over the angular momentum variables $L = lm$, $\delta_i^M(\varepsilon)$ is the exchange splitting of energy for the magnetic atom M and $\bar{g}_{ij}^{M,M\uparrow}(\varepsilon)$ are the site off-diagonal blocks of the Green function. The advantage with the Liechtenstein formula compared to model Hamiltonians for the exchange is that no assumptions have to be made on the nature of the exchange. [1]. The expression Eq. 3.40 has been implemented in numerous Green function electronic codes in the KKR [63] or LMTO [61, 62] family. When using the Liechtenstein formula the exchange parameters are usually calculated from a FM configuration by making infinitesimal rotations away from the strict FM configuration (or from DLM configurations, see below). In general the J_{ij} can be dependent on the magnetization configurations, and implicitly or directly on temperature.

Exchange interaction parameters can also be calculated with the Generalised Perturbation Method (GPM) by Ruban *et al.* [76]. This method is argued to give more realistic values for the parameters for systems that are in the paramagnetic state. The paramagnetic state lacks long range ordering but magnetic moments can be correlated on shorter distances. To calculate parameters the high temperature limit of completely uncorrelated spins is used. The disordered local moments (DLM) configuration is defined as the state where there are no correlation between the magnetic moments on any distance. The GPM also provides a means to parametrize longitudinal fluctuations and include biquadratic and higher order terms in the expansion of the interatomic exchange interaction.

An important alternative to the Liechtenstein formula and the GPM is the so called frozen magnon approximation [50, 51, 77]. Here spin spiral configurations excitations are enforced in the electronic structure calculations with

[1] For a description of different exchange mechanisms such as direct exchange, RKKY, superexchange, see the monograph by Yosida [19] Exchange interactions in diluted magnetic semiconductors are discussed in the reviews Refs. [75, 13]

the help of constraining fields. By calculating for a set of spin spirals the total energy is obtained as function of the spin spiral wave vector q. From the minima of the total energy one can immediately observe if the groundstate of the system is ferromagnetic which it is if the total energy has a minima for $q = 0$. The frozen magnon energies also often match well with the actual magnon dispersion relations measured in experiments.

A more complete parametrization of the magnetic energy does also include contributions from magnetocrystalline anisotropy energy and anisotropic interatomic exchange energy. The TB-LMTO program [62] and KKR-program [63] that were used in most calculations presented in this Thesis did not have spin-orbit coupling included. Magnetocrystalline anisotropy is a relativistic effect that cannot be captured in calculations without spin-orbit coupling. For this reason the magnetocrystalline anisotropy energy was input with values either from experiment or from calculations using other programs. It is not uncommon that LMTO and KKR-programs lack spin-orbit coupling. When a more general parametrization of the magnetic energy is needed it is necessary to use full-potential programs and spin-orbit coupling. The LAPW method, explained in detail in a monograph by Singh and Nordström [78], is suitable for full potential calculations. Examples are FP-LAPW/FP-APW+lo, (+local orbitals) programs as Wien2k [79], Fleur [80], ELK [81] or Exciting [82]. In these programs the frozen magnon approximation can be used to parametrize isotropic exchange, anisotropy and Dzyaloshinskii-Moriya interactions [83]. This has been used in combined experimental and theoretical investigations [84, 85] of the magnetism of Mn/W(110), a monolayer of Mn on deposited on a tungsten surface.

The full-potential LMTO method (FP-LMTO), described in the monograph by Wills, Eriksson *et al.* [86] and Chapter 4 of Ref. [87], allows for very precise calculation of total energies, important in accurate investigations of magnetocrystalline anisotropy energies. Using the FP-LMTO program RSPt [88], Burkert *et al.* calculated the giant magnetic anisotropy in tetragonal FeCo Alloys [89] and the uniaxial magnetic anisotropy energy of tetragonal and trigonal Fe, Co, and Ni [90]. The RSPt program is at present restricted to collinear spin configurations, but the FP-LMTO method as such can be used also for noncollinear magnetic configurations. For the FP-LAPW/FP-APW and the FP-LMTO method alike, the computational effort increases drastically for the case of noncollinear magnetic configuration. Methods without spin-orbit coupling can use the generalised Bloch theorem [38], this is not possible in the full potential formulation.

Udvardi *et al.* [70, 71] have developed a technique, based on infinitesimal rotations and the Andersen force theorem, to map the magnetic energy to the general interatomic exchange Hamiltonian, including relativistic contributions as the Dzyaloshinskii-Moriya interaction, pseudo-dipolar interaction and on-site anisotropy. This has been implemented into a program based on SKKR, the screened KKR method [91, 92]. The technique comes to good use in in-

vestigations on systems with reduced dimensionality and symmetry, where Dzyaloshinskii-Moriya interactions and anisotropies can be larger and hence more important, than in bulk systems. This was the case in calculations on monolayers of iron on tungsten, Fe/W(110) [71], and of the spin interactions and the magnetic ground states of Cr trimers on Au(111) [93].

3.10 Relaxation

The local moment equation Eq. 3.25 does only contain a term expressing the precession of the local moment around the effective magnetic field. This describes the conservative dynamics of an ideal spin system that does not exchange energy with its environment. Unless initially in its (possibly degenerate) ground state, the spin system will remain in configurations that have a constant, higher energy. The spin system cannot respond to changes in the temperature of its environment. In Chapter 4 the characteristics of spin dynamics, with or without a mechanism for relaxation and at zero or finite temperature is discussed. This section on relaxation will describe how damping can be introduced phenomenologically and also the more recent developments that strive to model damping from first principles.

3.10.1 Phenomenological damping

Landau and Lifshitz did, already in their first paper [3] on magnetization dynamics, include a term in the EOM that account for relaxation. They proposed a double cross product damping term in addition to the precession term, yielding the equation known as the Landau Lifshitz (LL) equation:

$$\frac{\partial \mathbf{m}}{\partial t} = -\gamma \mathbf{m} \times \mathbf{B} - \frac{\lambda}{m} \mathbf{m} \times (\mathbf{m} \times \mathbf{B}). \tag{3.41}$$

The damping torque is perpendicular to the precession torque. The motion of a single spin exerted to an external magnetic field is a spiral motion where the spin eventually aligns with the field. For a system of interacting spins the motion is more complex but also here each spin momentarily exercise spiral motion around the effective magnetic field acting on it.

In classical mechanics, the friction force acting on a particle moving through a viscous media is to first order approximation proportional to, and negative in direction to, its velocity [94]. Gilbert [95] introduced an analogous damping force for magnetization dynamics resulting in the Landau-Lifshitz-Gilbert (LLG) equation):

$$\frac{\partial \mathbf{m}}{\partial t} = -\gamma \mathbf{m} \times \mathbf{B} + \frac{\alpha}{m} \mathbf{m} \times \frac{\partial \mathbf{m}}{\partial t}. \tag{3.42}$$

Just as the LL damping torque, the Gilbert damping torque is perpendicular to the precession torque. In the limit of small damping the solutions of the LL and the LLG equations are close to each other. For larger damping the discrepancy is substantial. [2] In the micromagnetic community, the Gilbert form of the damping has been the more popular choice, and it was indeed shortcomings of the LL for of damping that motivated Gilbert's research.

3.10.2 Mechanisms for damping

The mechanisms for damping of the magnetic precession are manifold. At first, it can be observed that for a closed magnetic system, the total angular momentum and total energy are preserved quantities. With magnetic system is here understood the whole magnetic solid, with spin, charge and lattice degrees of freedom. In the case of ideal precessional dynamics with only interatomic exchange contributing to the effective field, the total angular momentum and energy for the spin system are constants of motion. In the presence of magnetocrystalline anisotropy, the spin exchange angular momentum with the lattice. Describing the dynamics in terms of conjugate variables for magnons (Holstein-Primakoff variables [96] or the analogues variables for classical spins), this is an example of magnon scattering. This mechanism, relevant for the phenomena of spin wave instabilities explored in Paper V, can result in longitudinal damping of the magnetization averaged over a finite part of the sample. This longitudinal damping of the average magnetization of a system of local magnetic moments should be contrasted to the possible restriction that the size of the local moment is constant.

The transfer of angular momentum to the lattice from the spin system is discussed mainly in terms of spin-orbit coupling. Magnetocrystalline anisotropy energy is a caused by spin-orbit coupling, allowing for the pure precessional torque dynamics described above to involve transfer of angular momentum. The spin-orbit coupling is arguably also very important in mechanisms for the damping torque on individual magnetic spins. Damping of magnons in scattering with the lattice involves spin-orbit coupling. The damping can be enhanced by impurities and other imperfections of the lattice.

Allowing for the magnetic system to interact with its environment opens many channels for angular momentum and energy transfer. Conducting electrons can drain or feed the magnetic system with angular momentum when they flow in or out of the system. This is the mechanism behind the spin-transfer-torque effect [68, 67, 66]. A dynamic magnetic system will, governed by Maxwell's equations, radiate electromagnetic fields, also here involving a transfer of angular momentum. This effect is utilised in design of, and experiments on, spin-torque oscillators [66]. Being in thermal contact with its

[2] As will be shown in Chapter 4 the LL and the LLG equations are identical in the case of isotropic damping, provided a renormalized gyromagnetic ratio is introduced

environment, the thermal motion of electrons and lattice connect to the spin degrees of freedom, once again involving transfer of angular momentum.

When investigating the physical origins of damping it often comes natural to use the spin wave picture and study how damping can occur for magnons. This is the case for impurity scattering and also for damping due to radiation of electromagnetic fields. In the following the formalism will however be in the local moment picture. Eventually, this is what is needed for ASD as it relies on an EOM for the local moments and not for the conjugate variables.

For an inhomogenously magnetized system one can assume that the relaxation is dependent on the local magnetization. Furthermore, it can be anisotropic with regard to the direction of the magnetization. Holding on to the Gilbert form, the damping can be expressed as a tensorial quantity

$$\frac{\mathbf{A}(\{\mathbf{m}_i\})}{m}\mathbf{m}_i \times \frac{\partial \mathbf{m}_i}{\partial t}, \tag{3.43}$$

where $\mathbf{A}(\{\mathbf{m}_i\})$ is a 3×3 tensor in spin space. A tensorial formulation of the Gilbert damping is useful in analysis of data from FMR for systems where the relaxation is anisotropic. It is here important to observe that the damping parameters extracted from the line widths of the resonance peaks, are for the global magnetization. Regardless of whether the damping is isotropic or not, it is in general the case that the damping parameter for a finite cell of the magnetic sample must not be identical with the damping parameter for the atomic magnetic moments. This implies that values for the damping damping parameters obtained from FMR experiments cannot indiscriminately be adopted as damping parameters for atomistic spin dynamics [97, 98, 99].

3.10.3 Damping from first principles

An important step towards a description of damping from first principles was taken by Kambersky who introduced the so called breathing Fermi surface (BFS) model [100]. In the adiabatic approximation for spin dynamics, it is assumed that the electronic degrees of freedom respond so fast to changes of the local magnetization directions that the system is always in a ground state. In the BFS model the assumption of adiabacity is loosened, to describe the situation where the electronic system does not respond instantaneously to the evolution of the magnetization. The BFS model was originally developed for electron band theory but was later [101, 47] combined with the single electron wave function formalism in DFT. The non-adiabacity is here realised by keeping the adiabatic single electron states but letting the occupation numbers relax at a rate inversely proportional to a scattering time τ. The group of Fähnle has extended the BFS model to allow for anisotropic damping and dependence on the local magnetic configuration. In a recent paper [102] they arrive to expressions that treat the noncollinear and collinear case on the same footing. An important difference between the collinear case and the noncollinear case

is that the former is dependent on spin-orbit coupling. In the latter case also electron kinetic energy associated with the noncollinear spin configurations contribute to the damping. Angular momentum is here scattered within the spin system. This contribution can be substantially stronger than contribution from spin-orbit coupling, which compares well with experimental observations of strongly enhanced damping in highly noncollinear configurations as domain walls or vortex cores. The BFS model combined with DFT can incorporate different source of relaxation through the calculation of energies and occupation numbers. The scattering time τ can however not be calculated from within DFT and remains a free parameter. This circumstance strongly limits the predictive power of the BFS.

Expressions similar to the ones in the BFS model can also be derived within the frame work of linear response. Kambersky [103] developed this method which was latter given the name torque-correlation model (TCM). Gilmore *et al.* concluded [104] that the BFS model actually is equivalent to the intraband contributions to the damping rate within the TCM. They demonstrated in calculations for Fe, Co and Ni that whereas the intraband contributation to damping dominates at low temperatures, it is the interband contribution, which is captured by the TCM, that dominates at room temperature.

The models presented so far presupposes a Gilbert form of the damping and are derived within a single electron formalism. Hickey and Modera proved with a non-relativistic expansion of the Dirac equation that the functional form $\frac{\alpha}{m}\mathbf{m} \times \frac{\partial \mathbf{m}}{\partial t}$ can be derived from first principles. The crucial step was to use the Maxwell equation $\nabla \times \mathbf{E} = -\frac{\partial \mathbf{B}}{\partial t}$ to identify the connection between the time-dependent magnetization and the curl of the electric field. The damping is here connected too electromagnetic radiation, a concept earlier proposed by Ho [105] and given the name radiation-spin-interaction. The expressions for α does depend on the typical frequency of the magnetization precessing in the exchange field. To incorporate these expressions within DFT would give access to material specific properties for the frequency dependent damping. However, this method also requires knowledge of a scattering time τ.

The are numerous other proposals on how to model damping. Some or them are for specific geometries and some are for specific materials. Brataas *et al.* developed [106] a scattering theory of Gilbert damping for a single domain ferromagnet in contact with a heat bath. The method is an extension of previous work by the same authors on spin pumping and enhanced Gilbert damping [107]. Zhang *et al.*, observing that the most significant source of damping in conducting ferromagnets is due to conduction electrons carrying away angular momentum, developed a model where conduction electron damping is explicitly included. Fähnle *et al.* demonstrated in constrained DFT calculations how the directions of the polarisation of the itinerant s- and p-electrons and the localized d-electrons can strongly deviate from each other and made the point that the s-d-model for magnetization dynamics, as described by

Zhang *et al.* [108], need to be extended to handle the situation where the different electrons are not collinear within the extent of an atom.

In conclusion, it can observed that although substantial progress has been made, the efforts to develop schemes to calculate damping from first principles still have some way to go. In the framework of DFT, the question on how to calculate damping (parameters) is connected to the developments of exchange-correlation functionals for time-dependent DFT [65, 109]. Remarkable is also, that there is an ongoing and lively discussion on the mechanisms that can explain ultrafast demagnetization [110, 111, 112, 113] that can be caused and probed with femtosecond lasers [114]. In the context of the present Thesis it should be emphasized that some of the processes involved in ultrafast demagnetization violate the condition of adiabacity and therefore cannot be captured by adiabatic atomistic spin dynamics.

4. Properties of the LL equation

The Landau-Lifshitz equations are nonlinear coupled equations, for which closed analytical solutions can only be obtained in a few cases. Analytical solutions are rare, not only for the trajectories in time of the individual magnetic moments, but also for the trajectories in time of the average magnetization and higher moments [115]. In early work on micromagnetics, techniques were developed to solve the LL equations approximately so that a larger class of problems could be handled. At a later stage, the possibility to perform large scale numerical simulations on computers have enabled still more complex geometries and problems to be investigated.

For ferromagnetic materials it is possible to define an exchange length over which changes to the magnetization direction are negligible. The exchange length determines how large elements can be used in finite difference and finite elements methods. For efficiency, adaptive meshes can be used, where for domainwalls and vortices, with large gradients of the magnetization vectorfield, a higher resolution is necessary. For homogenously magnetized parts of the magnetic sample, lower resolutions are possible. In simulations of the soft magnetic permalloy, $Fe_{20}Ni_{80}$ a typical value for the spatial discretization is 3 nm [116].

For compounds with an antiferromagnetic, ferrimagnetic or noncollinear ground state configuraation it is not possible to coarse grain the magnetization in the same way as for ferromagnets. The length scale is here set by the lattice parameters, which for small chemical unit cells are only a few Å. In comparison with the discretization lengths that can be used in micromagnetism, it is clear that the computational effort per unit volume is drastically larger for atomistic spin dynamics.

4.1 Spin systems at finite temperatures

The equilibrium properties of quantum mechanical and classical spin models is a very well established field of condensed matter and statistical physics. The physics that take place in the vicinity of phase transitions has for long time been of particular interest [117]. A large body of theory and results have been worked out, with important concepts as finite size scaling, universality classes and the renormalization group [118, 119]. For less technical introductions to these topics the papers of Stanley [120] and Delamotte [121] are suggested

reading. For atomic spin dynamics, the theory of dynamic critical phenomena [122] is relevant, connecting to phenomena such as critical slowing down [123], and relaxation of frustrated systems [124].

The thermal equilibrium properties of a spin system modelled by a classical Hamiltonian follow Boltzmann statistics [7]. Extensive Monte Carlo simulations allowed Chen *et al.* to determine the exponents for the static critical behaviour of the Heisenberg model for spins on the sites of a sc and a bcc lattice. The Boltzmann statistics is an important starting point also for simulations of atomistic spin dynamics at finite temperatures. Following up on their study of static behaviour, Chen *et al.* [123] performed spin dynamics simulations on the Heisenberg model. At first, thermalized spin configurations were calculated in Monte Carlo simulations. In the subsequent spin dynamics simulations, no damping term was used. This being conservative dynamics, the energy of the spin system is preserved during the simulation. A motivation, for the choice not to include a damping term in the equation of motion, is that the dynamic structure factor $S(\mathbf{q}, \omega)$ typically is easier to sample in the absence of damping.

4.2 Atomistic spin dynamics at finite temperatures

At finite temperature, the atomic magnetic moments will be excerted not only to the deterministic precession torque and the damping torque connected to the effective field $\mathbf{B}_i$. In addition also stochastic torques will act on the atomic magnetic moments, due to presence of fluctuating moments. The stochastic torques can be included as fluctuating fields $\mathbf{B}_i^{\text{fl}}$ in the LL or LLG equations. As will be developed in this section, the power of fluctuating torques needs to be connected to the mechanisms for damping. That fluctuations and relaxations are intimitly connected is a very important result of equilibrium statistical physics that is expressed in the fluctuation-dissipation theorem [125, 126, 7].

The first investigations on how to include fluctuations in magnetization dynamics were undertaken by Brown [44] who let a stochastic torque contribute to both the precessional and the damping motion. To find out a relation between the strength of the fluctuating field and the rate of damping, he formulated the Fokker-Planck equation [127] for the stochastic version of the LLG equation. The result is an equation that couples the amplitude of the stochastic field $\mathbf{B}_i^{\text{fl}}$ to the damping parameter α and the temperature T. The size of the magnetic moment $\mathbf{m}_i$ and the gyromagnetic ratio γ also enters the expression. The relation is of a form similar to the relation between the fluctuating forces and the diffusion constant that Einstein derived in his theory of Brownian [1] motion [128]. Choosing to include the fluctuating fields only in the precession

[1] Named after the botanist Robert Brown who in the 19th century observed the seemingly random movements of pollen particles floating in water.

term, Kubo and Hashitsume [45] worked out a formalism similar to, but not identical to, Brown's expressions. Brown and Kubo were modelling single-domain magnetic particles and single spins respectively. It was proposed by Antropov *et al.* [41] that the same formalism is applicable to atomic magnetic moments.

In the original works [44, 45] restrictions were made to the specific situation of spins precessing in an axially symmetric potential. Garcia-Palacios *et al.* formulated the Fokker-Planck equation for a general system of spins. They eventually arrived to the same relations between the fluctuating fields and the rate of damping as Brown and Kubo, but had proven that the fluctuation-dissipation relation is applicable also in the general case of a system of interacting, or non-interacting, magnetic moments excerted to an external magnetic field.

4.3 Langevin dynamics

Including stochastic fields in both the precession term and the damping term, the stochastic Landau-Lifshitz (SLL) equation is written

$$\frac{d\mathbf{m}_i}{dt} = -\gamma \mathbf{m}_i \times [\mathbf{B}_i + \mathbf{B}_i^{\mathrm{fl}}(t)] - \gamma \frac{\alpha}{m} \mathbf{m}_i \times \{\mathbf{m}_i \times [\mathbf{B}_i + \mathbf{B}_i^{\mathrm{fl}}(t)]\}. \tag{4.1}$$

This can be classified as a Langevin equation with multiplicative noise introduced as Langevin forces [129]. The term multiplicative implies that the Langevin forces enter the equation with coefficients depending on the system variables. This indeed is the case for the SLL equation as $\mathbf{B}_i^{\mathrm{fl}}(t)$ is a noise term that occurs in a cross-product or double cross-product with the system variable $\mathbf{m}_i$. The Langevin equation, stochastic differential equations and many other aspects of stochastic processes in physics and chemistry are covered in the textbook of van Kampen [129]. As will be discussed later, for every Langevin equation there is an equivalent Fokker-Planck equation. The Fokker-Planck equation and techniques for how to solve it is discussed in detail in the monograph of Risken [127].

As the fluctuating fields are being caused by a large number of weakly coupled microscopic events they are because of the central limit theorem described by a Gaussian distribution. In principle the noise can be correlated both in ordinary space and in spin space. In the following it is assumed that the components $B_{i,\mu}^{\mathrm{fl}}$, with $\mu = \{x, y, z\}$, are uncorrelated and that the fluctuating field for different atomic magnetic moments $\mathbf{m}_i$ is uncorrelated. The autocorrelation function is denoted $f(t,s)$. Assuming also that the average of the fluctuation is zero, the two first moments of the fluctuating field are given by the expressions

$$\langle B_{i,\mu}^{\mathrm{fl}}(t) \rangle = 0, \quad \langle B_{i,\mu}^{\mathrm{fl}}(t) B_{j,\nu}^{\mathrm{fl}}(s) \rangle = 2D\delta_{\mu\nu}\delta_{ij} f(t,s). \tag{4.2}$$

Physical process that are stationary can be described with an autocorrelation function $f(t-s,0) \rightarrow f(t')$ that depends only on the difference of the time arguments. A short, but finite, correlation in time can be modelled for example by expontially correlated coloured noise [130],

$$\langle B^{\mathrm{fl}}_{i,\mu}(t)\rangle = 0, \quad \langle B^{\mathrm{fl}}_{i,\mu}(t) B^{\mathrm{fl}}_{j,\nu}(s)\rangle = \frac{b^2}{2a} exp^{(-a|t-s|)}. \tag{4.3}$$

Fluctuations that have finite correlation time are characterized by a noise power that depends on frequency. This can be infered through the Wiener-Khintchine theorem which states that the power spectrum of a stationary fluctuating process can be calculated as the Fourier transform of the autocorrelation function

$$S(\omega) \quad = \quad \int_{-\infty}^{\infty} f(t') e^{i\omega t'}\, dt'. \tag{4.4}$$

If the stochastic process is very fast in comparison to the deterministic part of the motion, the autocorrelation function is often approximated as the product $f(t') = q\delta(t')$ of an amplitude q and a Dirac δ-function. Actual physical processes always have a finite correlation time, and are never completely stationary. In that regard the assumption of a stationary process with zero correlation time is a strong approximation. That noise with zero correlation time has a flat power spectra, completely lacking a dependence of frequency, is easily shown

$$\begin{aligned} S(\omega) &= \int_{-\infty}^{\infty} q\delta(t') e^{i\omega t'}\, dt' \\ &= 2q. \end{aligned} \tag{4.5}$$

This kind of noise is called white noise, as it has the same power for all frequencies. For the reason that coloured noise is more difficult to handle mathematically than white noise, the assumption of noise with zero correlation time is often used in description of fluctuations in physical systems. The Langevin forces that play a role in atomistic spin dynamics are caused by microscopic events that can have a bandwith with finite power as high up in frequencies as 10^{13} Hz. The shortest time scale in atomistic spin dynamics is given by the precession of individual atomic moments in their exchange fields. These frequencies can be very high. The exchange field can for bcc Fe be of the order of 1000 T, corresponding to frequencies of the order 30 THz. This circumstance potentially render the approximation of white noise inappropriate. In practice, many practitioners of atomistic spin dynamics are using white noise. Three observations should here be stated: The first is that whereas the precession in the exchange field is very high in frequency, the precession of the average magnetic moment in anisotropy and applied magnetic fields are typically orders of magnitude lower. The second observation is that white noise, with the power prescribed by the appropriate fluctation dissipation relation, is

good enough to ensure that the system of magnetic moment will evolve towards the Boltzmann distribution. The third observation is based on the fact that in the limit of low damping α, the damping and fluctuating part of the motion can be regarded as a weak perturbation to the deterministic precessional motion. This circumstance inspires a, somewhat speculative, assertion that the influence of an imprecise treatment of the correlation time of the noise matters less in the case of weak damping than in the case of stronger damping. Finally, these observations do by no means imply that investigations, on how the possible breakdown of the white noise assumption can affect the validity of simulations, are not motivated. Rather, they can give a hint on why a white noise Langevin dynamics approach *seems* to work fine for atomistic spin dynamics. Ultimately, the question is something that needs to be clarified in a collaborative effort between theory and experiment.

For the results presented in this Thesis, all the data from atomistic spin dynamics simulations were obtained in simulations where the standard Gaussian white noise was used. A Gaussian distribution can be specified uniquely by its two first moments and a complete expression of the fluctuating field is given by the expressions

$$\langle B^{\mathrm{fl}}_{i,\mu}(t)\rangle = 0, \quad \langle B^{\mathrm{fl}}_{i,\mu}(t)B^{\mathrm{fl}}_{j,\nu}(s)\rangle = 2D\delta_{\mu\nu}\delta_{ij}\delta(t-s). \tag{4.6}$$

The first moment, $\langle B^{\mathrm{fl}}_{i,\mu}(t)\rangle = 0$, is the average value of the stochastic process and the second moment, $\langle B^{\mathrm{fl}}_{i,\mu}(t)B^{\mathrm{fl}}_{j,\nu}(s)\rangle$, is its variance.

4.4 Stochastic differential equations

Introducing the Einstein convention, with summation over repeated indices without writing the summation sign, the general form of a multidimensional Langevin equation is written

$$\frac{\partial X_i}{\partial t} = h_i(\{X\},t) + g_{ij}(\{X\},t)\Gamma_j(t). \tag{4.7}$$

$$\tag{4.8}$$

This is a stochastic differential equation (SDE) of the Ito form. The first term, $h_i(\{X\},t)$ accounts for the *deterministic drift*, the second term represents *stochastic diffusion*. To solve a SDE, the techniques for solving ordinary differential equations (ODE) must be extended with techniques for stochastic processes. The reason is that the integral forms of SDEs are not directly integrable in the standard Riemann or Lebesgue sense. The problem occurs in the second term which contains the Langevin force $\Gamma_j(t)$, which is not a continuous function, but a stochastic variable. In the following, small letters denote specific values taken by the stochastic variables. Stating the Ito SDE in

integral equation form,

$$X_i(t+\tau) \quad = \quad x_i(t) + \int_t^{t+\tau} h_i(\{X(t')\},t')dt' + \int_t^{t+\tau} g_{ij}(\{X(t')\},t')\Gamma_j(t')dt', \tag{4.9}$$

the way forward is to replace the integral including the stochastic variable $\Gamma_j(t')$ with an integral containing the increment $dW_j(t') = \int_0^\tau \Gamma_j(t')dt'$. This transforms the second integral into a Riemann-Stiltjes integral,

$$X_i(t+\tau) \quad = \quad x_i(t) + \int_t^{t+\tau} h_i(\{X(t')\},t')dt' + \int_t^{t+\tau} g_{ij}(\{X(t')\},t')dW_j(t'). \tag{4.10}$$

The distribution of the increment $dW_j(t')$ has the same form as the distribution of the Langevin force. In the case of the Gaussian white noise in Eq. 4.6, the moments of $dW_j(t')$ are given by

$$\langle dW_{i,\mu}\rangle = 0, \quad \langle dW_{i,\mu}dW_{j,\nu}\rangle = 2D\tau\delta_{\mu\nu}\delta_{ij}. \tag{4.11}$$

The integral form of the SDE is still not a uniquely defined expression as the stochastic calculus requires a prescription on how the second integral should be evaluated. In informal wording, it must be specified for which times t', and with which weights, the term $g_{ij}(\{X(t')\},t')$ should be multiplied with the increment $dW_j(t')$. Stochastic integrals can be calculated as the mean square limit of a sum over n terms with $n \to \infty$. In the notation of Kloeden [131], with w denoting specific values of the stochastic variable W, the expression for the integral is

$$\begin{aligned} & (\lambda)\int_0^T f(t,w)\, dW_t(w) \qquad (4.12)\\ = \quad & \lim_{n\to\infty}\sum_{j=1}^{n}\left\{(1-\lambda)f\left(t_j^{(n)},w\right)+\lambda)f\left(t_{j+1}^{(n)},w\right)\right\}\left\{W_{t_{j+1}^{(n)}}(w)-W_{t_j^{(n)}}(w)\right\}. \end{aligned}$$

with evaluation points $t_j^{(n)}$ for partitions $0 = t_1^{(n)} < t_1^{(n)} < \cdots < t_{n+1}^{(n)} < T$ for which

$$\delta^{(n)} = \max_{1\le j\le n}\left(t_{j+1}^{(n)} - t_j^{(n)}\right) \to 0 \text{ when} \qquad n \to \infty. \tag{4.13}$$

The parameter λ specifies where in the interval $\left[t_j^{(n)}, t_{j+1}^{(n)}\right]$ the integrand should be evaluated. The two common choices for the stochastic integral are the Ito and Stratonovich integrals. The Ito integral is defined by the choice $\lambda = 0$, the Stratanovich integral by the choice $\lambda = 1/2$. For Langevin equations of the form of Eq. 4.7, it is often, but not always, the Stratonovich calculus that gives the solution that is related to a physical process [129, 131].

Both definitions are remniscent to the standard Riemann integral in so far they are the $n \to \infty$ limit of a sum of n terms. In the Ito integral, only the value $f\left(t_j^{(n)}, w\right)$ of the integrand is included. In the Stratonovich integral also the value $f\left(t_{j+1}^{(n)}, w\right)$ is used, with the values at $t_j^{(n)}$ and $t_{j+1}^{(n)}$ contributing with equal weight. In terms of a physical process, the Ito definition describes the situation where the stochastic contribution during the time interval $\left[t_{j+1}^{(n)}, t_j^{(n)}\right]$ does not affect the deterministic contribution during the same time interval. For many physical processes it is more appropriate to use the Stratonovich calculus. Here the stochastic contribution for the time interval $\left[t_j^{(n)}, t_{j+1}^{(n)}\right]$ does affect the deterministic contribution for the same time interval. At an intermediate time $\tilde{t}$, with $t_j^{(n)} < \tilde{t} < t_{j+1}^{(n)}$, the system variable $x_{\tilde{t}}$ can have a different value in the presence of the stochastic force than it would have had in the absence of the stochastic force. The deterministic evolution of the system variable from time $\tilde{t}$ and onwards depend on the value $x_{\tilde{t}}$ and its clear that the presence of a stochastic force can affect the deterministic evolution. This contribution to the otherwise deterministic drift term is called noise-induced drift, or alternatively, spurious noise. The calculation of the noise-induced drift is not trivial but is well described in textbooks on stochastic calculus [127, 131]. The final expressions for the drift coefficient with noise-induced drift included, $D_{ij}(\{x\},t)$, and the diffusion coefficient $D_{ij}(\{x\},t)$ of the multidimensional Langevin equation are written

$$D_i(\{x\},t) = h_i(\{x\},t) + g_{kj}(\{x\},t)\frac{\partial g_{ij}(\{x\},t)}{\partial x_k}, \tag{4.14}$$

$$D_{ij}(\{x\},t) = g_{ik}(\{x\},t)g_{jk}(\{x\},t). \tag{4.15}$$

It turns out that the Stratonovich integral, by construction, takes account for the noise-induced drift. This implies that the integrands can be used as they are with no explicit addition of a noise-induced part to the drift coefficient. It can be shown [115] that for the SLL with Gaussian white noise, the Ito calculus gives a solution that fails to reproduce the Boltzmann distribution for the energies of the magnetic moments in the effective field. Instead the Stratonovich definition of the stochastic integral should be used. The expressions for the drift coefficient with noise-induced drift and the diffusion constant are still useful as they will be used in the Fokker-Planck equation.

4.5 Finite difference approximations to SDEs

The schemes that are used to solve ordinary differential equations (ODE) can be extended to be applicable to the case of stochastic differential equations.

In the following the solvers Euler and Heun will be discussed. These are both Runge-Kutta type explicit schemes where time is discretized $t_0 < t_1 < t_2 < \ldots < t_n$ and the solutions are obtained as sequences $x_0 < x_1 < x_2 < \ldots < x_n$. There are also semi-implicit and implicit schemes that have some attractive properties for the LL equation, as will be commented in section 4.9. It is important to ensure that the stochastic counterpart to an ODE solver gives a solution that converges to the kind of stochastic calculues that has been chosen to apply to the SDE that is investigated. The properties of an ODE scheme can be analysed in terms of the order of the local (one step) and the global (after n steps) discretization error [131]. The corresponding analyses of the local and global properties of an SDE is more involved and concepts as convergence in the quadratic mean, weak convergence, strong convergence are introduced [131].The stochastic extension of the Euler scheme for ODE is given as

$$x_i(t+\tau) = x_i(t) + A_i(\{x\},t)\tau + \sum_k B_{ik}(\{y\},t)dW_k, \tag{4.16}$$

where τ is the time step and the moments of the stochastic increments are given by Eq. 4.11. To obtain the value $x_i(t+\tau)$, the Euler scheme uses only the value of $x_i(t)$ at a time t_i. By comparing with the definition of the Stratonovich and the Ito integrals, it seems that the Euler scheme corresponds to the solution given by the Ito integral, as the definition of the Ito integral uses the value of the integrand only at $\left(t_j^{(n)}\right)$. In can indeed be proved [132, 133] that the Euler solution converges to the Ito integral in the quadratic mean. The Euler scheme can still be used to obtain the numerical solution in the Stratonovich sense. This is achieved by explicitly adding the noise-induced drift to the SDE which then takes the form of a Stratonovich SDE [131]. The Euler scheme that converges in the quadratic mean to the Stratonovich solution can then be written

$$x_i(t+\tau) = x_i(t) + D_i(\{x\},t)\tau + D_{ij}(\{x\},t)dW_k. \tag{4.17}$$

The stochastic extension of the Heun scheme,

$$x_i(t+\tau) = x_i(t) + \frac{1}{2}[A_i(\{\tilde{x}\},t+\tau) + A_i(\{x\},t)]\tau \tag{4.18}$$

$$+\frac{1}{2}\sum_k [B_{ik}(\{\tilde{x}\},t+\tau) + B_{ik}(\{x\},t)]dW_k, \tag{4.19}$$

where $\tilde{x}_i$ are Euler-type supporting values,

$$\tilde{x}_i(t+\tau) = x_i(t) + A_i(\{x\},t)\tau + \sum_k B_{ik}(\{x\},t)dW_k, \tag{4.20}$$

can be proved to converge to the Stratonovich integral. This means that one does not need to introduce the noise-induced drift term in the SDE equation, it

can be integrated as it stands in the form of an Ito equation. For this reason, and also the circumstance that yet higher order stochastic Runge-Kutta schemes not necessarily converge to a higher order [132], as would be the case for ODE:s, the stochastic Heun solver has among the explicit schemes been one of, or the most, popular solver. For simulations where the fluctuating noise is modelled with a finite correlation time, solvers developed for the case of coloured noise should be used [130].

4.6 The Fokker-Planck equation

A system described by a Langevin equation can also be described with a Fokker-Planck (FP) equation. The FP equation governs the time evolution of the probability distribution of the states, or transition probabilities, of the system [127]. The Fokker-Planck equation for the probability density $P(\{x\},t)$, is expressed in terms of the drift coefficient and the diffusion coefficient,

$$\frac{\partial P(\{x\},t)}{\partial t} = \left[-\frac{\partial}{\partial x_i}D_i(\{x\},t)+\frac{\partial}{\partial x_i x_j}D_{ij}(\{x\},t)\right]P(\{x\},t). \tag{4.21}$$

The drift coefficient and the diffusion coefficient are here the ones given by Eqs. 4.14,4.15. With the probability current $J(\{x\},t)$ defined by

$$J(\{x\},t) = \left[D_i(\{x\},t)-\frac{\partial}{\partial x_j}D_{ij}(\{x\},t)\right]P(\{x\},t), \tag{4.22}$$

the Fokker-Planck equation can be written on the form of a continuity equation for the probability density,

$$\frac{\partial P(\{x\},t)}{\partial t}+\frac{\partial J(\{x\},t)}{\partial x_i} = 0. \tag{4.23}$$

Inserting the expressions for the drift coefficient and the diffusion coefficient the resulting Fokker-Planck equation for the multidimensional Langevin equation is written

$$\begin{aligned}\frac{\partial P(\{x\},t)}{\partial t} = &-\frac{\partial}{\partial x_i}\left[h_i(\{x\},t)+g_{kj}(\{x\},t)\frac{\partial g_{ij}(\{x\},t)}{\partial x_k}\right.\\ &\left.-\frac{\partial}{\partial x_j}g_{ik}(\{x\},t)g_{jk}(\{x\},t)\right]P(\{x\},t).\end{aligned} \tag{4.24}$$

Following Garcia *et al.* [115], the terms of the FP equation are regrouped in a form of the equation that will be suitable for the SLL equation,

$$\begin{aligned}
&\frac{\partial P}{\partial t} \\
&= -\sum_i \frac{\partial}{\partial y_i}\left[\left(A_i + D\sum_{jk} B_{jk}\frac{\partial B_{ik}}{\partial y_j}\right)P\right] + \sum_{ij}\frac{\partial^2}{\partial y_i \partial y_j}\left[\left(D\sum_k B_{ik}B_{jk}\right)P\right] \\
&= -\sum_i \frac{\partial}{\partial y_i}\left\{\left[A_i - D\sum_k B_{ik}\left(\frac{\partial B_{jk}}{\partial y_j}\right) - D\sum_{jk} B_{ik}B_{jk}\frac{\partial}{\partial y_j}\right]P\right\}. \qquad (4.25)
\end{aligned}$$

4.7 The Fokker-Planck equation for the SLL equation

In dimensionless variables (See Chapter 5), the SLL equation is written

$$\frac{\partial \hat{\mathbf{e}}_i}{\partial \tau} = -\hat{\mathbf{e}}_i \times [\mathbf{b}_i + \mathbf{b}_i^{\mathrm{fl}}] - \alpha \hat{\mathbf{e}}_i \times (\hat{\mathbf{e}}_i \times [\mathbf{b}_i + \mathbf{b}_i^{\mathrm{fl}}]), \qquad (4.26)$$

with,

$$\langle b_{i,\mu}^{\mathrm{fl}}(t)\rangle = 0, \quad \langle b_{i,\mu}^{\mathrm{fl}}(t) b_{j,\nu}^{\mathrm{fl}}(s)\rangle = 2\tilde{D}\delta_{\mu\nu}\delta_{ij}\delta(t-s). \qquad (4.27)$$

Here the dimensionless noise power $\tilde{D}$ is not the same as the noise power D in Eq. 4.2 which has dimension (*magnetic field*)^2. To write the SLL equation on the form of a general Langevin equation, terms containing $\mathbf{b}_i$ and $\mathbf{b}_i^{\mathrm{fl}}$ are separated. Details are given in Appendix B. After simplifications the expressions are obtained as

$$\begin{aligned}
A_i(\hat{\mathbf{e}}, \tau) &= \sum_k [(\sum_j -\varepsilon_{ijk} e_j) - \alpha e_i e_k + \alpha \delta_{ik} e^2] b_k, \qquad (4.28) \\
B_{ik}(\hat{\mathbf{e}}, \tau) &= (\sum_j -\varepsilon_{ijk} e_j) - \alpha e_i e_k + \alpha \delta_{ik} e^2. \qquad (4.29)
\end{aligned}$$

The expressions for for A_i and B_{ik} can be substituted into three terms in the square brackets of the right hand side of the FP equation on the form of Eq. 4.25. The calculations are lengthy and given in full detail in Appendix B. Eventually the FP equation for the SLL equation, on the form of a continuity equation for the probability distribution, can be written

$$\frac{\partial P}{\partial \tau} = -\frac{\partial}{\partial \hat{\mathbf{e}}}\left\{\left[-\hat{\mathbf{e}} \times \mathbf{b} - \alpha \hat{\mathbf{e}} \times (\hat{\mathbf{e}} \times \mathbf{b}) + D(1+\alpha^2)\hat{\mathbf{e}} \times \left(\hat{\mathbf{e}} \times \frac{\partial}{\partial \hat{\mathbf{e}}}\right)\right] P\right\}. \qquad (4.30)$$

In equilibrium the time-derivative of the probability distribution P_0 should vanish, $\frac{\partial P_0}{\partial t} = 0$, and the probability distribution should be a Boltzmann distri-

bution, $P_0(\mathbf{m}) = e^{-\beta\mathscr{H}(\mathbf{m})}$, where $\beta = (k_B T)^{-1}$. The spatial derivative in the last term of the FP equation act on the probability distribution. Observing that $\mathbf{B} = -\frac{\partial\mathscr{H}(\mathbf{m})}{\partial\mathbf{m}}$, the derivative is swiftly calculated,

$$\frac{\partial P_0}{\partial \mathbf{m}} = \frac{\partial\left\{e^{-\beta\mathscr{H}(\mathbf{m})}\right\}}{\partial\mathbf{m}} = -\beta\frac{\partial\mathscr{H}(\mathbf{m})}{\partial\mathbf{m}}e^{-\beta\mathscr{H}(\mathbf{m})} = \beta\mathbf{B}P_0. \quad (4.31)$$

In terms of dimensionless variables, τ, m, $\hat{\mathbf{e}}$ and $\mathbf{b}$, the corresponding expressions are,

$$\begin{aligned}\frac{\partial P_0}{\partial\hat{\mathbf{e}}} &= 0,\\ \frac{\partial\mathscr{H}(\hat{\mathbf{e}})}{\partial\hat{\mathbf{e}}} &= \frac{\partial\mathscr{H}(\mathbf{m})}{\partial\mathbf{m}}\frac{\partial\mathbf{m}}{\partial\hat{\mathbf{e}}} = -\mu_B m B_0\mathbf{b}, \quad (4.32)\\ \frac{\partial P_0}{\partial\tau} &= \frac{\partial\left\{e^{-\beta\mathscr{H}(\hat{\mathbf{e}})}\right\}}{\partial\hat{\mathbf{e}}} = -\beta\frac{\partial\mathscr{H}(\hat{\mathbf{e}})}{\partial\hat{\mathbf{e}}}e^{-\beta\mathscr{H}(\hat{\mathbf{e}})} = \beta\mu_B m B_0\mathbf{b}P_0.\end{aligned}$$

The last equation is inserted into the FP equation, resulting in an equation from which it is possible to extract the relation between $\tilde{D}$, α and T that is required for thermodynamic consistency,

$$\begin{aligned}&\frac{\partial P_0}{\partial\tau} \quad (4.33)\\ &= -\frac{\partial}{\partial\hat{\mathbf{e}}}\left\{\left[-\hat{\mathbf{e}}\times\mathbf{B} - \alpha\hat{\mathbf{e}}\times(\hat{\mathbf{e}}\times\mathbf{B}) + \tilde{D}(1+\alpha^2)\beta\mu_B m B_0\hat{\mathbf{e}}\times(\hat{\mathbf{e}}\times\mathbf{B})\right]P_0\right\}.\end{aligned}$$

The first term is divergence-less, hence the derivative of the probability distribution will vanish when

$$\alpha = \tilde{D}(1+\alpha^2)\beta\mu_B m_i B_0. \quad (4.34)$$

Solving for $\tilde{D}$ and substituting for β gives the relation

$$\tilde{D} = \frac{\alpha}{1+\alpha^2}\frac{k_B T}{\mu_B m B_0}. \quad (4.35)$$

This equation is the Einstein type fluctuation dissipation relation for the SLL equation. The noise power, $\tilde{D}$, turns out to be frequency independent, precisely as the Wiener-Khintchine theorem had already revealed. Observing that m is in the denominator, it follows that large magnetic moments are less susceptible to fluctuations than small magnetic moments. The derivation above has been the traditional one, involving the FP equation. The fluctuation dissipation relation Eq. 4.35 can also be derived without calculating the terms of the Fokker-Planck equation. The suggested starting point is here to use linear response and a general formulation of the fluctuation dissipation theorem [126].

This approach is more general and in that regard a better choice, in particular if a fluctuation dissipation relation for coloured noise is required.

4.8 Relation between the LL and the LLG equations

The Landau-Lifshitz (LL) (Eq. 3.41) and the Landau-Lifshitz-Gilbert (LLG) (Eq. 3.42) equations, are closely related. In the case of isotropic damping they are identical if a renormalized gyromagnetic ratio is introduced. This will be shown below. That the LL and the LLG equations are not identical in the case of anisotropic damping is discussed by Steiauf *et al.* [134]. The precession torque and the damping torque, wether on the LL form or the Gilbert form, preserve the magnitude of the magnetization $\mathbf{m}$. This is easily proved by scalar multiplication with m, here for the LLG equation,

$$\begin{aligned}
\mathbf{m}\cdot\frac{\partial\mathbf{m}}{\partial t} &= -\gamma\mathbf{m}\cdot(\mathbf{m}\times\mathbf{B})+\frac{\alpha}{m}\mathbf{m}\cdot\left(\mathbf{m}\times\frac{\partial\mathbf{m}}{\partial t}\right)\\
&= \{\text{Use that } \mathbf{a}\cdot(\mathbf{b}\times\mathbf{c})=\mathbf{c}\cdot(\mathbf{a}\times\mathbf{b})\}\\
&= -\gamma\mathbf{B}\cdot(\mathbf{m}\times\mathbf{m})+\frac{\alpha}{m}\frac{\partial\mathbf{m}}{\partial t}\cdot(\mathbf{m}\times\mathbf{m})\\
&= 0. \qquad (4.36)
\end{aligned}$$

and observing that,

$$\frac{\partial\mathbf{m}^2}{\partial t} = 2\mathbf{m}\cdot\frac{\partial\mathbf{m}}{\partial t}=0. \qquad (4.37)$$

The proof for the LL equation is very similar. Starting from the LLG equation, the LL equation can be obtained after multiplication with $\mathbf{m}$ from the left,

$$\begin{aligned}
\mathbf{m}\times\frac{\partial\mathbf{m}}{\partial t} &= -\gamma\mathbf{m}\times(\mathbf{m}\times\mathbf{B})+\frac{\alpha}{m}\mathbf{m}\times(\mathbf{m}\times\frac{\partial\mathbf{m}}{\partial t}) \qquad (4.38)\\
&= -\gamma\mathbf{m}\times(\mathbf{m}\times\mathbf{B})+\frac{\alpha}{m}\left[\mathbf{m}(\mathbf{m}\cdot\frac{\partial\mathbf{m}}{\partial t}-\frac{\partial\mathbf{m}}{\partial t}(\mathbf{m}\cdot\mathbf{m})\right].
\end{aligned}$$

Using now the relation $\mathbf{m}\cdot\frac{\partial\mathbf{m}}{\partial t}=0$, which was derived above,

$$\mathbf{m}\times\frac{\partial\mathbf{m}}{\partial t} = -\gamma\mathbf{m}\times(\mathbf{m}\times\mathbf{B})-\alpha m\frac{\partial\mathbf{m}}{\partial t}. \qquad (4.39)$$

This is substituted into the right hand side of the LLG equation,

$$\begin{aligned}
\frac{\partial\mathbf{m}}{\partial t} &= -\gamma\mathbf{m}\times\mathbf{B}-\frac{\alpha}{m}\left[\gamma\mathbf{m}\times(\mathbf{m}\times\mathbf{B})+\alpha m\frac{\partial\mathbf{m}}{\partial t}\right]\\
&= -\gamma\mathbf{m}\times\mathbf{B}-\frac{\alpha}{m}\gamma\mathbf{m}\times(\mathbf{m}\times\mathbf{B})-\alpha^2 m\frac{\partial\mathbf{m}}{\partial t}. \qquad (4.40)
\end{aligned}$$

The terms containing $\frac{\partial \mathbf{m}}{\partial t}$ are collected on the left to give,

$$\begin{aligned}(1+\alpha^2)\frac{\partial \mathbf{m}}{\partial t} &= -\gamma \mathbf{m}\times\mathbf{B} - \frac{\alpha}{m}\gamma\mathbf{m}\times(\mathbf{m}\times\mathbf{B}), \qquad (4.41)\\ \frac{\partial \mathbf{m}}{\partial t} &= -\frac{\gamma}{(1+\alpha^2)}\mathbf{m}\times\mathbf{B} - \frac{\alpha}{(1+\alpha^2)m}\gamma\mathbf{m}\times(\mathbf{m}\times\mathbf{B}),\end{aligned}$$

on the LL form with the relaxation expressed as a double cross product. Defining an effective gyromagnetic ratio γ_L and expressing the LL relaxation parameter λ in units of the Gilbert damping parameter α,

$$\gamma_L = \frac{\gamma}{(1+\alpha^2)}, \qquad (4.42)$$

$$\lambda_L = \frac{\gamma\alpha}{(1+\alpha^2)} = \gamma_L\alpha, \qquad (4.43)$$

the LL equation can be written,

$$\frac{\partial \mathbf{m}}{\partial t} = -\gamma_L \mathbf{m}\times\mathbf{B} - \gamma_L\frac{\alpha}{m}\mathbf{m}\times(\mathbf{m}\times\mathbf{B}). \qquad (4.44)$$

This expression is known as the LL equation in the Gilbert form. For isotropic damping, the LL and the LLG equation differs only in the regard that $\gamma_L \neq \gamma$. A common practice, that will be used in the remaining of the Thesis, is to use the LL equation but specify the damping as a Gilbert damping parameter α. In the limit of vanishing damping, $\alpha \to 0$, the gyromagnetic ratios become equal, $\gamma_L \to \gamma$. In studies of dynamics in the presence of a time-dependent external field, it is important that the correct gyromagnetic ratio γ_L is used during the simulation. In other cases it is also possible to rescale the time after the simulation, corresponding to a different gyromagnetic ratio.

4.9 Conservation properties of the LL equation

The pure precessional motion of magnetic moments is conservative dynamics where the total energy of the magnetic system is preserved. Energy can however be transfered within the magnetic system. The precession torque of the LL equation can be derived from a classical spin Hamiltonian through Hamilton's equations

$$i\hbar\frac{d\hat{A}}{dt} = [[\hat{A},\mathscr{H}]] = i\{A,\mathscr{H}\}. \qquad (4.45)$$

Here the classical analogue $[[,]]$ of the quantum mechanical commutator $[,]$ is defined by a Poisson bracket $\{,\}$ multiplied with i. To calculate the Poisson

brackets [94] for classical spins one can use Mermin's formula [135],

$$[[A,B]] = i\sum_j \mathbf{m}\cdot\frac{\partial A}{\partial \mathbf{m}_j}\times\frac{\partial B}{\partial \mathbf{m}_j}. \tag{4.46}$$

The time derivative of different parts of the magnetic energy can be calculated from the commutator of $\mathscr{H}_p$ and the total magnetic Hamiltonian,

$$\frac{d\mathscr{H}_p}{dt} = -\frac{i}{\hbar}[[\mathscr{H}_p,\mathscr{H}_{\text{iex}}+\mathscr{H}_{\text{ma}}+\mathscr{H}_{\text{dd}}+\mathscr{H}_{\text{ext}}]]. \tag{4.47}$$

Consider now magnetic systems where two out the four terms in the Hamiltonian are present. Calculating the commutator for pairs of different terms in the parametrized magnetic Hamiltonian Eq. 3.39 gives insight in how energy can be transfered within the magnetic system [136]. The discussion will here be limited to the case of magnetic systems where all atomic magnetic moments have the same gyromagnetic ratio. The commutator of the (Heisenberg part of the) interatomic exchange energy and the Zeeman energy is always zero,

$$\begin{aligned}
[[\mathscr{H}_{iex},\mathscr{H}_{ext}]] &= i\sum_j \mathbf{m}\cdot\frac{\partial\mathscr{H}_{iex}}{\partial\mathbf{m}_j}\times\frac{\partial\mathscr{H}_{ext}}{\partial\mathbf{m}_j}\\
&= i\sum_j \mathbf{m}_j\cdot\left(\sum_i J_{ij}\mathbf{m}_i\times\mathbf{B}_{ext}\right)\\
&= i\sum_{ij} J_{ij}\mathbf{m}_j\cdot(\mathbf{m}_i\times\mathbf{B}_{ext})\\
&= i\sum_{ij} J_{ij}\mathbf{B}_{ext}\cdot(\mathbf{m}_j\times\mathbf{m}_i) = \{J_{ii}=0\}\\
&= i\sum_{i\neq j} J_{ij}\mathbf{B}_{ext}\cdot(\mathbf{m}_j\times\mathbf{m}_i) = \{J_{ij}=J_{ji}\}\\
&= i\sum_{i<j} J_{ij}\mathbf{B}_{ext}\cdot(\mathbf{m}_j\times\mathbf{m}_i+\mathbf{m}_i\times\mathbf{m}_j)\\
&= 0.
\end{aligned} \tag{4.48}$$

This has the important implication that the total exchange energy of the system cannot be changed directly by an external magnetic field. All magnetic moments precess with the same frequency around the external magnetic field with all angles between the moments left unchanged. The commutator between Heisenberg exchange energy and the magnetocrystalline anistropy is

calculated as

$$
\begin{aligned}
[[\mathscr{H}_{iex},\mathscr{H}_{ext}]] &= i\sum_j \mathbf{m}\cdot\frac{\partial\mathscr{H}_{iex}}{\partial\mathbf{m}_j}\times\frac{\partial\mathscr{H}_{ani}}{\partial\mathbf{m}_j} \\
&= -i\sum_j \mathbf{m}_j\cdot\left(\sum_i J_{ij}\mathbf{m}_i\times\frac{\partial\mathscr{H}_{ani}}{\partial\mathbf{m}_j}\right) \\
&= -i\sum_{i\neq j} J_{ij}\mathbf{m}_j\cdot\left(\mathbf{m}_i\times\frac{\partial\mathscr{H}_{ani}}{\partial\mathbf{m}_j}\right) \\
&= i\sum_{i\neq j} J_{ij}\frac{\partial\mathscr{H}_{ani}}{\partial\mathbf{m}_j}\cdot(\mathbf{m}_i\times\mathbf{m}_j) \\
&= i\sum_{i<j} J_{ij}\left[\frac{\partial\mathscr{H}_{ani}}{\partial\mathbf{m}_j}\cdot(\mathbf{m}_i\times\mathbf{m}_j)+\frac{\partial\mathscr{H}_{ani}}{\partial\mathbf{m}_i}\cdot(\mathbf{m}_i\times\mathbf{m}_j)\right] \\
&= i\sum_{i<j} J_{ij}\left[\frac{\partial\mathscr{H}_{ani}}{\partial\mathbf{m}_j}-\frac{\partial\mathscr{H}_{ani}}{\partial\mathbf{m}_i}\right]\cdot(\mathbf{m}_j\times\mathbf{m}_i)\,, \qquad (4.49)
\end{aligned}
$$

which in general is not zero. This implies that energy can be transfered from (to) magnetocrystalline anisotropy energy to (from) exchange energy also in the case of conservative dynamics. The transfer of energy is accompanimented by a transfer of angular momentum. It is the spin orbit coupling that enables a transfer of energy and angular momentum from magnetocrystalline energy to exchange energy. In the case that magnetocrystalline anisotropy energy and an external field are present at the same time, energy can be transfered directly between magnetocrystalline anisotropy energy and Zeeman energy if the applied field is not parallel with the anisotropy axis. Magnetocrystalline anisotropy energy and exchange energy can also be transfered into eachother via exchange energy.

Similarily, energy can flow between magnetostatic energy and exchange energy. Also in this case, the transfer of energy is accompanimented by a transfer of angular momentum. The magnetostatic interaction energy is governed by Maxwell's equations and do not depend on spin orbit coupling. The coupling between spin space and ordinary space is here possible due to the solenoidal nature of the magnetic field lines. This is manifest in that the coordinates of the magnetic atoms show up in the expression for the magnetostatic dipole-dipole energy.

The flow of energy within a conservative magnetic system can be vizualized as a graph with four vertices, all mutually connecte by in total six edges. Out of the six energy channels, some channels are always closed (e.g. exchange energy $\leftrightarrow$ Zeeman energy), whereas some of the others can be opened or closed depending on geometry, interactions and the magnetic configuration at an instant of time. If all the four energy types are connected, directly or over the other sorts of energy, the amount of energy of different types, will evolve

over time, reflecting the nature of how the magnetic moments precess. This evolution in time of the energies can be sampled during numerical simulations. The measure is an important part of the μ-mag problem 4, a benchmark problem for numerical solutions of the LL(G) equation [137]. The energies are also sampled in studies of spin wave instabilities as in Paper V and in Ref. [136].

Next the conservation properties for angular momentum are investigated. Also here the dissipationless $\alpha = 0$ dynamics is the starting point. If the magnetic Hamiltonian only includes isotropic exchange interactions, the total angular momentum is a conserved property as no external torque acts on the system. In precession in an external field the total angular momentum associated with the magnetic moments also precess. This is the essence of gyroscopic precession, angular momentum precess with the tangent vector for the motion of the tip of the angular momentum vector parallel to the applied torque. Obviously the total angular momentum is here not a preserved quantity, however, the projection of the angular momentum in the direction of the applied field is a constant of motion. Examples on how the conservation properties for angular momentum can be used to asses the performance of different SDE solvers for the SLL equation can be found in Mentink *et al.* [138].

To conclude this section on the conservation properties of energy and angular momentum, three different cases of spin dynamics will be listed:

- $\alpha = 0 \rightarrow T = 0$: Conservative dynamics. The energy of the magnetic systems is preserved, also in the presence of an external field. No direct channel for transfer between Zeeman energy and exchange energy. A direct channel between anisotropy energy and exchange energy is possible. See examples in paper V on spin wave instabilities.
- $\alpha \geq 0, T = 0$: Dissipative dynamics. Energy is transfered out from the magnetic system. The dynamics have a Lyapunov structure, which means that in the case that the external magnetic field does not depend on time, the free energy is monotonously decreasing [137]. Dissipative dynamics without a heatbath is the standard in micromagnetics simulations, but it is becoming more and more common that heatbaths are included in micromagnetics simulations.
- $\alpha \geq 0, T \geq 0$: Dissipative dynamics in the presence of a heat bath, canonical ensemble. This is the standard in atomistic spin dynamics. Averaging over heat baths is essential, as the finite size of the simulation cells make the evolution of the spin system sensitive to random-walk like drift of the total angular momentum.

For small α the dynamics, in some sense for zero temperature, but particularily for finite temperatures can be regarded as a perturbation to $\alpha = 0$ dynamics. This is important to keep in mind, when analyzing and choosing SDE solvers. For further reading, the monograph of Bertotti *et al.* [116], concentrating on ferromagnets, is a comprehensive description of the rich flora of the dynamics and solutions that the LL equation give rise to for different geome-

tries, anisotropies, driving fields and materials properties. The monograph of Gurevihvc and Melkov [25], on magnetic oscillations and waves, covers the dynamics of antiferromagnets and ferrimagnets.

4.10 The choice of SDE solver

The conservation properties for $\alpha = 0$ spin dynamics, should be respected as carefully as possible in numerical simulations, for the case of zero as well as finite damping. It is well known that explicit solvers as Euler and Heun fail to preserve the size of the individual magnetic moments. In implementations of the Heun scheme for atomistic spin dynamics, an additional projection step is needed, where the length of each spin is normalized. Furthermore, Heun does not preserve the total angular momentum. Implicit and semi-implicit schemes are better suited to respect the conservation properties of the LL equation. In the case of finite temperature it is also important that the schemes converge to the Stratonovich solution of the Langevin equations. An overview of different solvers will not be given here, but can be found in detail in recent papers, where also new solvers have been proposed. d'Aquino *et al.* have developed a scheme for geometrical integration of the LLG equation based on the midpoint rule [137] and a midpoint numerical technique for stochastic LLG dynamics [139]. Mentink *et al.* [138] have recently developed a semi-implicit scheme for the SLL equation, a scheme sharing the conservation qualities known from implicit solvers, with the lower computational effort known from explicit solvers.

4.11 Recent developments

The Langevin dynamics approach requires the temperature of the heatbath for the magnetic system to be specified. Phenomenological three-temperature models with a magnetic, an electronic and a lattice heat reservoir were used in the early experiments on ultrafast demagnetization [110]. The flow of heat between the reservoirs is modelled in terms of heat capacities of dissipation rates [140]. In Paper I, it is described how a two-temperature model can be incorporated for the SLL equation, and how simulations with two heatbaths compare with experiments. Recently, a method for how to measure the emperature for a dynamic spin ensemble was proposed by Ma *et al.* [141]. Another recent development is a method to model fluctuations with finite correlation time proposed by Atxitia *et al.* [142].

For simulations of larger magnetic samples, the atomistic spin dynamics method becomes computationally very expensive. To tackle this dilemma, schemes for multiscale modelling have been suggested. The Landau-Lifshitz-Bloch (LLB) equation, at first formulated for magnetic

nanoparticles by Garanin *et al.* [143], and later generalised to systems of interacting magnetic moments [144], is an alternative approach. The magnetic system is here characterized by longitudinal and transversal relaxation times and susceptibilities. Kazantseva *et al.* [145] developed a two-step scheme, where at first atomistic spin dynamics simulations are used to calculate the relaxation times and susceptibilities for a magnetic material. In the second step the LLB equation can be used to investigate magnetization on a larger length scale, e.g. domain wall motion and ultrafast switching. In Ref. [145] simulations using multiple LLB macrospins were performed to investigate the relaxation of FePt, in applied field and also impact of a heat pulse. Recently the multiple macrospin formulation was used to simulate how the magnetization switches [146] in the groundbreaking all-optical magnetization switching experiments [147, 114].

5. Implementation and examples

The atomistic spin dynamics simulations, for which results are presented in this Thesis, have all been performed with the UppASD program [164]. The implementation and the functionality of the program as of the year 2008 is described in detail in Paper I. The present chapter serve to complement Paper I and emphasizes new developments. In the first section, full details on the expressions for the SLL equation, the Hamiltonian and the effective field in dimensionless quantities are given. In the section on measurement, some comments on how to sample correlation functions are given. Information on the UppASD program is also given in Appendix A.

5.1 Dimensionless and normalized SLL equation

The terms on the left and right hand side of the SLL equation have dimension *energy/(magnetic field · time)* and, using the SI-system, are in units of J/Ts. This follows since the magnetic moments are in Bohr magnetons with dimension *energy/magnetic field* and are in units of J/T, the magnetic field is in units of T and the gyromagnetic ratio with dimension *1/(magnetic field · time)* is in units of 1/Ts.

The atomic magnetic moments $\mathbf{m}_i$ can be expressed as a product $\mathbf{m}_i = \mu_B m_i \hat{\mathbf{e}}_i$ where $m_i = \frac{|\mathbf{m}_i|}{\mu_B}$ are the sizes of the moments in multiples of Bohr magnetons, and $\hat{\mathbf{e}}_i = \frac{\mathbf{m}_i}{\mu_B m_i}$ is the directions represented by unit vectors. Note that in this notation $|\mathbf{m}_i| \neq m_i$ but $|\mathbf{m}_i| = \mu_B m_i$. A transformation of the SLL equation into a set of dimension-less equations can now be done as follows: A magnetic reference field strength B_0 is introduced with the dimensionsless magnetic field $\mathbf{b}$ defined as $\mathbf{B} = B_0\mathbf{b}$. Together with the gyromagnetic ratio, the reference field strength provides a dimensionless rescaled time $\tau = \gamma B_0 t$. The size of the reference magnetic field B_0 is arbitrary. With the unitary value, $B_0 = 1$ T, the conversion factor $(\gamma B_0)^{-1} = 5.7$ ps, so that one unit of dimensionless time $\Delta\tau = 1$ corresponds to $\Delta t = 5.7$ ps. Alternatively, it is also possible to express time and temperature in terms of the exchange parameter(s) J. This is common practice in spin dynamics simulations on model Hamiltonians. The conversion to and from dimension-less variables is presented in Table 5.1. The time derivative of the magnetization with regard to τ is calculated

Table 5.1: *Relations between the dimensionless variables and the original variables.*

$$\begin{aligned} \hat{\mathbf{e}}_i &= \frac{\mathbf{m}_i}{\mu_B m_i} & \qquad \mathbf{m}_i &= \mu_B m_i \hat{\mathbf{e}}_i \\ \mathbf{b}_i &= \frac{\mathbf{B}_i}{B_0} & \qquad \mathbf{B}_i &= B_0 \mathbf{b}_i \\ \tau &= \gamma B_0 t. & \qquad t &= \frac{1}{\gamma B_0}\tau. \end{aligned}$$

as

$$\frac{\partial \mathbf{m}_i}{\partial t} = \frac{\partial(\mu_B m_i \hat{\mathbf{e}}_i)}{\partial \tau}\frac{\partial \tau}{\partial t} = \gamma B_0 \mu_B m_i \frac{\partial \hat{\mathbf{e}}_i}{\partial \tau}. \tag{5.1}$$

Using this relation and dividing the SLL equation with $\gamma B_0 \mu_B m_i$,

$$\frac{1}{\gamma B_0 \mu_B m_i}\gamma B_0 m_i \frac{\partial \hat{\mathbf{e}}_i}{\partial \tau} = -\frac{\gamma}{\gamma B_0 \mu_B m_i} B_0 \mu_B m_i \hat{\mathbf{e}}_i \times \mathbf{b}_i \tag{5.2}$$

$$-\frac{\gamma\alpha}{\mu_B m_i}\frac{1}{\gamma B_0 \mu_B m_i} B_0 \mu_B^2 m_i^2 \hat{\mathbf{e}}_i \times (\hat{\mathbf{e}}_i \times \mathbf{b}_i), \tag{5.3}$$

the SLL equation on dimensionless form is written

$$\frac{\partial \hat{\mathbf{e}}_i}{\partial \tau} = -\hat{\mathbf{e}}_i \times \mathbf{b}_i - \alpha \hat{\mathbf{e}}_i \times (\hat{\mathbf{e}}_i \times \mathbf{b}_i). \tag{5.4}$$

A programmer can choose to have either $\{m_i e_i^x, m_i e_i^y m_i, e_i^z\}$ or $\{e_i^x, e_i^y, e_i^z\}$ as primary variables for the magnetic configuration. In an implementation of atomistic spin dynamics one can also work with spherical coordinates, with the well known problems around the poles, or use generalised coordinates, as in e.g. Ref. [136].

5.2 The effective magnetic field

The Heisenberg Hamiltonian can be formulated in slightly different but similar ways, depending on the choice to express it in terms of magnetic moments or unit vectors. Three different choices are

$$\mathscr{H}_{\text{iex}} = -\frac{1}{2}\sum_{i\neq j} J_{ij}\mathbf{m}_i \cdot \mathbf{m}_j \tag{5.5}$$

$$= -\frac{1}{2}\sum_{i\neq j} \tilde{J}_{ij}\hat{\mathbf{e}}_i \cdot \hat{\mathbf{e}}_j \tag{5.6}$$

$$= -\frac{1}{2}\sum_{i\neq j} J'_{ij} m_i m_j \hat{\mathbf{e}}_i \cdot \hat{\mathbf{e}}_j, \tag{5.7}$$

where the relations between J, $\tilde{J}$ and J' are $J'_{ij} = J_{ij}\mu_B^2$ and $\tilde{J} = J_{ij}\mu_B^2 m_i m_j$. It is common that electronic structure programs output exchange parameters where the sizes of the magnetic moments are included in the exchange parameters. The Heisenberg Hamiltonian is then expressed in unit vector spins. Using the notation above the exchange couplings are of the form $\tilde{J}_{ij}$ and have dimension *energy*. To describe magnetic systems with more than one type of magnetic moments it is convenient to work with exchange couplings of the form J'_{ij}. In an implementation of ASD one then reads $\tilde{J}_{ij}$-values and evaluate and store away J'_{ij}-values. These J'_{ij} are then the variables that are used in the subroutines that evaluate the effective fields. The Dzyaloshinskii-Moriya vectors $\mathbf{D}_{ij}$ are rescaled in the same way, $\mathbf{D}'_{ij} = \mathbf{D}_{ij}\mu_B^2$ and $\tilde{\mathbf{D}} = \mathbf{D}_{ij}\mu_B^2 m_i m_j$. The onsite anisotropy energy for each atomic magnetic moment depends only on the moment itself. When the anisotropy is calculated in an electronic structure program it is typically obtained as a function of the direction of the atomic moment with the size of the moment included in the anisotropy constant(s) $\tilde{K}$. This constant is what is necessary in the ASD program and there is no need for to also calculate a constant K'. Anisotropies measured in experiments are often reported in units of $\mathrm{J/m^3}$ and have to be converted to units of mRyd/atom. Expressed in unit vectors $\hat{\mathbf{e}}_i$, the moment sizes m_i and the parameters J', D' and $\tilde{K}$ the Hamiltonian takes the form

$$\begin{aligned}\mathscr{H}_{\text{magn}} &= -\frac{1}{2}\sum_{i\neq j} m_i m_j \left\{ J'_{ij}\hat{\mathbf{e}}_i\cdot\hat{\mathbf{e}}_j + \hat{\mathbf{e}}_i \mathscr{J}'^{S}_{ij}\hat{\mathbf{e}}_j + \mathbf{D}'_{ij}\cdot(\hat{\mathbf{e}}_i\times\hat{\mathbf{e}}_j)\right\} + \sum_i \tilde{K}(\hat{\mathbf{e}}_i) \\ &\quad -\frac{\mu_0}{8\pi}\sum_{i\neq j} m_i m_j \frac{3(\mathbf{R}_{ij}\cdot\hat{\mathbf{e}}_i)(\mathbf{R}_{ij}\cdot\hat{\mathbf{e}}_j) - R_{ij}^2(\hat{\mathbf{e}}_i\cdot\hat{\mathbf{e}}_j)}{R_{ij}^{-5}} - \mathbf{B}_{\text{ext}}\cdot\sum_i \mu_B m_i \hat{\mathbf{e}}_i.\end{aligned}$$

The Hamiltonian is not dimensionless, it has the dimension of energy. The effective magnetic field, in Tesla or in units of the reference field strength B_0 can be calculated from the Hamiltonian as,

$$\mathbf{B}_i = -\frac{\partial\mathscr{H}_{\text{magn}}}{\partial\mathbf{m}_i}, \qquad \text{(field in T)} \tag{5.8}$$

$$\mathbf{b}_i = -\frac{1}{\mu_B m_i B_0}\frac{\partial\mathscr{H}_{\text{magn}}}{\partial\hat{\mathbf{e}}_i}, \qquad \text{(dimensionless field)} \tag{5.9}$$

It is straightforward to calculate the contributions to the effective magnetic field one by one. The expressions will be given in form of the dimensionless

field. The exchange field $\mathbf{b}_{i,\mathrm{iex}}$ is calculated as

$$\begin{aligned}
\mathbf{b}_{i,\mathrm{iex}} &= -\frac{1}{\mu_B m_i B_0}\frac{\partial \mathscr{H}_{\mathrm{ex}}}{\partial \hat{\mathbf{e}}_i} = \frac{1}{2\mu_B m_i B_0}\sum_{i\neq j} J'_{ij} m_i m_j \frac{\partial[\hat{\mathbf{e}}_i\cdot\hat{\mathbf{e}}_i]}{\partial \hat{\mathbf{e}}_i} \\
&= \frac{1}{2\mu_B m_i B_0}\sum_{i\neq j} J'_{ij} m_i m_j \left(\frac{\partial}{\partial e_i^x},\frac{\partial}{\partial e_i^y},\frac{\partial}{\partial e_i^z}\right)\left(e_i^x e_j^x + e_i^y e_j^y + e_i^z e_j^z\right) \\
&= \frac{1}{2\mu_B m_i B_0}\sum_{i\neq j} J'_{ij} m_i m_j \left[\frac{\partial \hat{\mathbf{e}}_i}{\partial \hat{\mathbf{e}}_i}\hat{\mathbf{e}}_j + \hat{\mathbf{e}}_i\frac{\partial \hat{\mathbf{e}}_j}{\partial \hat{\mathbf{e}}_i}\right] \\
&= \frac{1}{2\mu_B m_i B_0}\sum_{i\neq j} J'_{ij} m_i m_j [\hat{\mathbf{e}}_j + \hat{\mathbf{e}}_i\delta_{ij}] = \{\text{summation is over } i\neq j\} \\
&= \frac{1}{2\mu_B m_i B_0}\sum_{i\neq j} J'_{ij} m_i m_j \hat{\mathbf{e}}_j = \{\text{note that } J_{ij}=J_{ji} \text{ and that } J_{ii}=0\} \\
&= \frac{1}{\mu_B B_0}\sum_j J'_{ij} m_j \hat{\mathbf{e}}_j. \qquad (5.10)
\end{aligned}$$

In order to calculate the expression for DM effective fields the scalar triple product is permuted, $\mathscr{H}_{\mathrm{DM}} = \frac{1}{2}\sum_{i\neq j} m_i m_j \hat{\mathbf{e}}_i\cdot(\mathbf{D}'_{ij}\times\hat{\mathbf{e}}_j)$ so that the effective field comes out immediately as

$$\mathbf{b}_{i,DM} = -\frac{1}{\mu_B B_0}\sum_j m_j \mathbf{D}'_{ij}\times\hat{\mathbf{e}}_j. \qquad (5.11)$$

In the case of easy axis anisotropy where K is negative, $\mathbf{b}_{i,\mathrm{ma}}$ the anisotropy field has the same direction as the projection of the local moment in the anisotropy axis,

$$\begin{aligned}
\mathbf{b}_{i,\mathrm{ma}} &= -\frac{1}{\mu_B m_i B_0}\frac{\partial \mathscr{H}_{\mathrm{ma}}}{\partial \hat{\mathbf{e}}_i} = -\frac{1}{\mu_B m_i B_0}K\sum_j \frac{\partial[(\hat{\mathbf{e}}_j\cdot\hat{\mathbf{e}}_K)^2]}{\partial \hat{\mathbf{e}}_j)} \qquad (5.12)\\
&= -\frac{1}{\mu_B m_i B_0}K\sum_j 2(\hat{\mathbf{e}}_j\cdot\hat{\mathbf{e}}_K)\hat{\mathbf{e}}_K\frac{\partial \hat{\mathbf{e}}_j}{\partial \hat{\mathbf{e}}_i} \qquad (5.13)\\
&= -\frac{2K}{\mu_B m_i B_0}\sum_j (\hat{\mathbf{e}}_j\cdot\hat{\mathbf{e}}_K)\hat{\mathbf{e}}_K\delta_{ij} \qquad (5.14)\\
&= -\frac{2K}{\mu_B m_i B_0}(\hat{\mathbf{e}}_i\cdot\hat{\mathbf{e}}_K)\hat{\mathbf{e}}_K. \qquad (5.15)
\end{aligned}$$

The magnetostatic dipole-dipole field is calculated as,

$$
\begin{aligned}
& \mathbf{b}_{i,\mathrm{dd}} \qquad (5.16)\\
= & -\frac{1}{\mu_B m_i B_0}\frac{\partial \mathscr{H}_{dd}}{\partial \hat{\mathbf{e}}_i}\\
= & \frac{1}{\mu_B m_i B_0}\frac{\mu_0\mu_B^2}{8\pi}\sum_{i\neq j}\frac{m_i m_j}{R_{ij}^{-5}}\frac{\partial\left[3(\mathbf{R}_{ij}\cdot\hat{\mathbf{e}}_i)(\mathbf{R}_{ij}\cdot\hat{\mathbf{e}}_j)-R_{ij}^2(\hat{\mathbf{e}}_i\cdot\hat{\mathbf{e}}_j)\right]}{\partial\hat{e}_i}\\
= & \frac{\mu_B}{m_i B_0}\frac{\mu_0}{8\pi}\sum_{i\neq j}\frac{m_i m_j}{R_{ij}^{-5}}\left[3\mathbf{R}_{ij}(\mathbf{R}_{ij}\cdot\hat{\mathbf{e}}_j)+3\mathbf{R}_{ij}(\mathbf{R}_{ij}\cdot\hat{\mathbf{e}}_i)\frac{\partial\hat{\mathbf{e}}_j}{\partial\hat{e}_i}-R_{ij}^2\hat{\mathbf{e}}_j-R_{ij}^2\hat{\mathbf{e}}_i\frac{\partial\hat{\mathbf{e}}_j}{\partial\hat{e}_i}\right]\\
= & \frac{\mu_B}{m_i B_0}\frac{\mu_0}{8\pi}\sum_{i\neq j}\frac{m_i m_j}{R_{ij}^{-5}}\left[3\mathbf{R}_{ij}(\mathbf{R}_{ij}\cdot\hat{\mathbf{e}}_j)+3\delta_{ij}\mathbf{R}_{ij}(\mathbf{R}_{ij}\cdot\hat{\mathbf{e}}_i)-R_{ij}^2\hat{\mathbf{e}}_j-\delta_{ij}R_{ij}^2\hat{\mathbf{e}}_i\right]\\
= & \frac{\mu_B}{m_i B_0}\frac{\mu_0}{4\pi}\sum_{j}\frac{m_i m_j}{R_{ij}^{-5}}\left[3\mathbf{R}_{ij}(\mathbf{R}_{ij}\cdot\hat{\mathbf{e}}_j)-R_{ij}^2\hat{\mathbf{e}}_j\right]\\
= & \frac{\mu_0\mu_B}{4\pi B_0}\sum_j m_j\left[\frac{3\mathbf{R}_{ij}(\mathbf{R}_{ij}\cdot\hat{\mathbf{e}}_j)}{R_{ij}^{-5}}-\frac{\hat{\mathbf{e}}_j}{R_{ij}^{-3}}\right].
\end{aligned}
$$

Alternatively, the expression for the magnetostatic field can be calculated from the magnetostatic energy on the form of Eq. 3.36. The magnetostatic interaction is the only term in the parametrized Hamiltonian that explicitly depends on the coordinates of the atomic magnetic moments. The proper lattice constants and vectors $\mathbf{R}_{ij}$ must therefore be used in order to get the right strength of the dipole-dipole field. The calculation of the dipole-dipole field for all atoms magnetic moments e_i constitutes a double summation over all sites in the simulation cell. In the limit of a large number of atomic magnetic moments, the computational effort for this operation can dominate the execution time in simulations of the SLL equation. Different techniques building on Ewald summation [6] or convolution and Fourier transforms [137] are commonly used in micromagnetics simulations. Similar techniques can be used also for atomistic spin dynamics. The external magnetic field in dimensionless units is simply $\mathbf{b}_{ext} = \mathbf{B}_{ext}/B_0$. Omitting the contribution from the pseudo-dipolar interaction, the complete expression for the dimensionless effective magnetic field $\mathbf{b}_i$ acting on the atomic magnetic moment $\hat{\mathbf{e}}_i$ is written as

$$
\begin{aligned}
\mathbf{b}_i = & \frac{1}{\mu_B B_0}\sum_j\left\{J'_{ij}m_j\hat{\mathbf{e}}_j-\mathbf{D}'_{ij}\times\hat{\mathbf{e}}_j-\frac{2K}{m_i}(\hat{\mathbf{e}}_i\cdot\hat{\mathbf{e}}_K)\hat{\mathbf{e}}_K \qquad (5.17)\right.\\
& \left.\frac{\mu_0\mu_B^2}{4\pi}m_j\left[\frac{3\mathbf{R}_{ij}(\mathbf{R}_{ij}\cdot\hat{\mathbf{e}}_j)}{R_{ij}^{-5}}-\frac{\hat{\mathbf{e}}_j}{R_{ij}^{-3}}\right]\right\}+\frac{\mathbf{B}_{\mathrm{ext}}}{B_0}, \qquad (5.18)
\end{aligned}
$$

where here the magnetocrystalline anisotropy field is for the lowest order contribution to a uniaxial anisotropy.

5.3 Implementation and examples

The implementation of the SLL for atomistic spin dynamics simulations within UppASD allows for the magnetic sample to have in principle arbitrary geometry. The hard restrictions are mainly in form of memory and execution time limitations. To describe a highly irregular structure, in form of a nanoscale magnetic heterostructure or device, is possible. The limitation is here mainly of a practical nature as coordinates and couplings, in the limiting case of irregularity, has to be specified individually for each atomic magnetic moment in the simulation cell. The atomic moments $\{\mathbf{e}_i\}$ are referred to primarily through the index i. If the dipole-dipole field is included in a simulation, the coordinates $\{\mathbf{r}_i\}$ have to be provided. The coordinates are also needed in sampling the space- and time-displaced connected correlation function and in calculating the dynamic structure factor $S(\mathbf{q}, \omega)$.

The Bloch theorem enables for the electronic structure of a bulk compound to be investigated in calculations on the chemical unit cell. Band structure methods and density functional theory calculations almost always make use of the Bloch theorem. An example of methods that do not use the Bloch theorem are real-space methods, for instance the linear scaling real space method developed and described in the PhD thesis of Bergman [148]. This method is suitable for investigations of the non-collinear magnetic behaviour of nanostructured materials.

Most of the time, the atomistic spin dynamics simulations are performed for magnetic samples with a crystal structure. The compound is represented in a simulation cell by duplication of the chemical unit cell. In simulations of the bulk phase of a material, the duplication is in the direction of the three lattice translation vectors, complemented with periodic boundary conditions. In simulations of a layered system, the duplication is in the directions of two of the lattice translation vectors. For a multilayer system it is possible to have different interatomic exchange interaction and magnetocrystalline anisotropy constants for each layer. Electronic structure programs that use surface Green functions are particularly suited for these semi-infite geometries [62, 70].

Chemically disordered systems are challenging as they break the translational symmetry of the lattice. The chemical disorder can be modelled in supercells, where a local chemical disorder can be taken into account. An efficient scheme for how to set up the disordered supercells is the technique of special quasirandom structures [149], An alternative is to use the coherent potential approximation, as described in e.g. Ref. [62]. The applications of the coherent potential approximation will be discussed in Chapter 6 in connection to Papers II-IV.

Event more complicated for first principles methods are amorphous compounds. There are methods [150] for how to investigate amourphous compounds within a electronic structure framework, but there is no immediate procedure how to combine this with mapping to a magnetic Hamiltonian of

the form of Eq. 3.39. In solid state magnetism, a strong motivation for interest in amorphous materials is the opportunity they offer for tuning of the magnetization and angular momentum compensation points in ferrimagnetic rare earth-transition metal alloys [151].

5.4 Thermal equilibrium and ergodicity

To equilibrate the system, either spin dynamics simulation evolution in presence of a heatbath or Monte Carlo techniques can be used. [1] Different measures are available to determine if a system of atomic magnetic moments have reached thermal equilibrium.

The crudest measure is the magnetic order parameter, in simulations calculated as the average of all magnetic moments in the simulation cell. In equilibrium the energy distribution of the spin-moments follows a Boltzmann distribution. The energy of spin i is given by

$$E_i = -\mathbf{m}_i \cdot \mathbf{B}_i + |\mathbf{m}_i||\mathbf{B}_i|. \tag{5.19}$$

In this expression parallel coupling between the moment and the local effective field is set to zero energy. During dynamical processes the distribution changes. In analog with the spin wave content one may calculate the change in the energy distribution at different points in times during a dynamic process.

Averages of an observable can be obtained either by averaging over time or by averaging over the magnetic moments in the simulation cell. The ergodic hypotheses [7] in statistical mechanics states that in the thermodynamic limit of long measuring times and large simulations cells, the average over time and over the simulation cell are equivalent. As a consequence, there is a certain freedom in how averages can be calculated for a system in thermal equilibrium. In simulations, where the number of magnetic moments, and the number of times steps, with necessity both are limited, the thermodynamic limit cannot be approached. Rather the choice is between a small or medium cell and simulation time invervals typically shorter than one nanosecond. It is then important to observe that the dynamics, also in the steady state of thermal equilibrium, is of different nature for simulations cell of varying size. The theory of finite-size scaling and the renormalization group [119] make it possible to extract qualitative and quantitive results in the thermodynamic limit from data collected in simulations on finite cells. This is very useful in order to investigate phase transitions. As mentioned already in Chapter 4, the theory of dynamic critical phenomena is important for atomistc spin dynamics. Whether a simulation aims to actually calculate dynamical critical exponents

[1] Bloch spin algorithms, such as the Wolff algorithm, are used in Monte Carlo simulations to speed up the approach to equilibrium. A similar method could be developed for Langevin dynamics of spin systems. That would then be the Björn algorithm.

or simulate e.g. the switching of a magnetic heterostructure, the mechanism of critical slowing down can potentially influence the evolution of the system. A consequence, with immediate relevance for simulations on switching behaviour, is that the time scale in simulation is not absolute. Not only is precise knowledge of the microscopic damping parameter typically not at hand, it is in principle also necessary to account for finite size effects when trying to determine the speed of reversal and relaxation as accurately as possible.

5.5 Measurements

5.5.1 Average magnetization and sublattice magnetization

As primary quantities, the average magnetization M and its Cartesian components M^k, are calculated as averages over the magnetic moments in the simulation cell,

$$M^k = \frac{1}{N}\sum_i m_i^k \tag{5.20}$$

$$M = \sqrt{M^x + M^y + M^z} \tag{5.21}$$

at an instant of time during the simulation. Here m_i^k, with $k = x, y, z$, are the Cartesian components of the atomic magnetic moments and N is the number of atoms in the simulation cell. For antiferromagnets, ferrimagnets, and materials with a complicated crystal structure, averages can be calculated over individual sublattices. When sampling a dynamic process over a time interval, the time scales of the dynamics for a specific system determines the appropriate sampling rate of the components M^k. A typical value of the sampling periodicity time is 10 ps, corresponding to a sampling frequency of 100 THz. It is also possible to write to file sequences in time of the individual atomic magnetic moments m_i^k. This provide information that can be used, together with conservation laws as described in Section 4.9, for testing and debugging of software implementing atomistic spin dynamics. In simulations of the SLL equation, averaging over different realisations of the heat bath, i.e. starting the random number generator with different seeds, is important. For geometrically disordered systems such as dilute magnetic semiconductors, also averaging over different configurations of the magnetic atoms in the lattice is important.

If a system has reached thermal equilibrium, averaging can be performed also over time. This is typically done for the average magnetization and the average sublattice magnetization over a range of temperatures. It is also possible to calculate higher order moments and cumulants as described in textbooks on Monte Carlo simulations in statistical physics, e.g. Ref. [28].

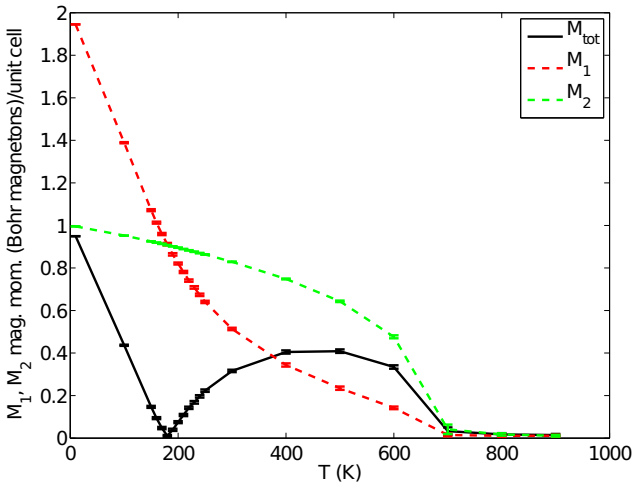

Figure 5.1: The magnetization $M(T)$ and sublattice magnetizations $M_1(T), M_2(T)$ versus temperature for the B2 model ferrimagnet described in the text. A simulation cell sized $L = 32$ was used in simulations with 20 heat bath averages.

5.5.2 An example: Ferrimagnetic resonance

Simulations have been performed for a model Ferrimagnet with B2 Caesium Chloride crystal structure. The magnetic moments were $M_1 = 2.0\ \mu_B$ and $M_2 = 1.0\ \mu_B$. The exchange interactions were $J_{11} = 1.00$ mRy, $J_{22} = 0.05$ mRy, and $J_{12} = -0.10$ mRy. At first simulations were run to obtain magnetic moment configurations in thermal equilibrium at different temperatures. Here 20 realisations of the heat bath were used. As can be seen in the error bars for the graphs, the standard deviation of the average magnetization in the 20 samples is small. The $M(T)$-graphs are shown in Fig. 5.1. At a temperature $T \approx 180$ K the magnetization of the M_1 and M_2 sublattices cancel each other. The temperature T_M where this happen is called the magnetization compensation temperature. If the atomic magnetic moments on the different sublattices have the same gyromagnetic ratio, the magnetization compensation temperature coincide with the angular momentum compensation temperature T_A. If the gyromagnetic ratios are different, the compensation of magnetization and angular moment occur at different temperatures $T_M \neq T_A$. In the present simulations, the steps in temperature was $T = 10$ in the interval $T = 150$ to $T = 250$ K. No particular effort was made to pinpoint the magnetic compensation temperature to a very precise value. It should be remarked that not all ferrimagnets have a compensation point. If the exchange couplings between the sublattices are too strong, the sublattice with the stronger magnetic moment at low

temperature will prevail over the other sublattice all the way up to the Curie temperature T_C.

The magnetic configurations in equilibrium at different temperatures were used as starting configurations for simulations of precession in a uniaxial anisotropy with the strength $K = -0.02$ mRy/atom. The anisotropy axis is along the z-direction. The magnetic configurations were rotated to have an initial angle of 10° to the anisotropy axis. The simulations were performed using the damping parameters $\alpha = 0.00$ or $\alpha = 0.01$. For the simulations with $\alpha = 0.01$ averaging was performed over 20 heat baths. For M_1 atoms the Lande g-factor was kept to $g_1 = 2.0$ in all simulations. For M_2 atoms two different values of the g factor was used, $g_2 = 2.0$ and $g_2 = 2.2$. In all simulations a precession of the average magnetization around the anisotropy axis could be observed. This constitutes a ferrimagnetic precession mode. What distinguises this as a ferrimagnetic mode is its dependence of the precession frequency on the temperature. In Fig. 5.2 are shown the graphs of the magnetization components at temperature $T = 10$ K. Far away from the compensation points, the evolution of the average magnetization is similar to that of a ferromagnet. In Fig 5.3 are shown the graphs of the magnetization components at temperature $T = 100$ K. The precession of the sublattice magnetization vector around the anisotropy axis is here much faster than for low temperatures.

The trajectories of the average magnetization and the magnetization for each sublattice were analysed by Fourier transforms. At first the M^x, M_1^x, M_2^x and M^y, M_1^y, M_2^y components were analysed. For most temperatures two resonance frequencies can be found. The Fourier transforms reveal that the frequencies present in the $\alpha = 0.01$ and the $\alpha = 0.00$ simulations are similar. These frequencies are the same for the average magnetization and for the sublattice magnetizations. The frequencies are associated with the ferromagnetic mode and the exchange mode respectively [26, 27]. Close to the compensation temperature, the frequencies are close together and it is hard to distinguish if there are two distinct frequencies or only one frequency. This corresponds to the theory of ferrimagnetic resonance, where the frequencies of the ferromagnetic mode and exchange mode coincide at the angular momentum compensation temperature.

Next the M^z, M_1^z, M_2^z components and M, M_1, M_2 were analysed. The exchange interactions within each sublattice ensure that the average sublattice magnetizations M_1 and M_2 are almost unaffected by the precession around the the anisotropy axis. This can be seen directly in the trajectories for M_1 and M_2 and also in their respective Fourier spectra. On the other hand, the total magnetization M oscillate in time. As the sublattice magnetizations are stable, an oscillation of M must be associated with an oscillation of the angle θ_{12} between $\mathbf{M_1}$ and $\mathbf{M_2}$. The angle can be calculated and analysed, but one can also observe oscillations directly in the M_1^z and $, M_2^z$ components. These are more pronounced in the beginning of the 50 ps long simulation interval when the angles θ_1 and θ_2 of the sublattice magnetizations to the anisotropy axis are

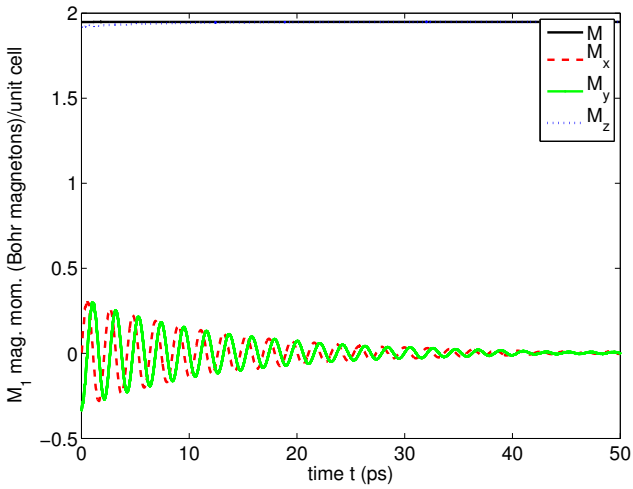

Figure 5.2: The sublattice magnetization $M_1(T)$ during precession at $T = 10$ K in a uniaxial anisotropy. A simulation cell sized $L = 32$ was used in simulations with 20 heat bath averages and $\alpha = 0.01$, $g_1 = 2.0$, and $g_2 = 2.0$.

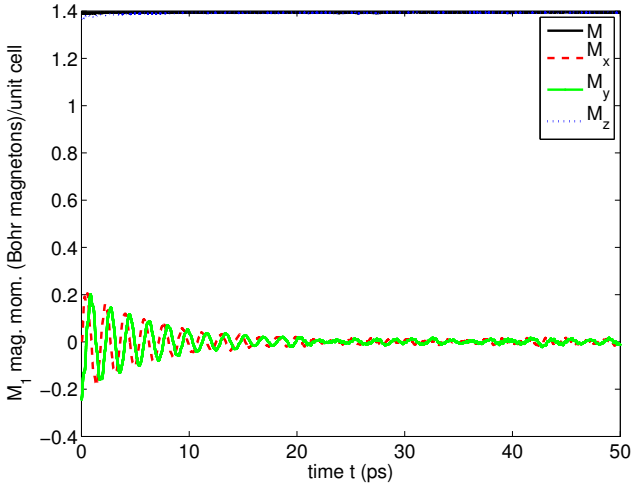

Figure 5.3: The sublattice magnetization $M_1(T)$ during precession at $T = 100$ K in a uniaxial anisotropy. A simulation cell sized $L = 32$ was used in simulations with 20 heat bath averages and $\alpha = 0.01$, $g_1 = 2.0$, and $g_2 = 2.0$.

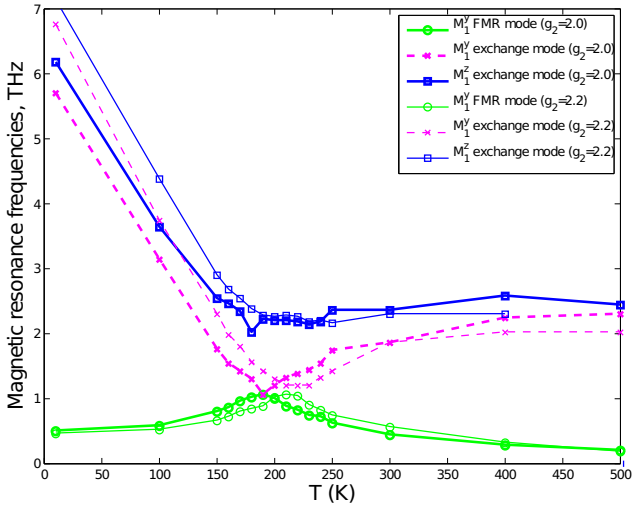

Figure 5.4: The resonance frequencies for the B2 model ferrimagnet. The frequencies of the ferromagnetic mode and the lower exchange mode were obtained from Fourier transforms of the M_1^y-component. The frequencies of the upper exchange mode were obtained from Fourier transforms of the M_1^z-component. The frequencies are shown for two sets of simulations, one set where $g_1 = g_2 = 2.0$ and one set where $g_1 = 2.0$, $g_2 = 2.2$.

close to 10°. At a later point, when the sublattice magnetizations both align close to the z-axis, all motion is mainly in the xy-plane and oscillations in the z-direction are small in magnitude. That the frequencies are close is indicative of that the oscillation in M is connected to the oscillation of M_1^z and M_2^z. This can also be confirmed by calculation of the angle θ_{12}. When comparing the graph for θ_{12} with the graphs for M_1^z, M_2^z, and the magnetization M, it is seen that they all have the same dependence on time.

The peak values of the frequencies have been plotted versus temperature in Figs. 5.4. Around T_A the lower lying frequency, connected to the precession around the anistropy axis, is seen to diverge. This corresponds to a divergence of the effective gyromagnetic ratio. Also in the case of equal g factors a divergence of the effective gyromagnetic ratio can be seen around T_A. The divergence is not very strong but the trend is clear. Remarkable is here that the frequency does not drop to zero around T_M. This is precisely what was observed in the experiments on ferrimagnetic resonance of GdFeCo by Stanciu *et al.* [35]. The lower exchange branch has a minima close to T_A. In the vicinity of the compensation temperatures this branch takes values close in magnitude to those of the ferromagnetic branch.

5.5.3 The autocorrelation function

It can be tempting to try to determine how well equilibrated a spin configuration is by optical inspection of the magnetic order parameter plotted as a function of time. This measure gives a hint on how far the system has evolved towards thermal equilibrium, but it can be misleading. For small systems, thermal fluctuations make the order parameter oscillate. This is to some part relieved by averaging over heatbaths, but if the order parameter only slowly approaches a limiting value it can be problematic nevertheless. A dynamic system that is out of equilibrium has physical observables that break time translation invariance during the relaxation towards thermal equilibrium. Two-time observables can sample the characteristics of the approach to equilibrium. The spin autocorrelation function,

$$C_0(t_w + t, t_w) = \langle \mathbf{m}_i(t_w) \cdot \mathbf{m}_i(t_w + t) \rangle, \tag{5.22}$$

is an important quantity as it provides a good measure to see how well equilibrated the spin system is. The autocorrelation function is used extensively in Papers II-IV to investigate the pace of relaxation. In Fig. 15 of Paper II the relaxation for plain bcc Fe is plotted. These relaxation of Fe provides a reference for which the relaxation of GaMaAs, with different rates of As antisites, is compared in Figs. 12-14 in the same paper. In Paper III on the archetypical spin glass alloy CuMn, the dependence of the relaxation on the α parameter is discussed. In Fig. 5.5 is shown the autocorrelation function from a simulation of the frustrated magnet $(Zn_{1-x}Mn_x)Se$. In contrast to the waiting times used in Papers II-IV, the waiting times here are completely regularly distributed on the logarithmic time axis.

The autocorrelation can also be misleading. The reason is that, for isotropic spin systems, there is no energy cost associated with global rotations of the whole spin simulation cell. As discussed in Section 4.9, it is important that the solver of the LL equation preserves the total angular momentum for a system described by only a Heisenberg Hamiltonian and $\alpha = 0$ dynamics. In the case of finite temperature and finite damping, there will always be a random walk like drift due to the fluctuating fields. To suppress this drift is yet another reason that it is important to average over different heatbaths.

5.5.4 Spatial correlation functions

In addition to the trajectories of the atomic moments, and the autocorrelations function, spatial correlations between atomic moments, provide fundamental information on the system. The connected correlation function is defined as

$$C^k(\mathbf{r} - \mathbf{r}', t, t') = \langle m^k_{\mathbf{r}}(t) m^k_{\mathbf{r}'}(t') \rangle - \langle m^k_{\mathbf{r}}(t) \rangle \langle m^k_{\mathbf{r}'}(t') \rangle, \tag{5.23}$$

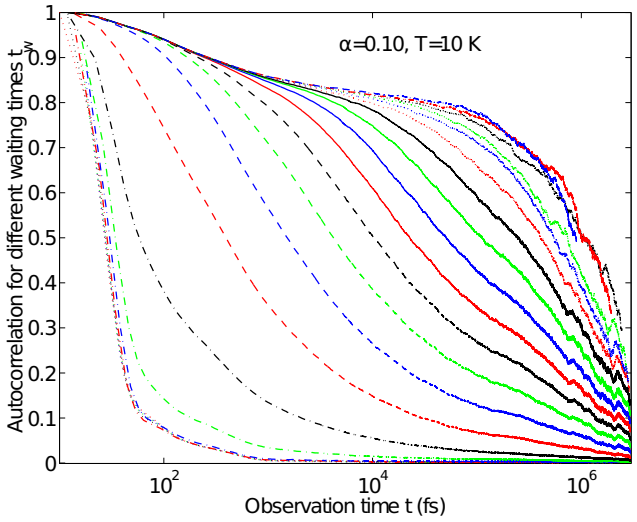

Figure 5.5: Sampling of the autocorrelation function for the diluted magnetic semiconductor ($Zn_{1-x}Mn_xSe$, x=0.25. An ensemble of 20 configurations of the Mn atoms was used. The simulation is following a quenching protocal where the initial magnetization configuration is random. At time $t_0 = 0$ the temperature is set to 10 K. This is below the spinn glas ordering temperature. The system relaxes over many orders of magnitude in time.

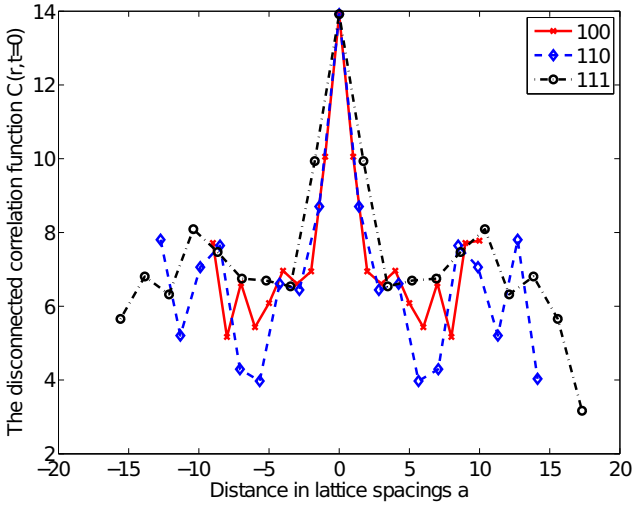

Figure 5.6: Sampling of the disconnected equal time spatial correlation function $G(\mathbf{r}-\mathbf{r}', t = t')$for the diluted magnetic semiconductor $(Ga_{1-x}Mn_x)As$, $x = 0.05$. The system is in thermal equilibrium at $T = 100$ K. The simulation cell has size $L = 20$. The correlation is plotted for arguments $[-L/2, L/2]$ in direction (100), $\sqrt{2}\cdot[-L/2, L/2]$ in direction (110), $\sqrt{3}\cdot[-L/2, L/2]$ in direction (111)

where $\langle ... \rangle$ denotes ensemble averages over heatbaths. The first term on the right hand side is the disconnected correlation function,

$$G^k(\mathbf{r}-\mathbf{r}',t,t') = \langle m^k_{\mathbf{r}}(t) m^k_{\mathbf{r}'}(t') \rangle, \tag{5.24}$$

which contains information on the magnetic order of the system. It will also prove useful to plot,

$$G(\mathbf{r}-\mathbf{r}',t=t') = \langle \mathbf{m}_{\mathbf{r}}(t) \cdot \mathbf{m}_{\mathbf{r}'}(t') \rangle, \tag{5.25}$$

which will be refered to as the disconnected equal time spatial correlation function. This simple measure has been used in Figs. 5-7 in Paper II to determine and vizualize how the correlation of spin grows with time in relaxation from either the ferromagnetic $T = 0$ K state or from a completely disordered state, i.e. the limit of infinite temperature, towards the equilibrium correlation. As the memory footprint for the space- and time-displaced correlation functions are high, in particular if they are sampled for all sites r and r' and also at different times, it is possible to write the correlation functions to file for a subset of all possible directions in the crystal structure. The data in Fig. 5.6 is for $T = 100$ K, $L = 20$ and no As antisites and shows the values of $G(\mathbf{r}-\mathbf{r}',t=t')$ along the 100, 110 and 111 high symmetry directions in the lattice. It is complementary to the black line for the correlation in thermal equilibrium shown in Fig. 5 in Paper II. The correlation function was sampled for distances $\mathbf{r}$ up to half the the edge length, $L/2$. The sampling of correlation functions can also be performed within or between individual sublattices, allowing for insight into how the dynamics can evolve on different timescales for atomic magnetic moments on chemically and magnetically inequivalent sites.

5.5.5 The dynamic structure factor

In order to evaluate the spin wave density of a system one may calculate the dynamics structure factor $S(\mathbf{q},\omega)$ by performing a space and time Fourier transform of the connected correlation function[123],

$$S^k(\mathbf{q},\omega) = \frac{1}{N\sqrt{2\pi}} \sum_{\mathbf{r},\mathbf{r}'} e^{i\mathbf{q}\cdot(\mathbf{r}-\mathbf{r}')} \int_{-\infty}^{+\infty} e^{i\omega t} C^k(\mathbf{r}-\mathbf{r}',t) dt, \tag{5.26}$$

where N is the number of terms in the summation. In Figs. 5.7 and 5.8 the dynamic structure is sampled for a model Heisenberg Ferromagnet with bcc lattice structure. Shown in the figures are here the intensity as a function of frequency f, for the q-value $q = 5(\pi/Na)$. $N = 20$ is the edge length of the simulation cell. In the initial step of the simulation, the spin systems were equilibrated with a heat bath at T=100 K. The sampling of $S(\mathbf{q},f)$ was in Fig. 5.7 performed with 'microcanonical' ensemble where $\alpha = 0$. The peak in the structure factor is sharp. That carries over to the case of finite damping $\alpha =$

0.01 in Fig. 5.8, where the peak is still well defined but a certain broadening occur. This is as expected.

In Fig. 5.9 the dynamic structure factor is measure for GaMnAs. The numerical effort to produce this data is substantial. An average over 20 realizations of the chemical disorder of the lattice was used. For a diluted system, the techniques that are applicable for stochiometric systems are hard to apply. A direct Fourier transform of the realspace interatomic exchange interactions give limited information as this fails to take into account that the system is diluted. The frozen magnon approximation is here not very practical as the necessary supercells would be large. This in combination with that a large number of individual calculations for different realizations of disorder are necessary renders the computational effort unwieldy. Direct sampling of $C^k(\mathbf{r}-\mathbf{r}',t,t')$ in spin dynamics simulations followed by Fourier transforms seems to be one of the few tractable means to calculate the spin wave spectra of diluted systems. There is at least one other technique at hand, the self-consistent local random phase approximation. This has recently been used by Bouzerar in a calculation on GaMnAs [152]. The data of Fig. 5.9 is from preliminary atomistic spin dynamics simulations. It shows resemblence with Fig. 2 of Ref. [152], and future more careful comparisons are motivated. It should be pointed out that the systems are not identical as they are for Mn concentration $x = 0.05$, and $x = 0.03$, respectively.

5.5.6 The susceptibility

In thermal equilibrium, the response to external perturbations can to first order be calculated in the formalism of linear response. For magnetism, one of the more important response functions is the susceptibility. It can be readily sampled in simulations as,

$$\chi = \frac{1}{Nk_BT}\langle(\mathbf{m}-\langle\mathbf{m}\rangle)^2\rangle. \tag{5.27}$$

The requirement that a system actually is in thermal equilibrium when measuring a response function or susceptibility is the same in numerical simulations as in experimental measurements. The simplest case is when a system is in proper thermal equilibrium, with all correlations in time being stationary. For systems that relax over many orders of magnitude in time, and actually never reaches complete equilibrium, response functions can still be described by linear response if the driving perturbation is slow with regard to the dynamics [124].

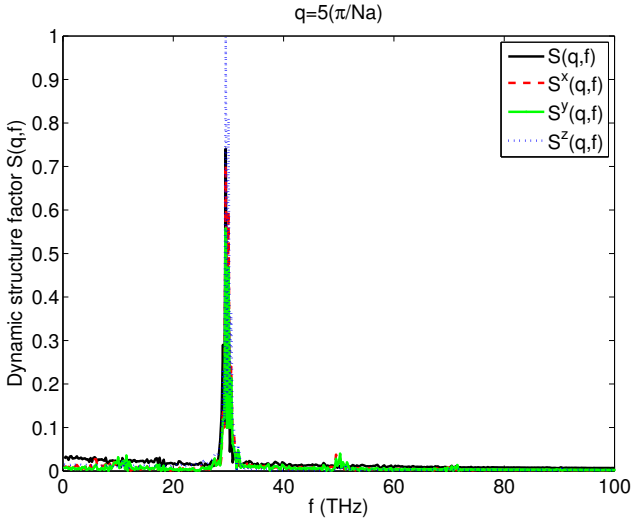

Figure 5.7: Sampling of the dynamic structure factor $S(\mathbf{q}, f)$ for a model Heisenberg ferromagnet with bcc crystal structure. Shown is here the intensity as a function of frequency f, for the q-value $q = 5(\pi/Na)$ where here $N = 20$ is the edge length of the simulation cell. In the initial step of the simulation, the spin system was equilibrated to a heat bath at T=100 K. The sampling of $S(\mathbf{q}, f)$ was performed with 'microcanonical' ensemble where $\alpha = 0$.

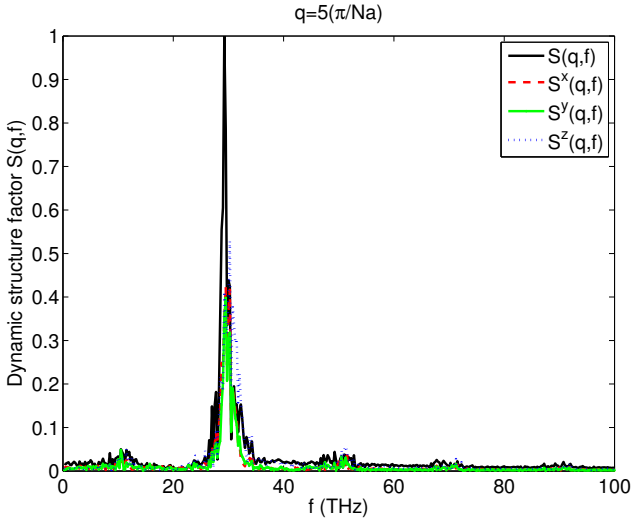

Figure 5.8: Same magnetic system as in Fig. 5.7 but here the sampling of $S(\mathbf{q}, f)$ was performed with a finite damping of $\alpha = 0.01$ and a heatbath of $T = 100$ K. In comparison, the peak is broader in this graph, as expected for finite damping versus zero damping. In both this graph and the graph of Fig. 5.7 the $S(\mathbf{q}, f)$ data was normalized to its respective peak value.

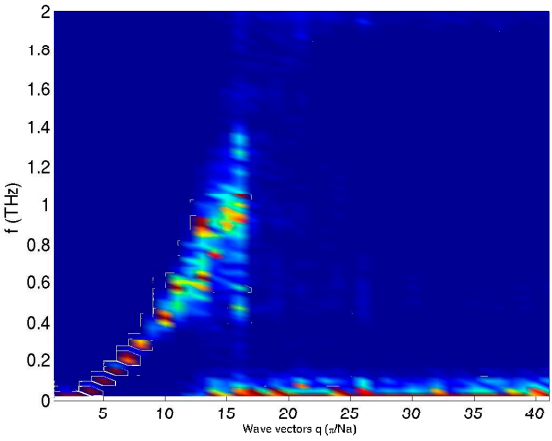

Figure 5.9: Sampling of the dynamic structure factor $S(\mathbf{q},\omega)$ for the diluted magnetic semiconductor $(Ga_{1-x}Mn_x)As$, x=0.05. An ensemble of 20 configurations of the Mn atoms was used. In the initial step of the simulation, the spin system was equilibrated to a heat bath at T=10 K. The sampling of $S(\mathbf{q},w)$ was performed with 'microcanonical' ensemble where $\alpha = 0$.

6. Introduction to the papers

This section introduces Paper I.

Paper I describes the method for, and implementation of, a scheme for atomistic spin dynamics. See also comments in the opening of Chapter 5 and Appendix A.

6.1 Chemically disordered magnets

This section introduces Papers II-IV.

In order to model chemically disordered magnets within the framework of density functional theory, special care is necessary. One approach is to set up a supercell, as large as possible depending on the available computing resources. The supercell approach has the advantage that it provides a local environment for the magnetic atoms. It is possible to investigate how chemical, structural and magnetic properties differs in the case of homogeneously distributed magnetic atoms as compared to the case where clustering occurs. This can be done by imposing different magnetic configurations in the solution of the electronic structure and calculate the total energy. The total energies for a set of different magnetic configurations can be used in an equation system to calculate nearest neighbour and possibly next nearest neighbour interactions. If the concentration of magnetic impurities is small, the supercell method faces the problem that a larger number of host atoms in the semiconductor needs to go into the calculation in order for the ratio of the atoms in the supercell to come close to the chemical composition that one wants to calculate for. A large supercell obviously also increases the computational effort.

The coherent potential approximation, briefly discussed in Chapter 5, is one of the techniques that can be used instead. This techique works very well for many problems in alloy theory. When applied to magnetic alloys with the goal in mind to extract interatomic exchange parameters and atomic magnetic moments, that can be used in subsequent Monte Carlo or spin dynamics simulations, two things need to be taken into account. One is whether the compound is known to be a homogeneous alloy or if clustering occur. The second is to what extent the magnetic exchange interaction depends on the local environment. In the investigations of the diluted magnetic compounds in Papers II-IV, the assumption was always that the compounds could be regarded as homo-

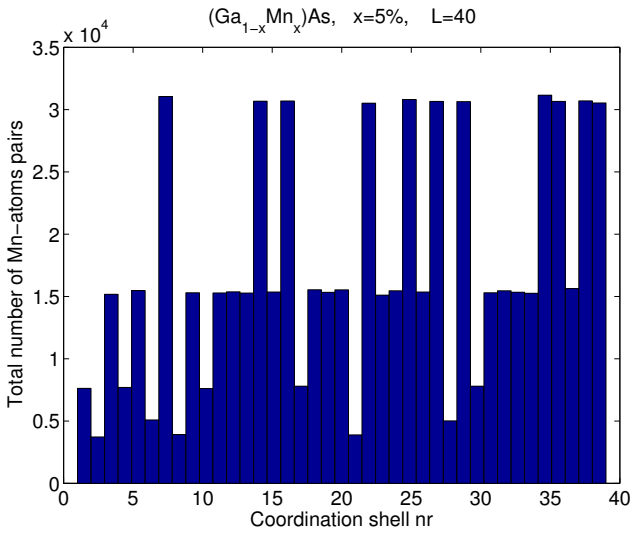

Figure 6.1: Histogram of the atomic pair correlation for a simulation cell $L = 40$ of the diluted magnetic semiconductor $(Ga_{1-x}Mn_x)As$, $x = 0.05$. The Mn atoms have here homogeneously substituted 5% of the Ga atoms. A consequence of this atomic pair correlation is that the combined effect of interactions over larger distances will be stronger than their individual values would indicate.

geneous and that the magnetic exchange interactions would not be too much dependent on the local environment.

To arrive to longe range magnetic ordering, the diluted magnetic compounds must have a mechanism to couple the magnetization throughout the sample. The mechanism is often exchange interactions, but also magnetic-dipole-dipole interactions can play a role. The exchange parameters used for the spin dynamics simulation on the diluted magnetic semiconductor $(Ga_{1-x}Mn_x)As$, $x = 0.05$, presented in Paper II, are displayed in Fig. 1 of that paper. As the Mn atoms occupy only 5% of the sites of one fcc lattice, it is clear that also exchange interactions for larger distances can play a role, as the number of such couplings can be larger than the numbers of nearest neighbour couplings. In Fig. 6.1 is shown a histogram of the atomic pair correlation. This histogram is for a homogenous substitution with 12800 Mn atoms distributed over the 256000 sites of the Ga lattice in a $L = 40$ simulation cell.

In materials with antiferromagnetic interatomic exchange interactions, it can happen that not all antiferromagnetic couplings can minimize their energy simultaneously. This effect is called frustration. The cause of frustration can be purely geometrical [153], as is the case for a triangular lattice, a Kagome lattice or the Pyrochlore lattice [154]. If a lattice of this type is occupied with chemically equivalent elements, all antiferromagnetically cou-

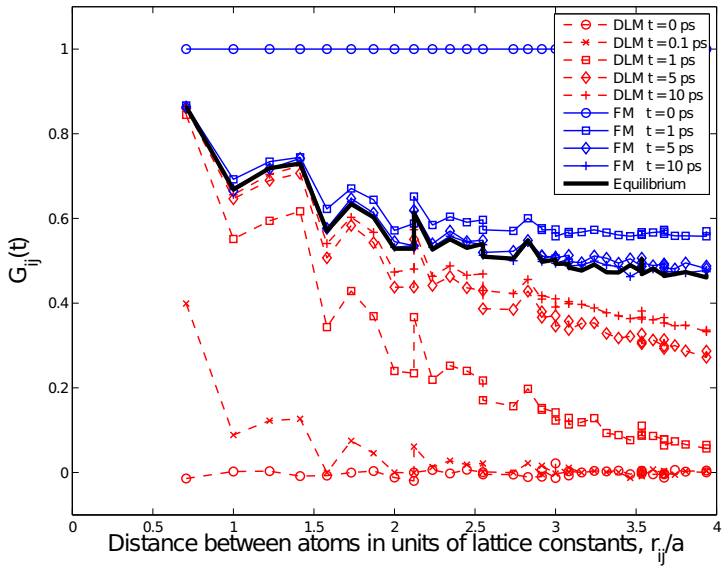

Figure 6.2: Time evolution of the pair correlation function $G_{ij}(t)$ starting from ferromagnetic (blue) respective random (red) configurations and with $L = 40$ in the simulation. Values are obtained for $y = 0.25$ % and $T = 100$ K. The equilibrium pair correlation is shown in black.

pled to each other, the groundstate will be highly degenerate. Such materials have particular thermodynamic properties that are investigated in experiments [154] and also in numerical simulations [155]

In the case that frustration is combined with chemical disorder, it can be that the materials will belong to the class of spin glasses [156, 124]. The disorder can be in form of bond disorder, where the exchange couplings take different values, or in form of site order, where the atoms are chemically essentially equivalent, but occupy the lattice sites randomly. Spin glasses are related to the frustrated magnets mentioned above, but also possess some distinct characteristics. One of them is that a spin glass will in experiments relax over a large order of times scales, potentially reaching geological time spans. In simulations of finite cells, it is possible to sample the phase space in order to explore the degenerate groundstates. This is computationally very demanding, and refined algorithms such as the heatbath algorithm and parallel tempering come to good use. For an introduction to the theory of slow dynamics and aging in spin glasses see e.g. Vincent *et al*, [157], Nordblad and Svedlindh in Chapter 1 of Ref. [124] and Bouchaud *et al.* in Chapter 6 of Ref. [124]. The PhD thesis of Peil [158] explores in detail how research on spin glasses can be performed combining materials specific density functional theory calculations and advanced Monte Carlo methods.

In the simulations that are reported in Papers II-IV the aim was not to sample the groundstates. Instead the emphasisis was on investigations on the relaxation and the aging over a continuum of time scales by means of sampling of the autocorrelation function. Direct comparisons with experiment are difficult as the section of the logarithmic time axis that can be targeted in numerical simulations are in the interval $10^{-14} - 10^{-9}$ s. This can be contrasted with the time scales of $10^{-5} - 10^{5}$ s in experimental protocols, such as e.g. thermoremanence magnetization measurements and susceptibility measurements.

6.1.1 Spin dynamics of Mn doped GaAs

Dilute magnetic semiconductors (DMS)constitute a class of materials where magnetic atoms, possessing stable magnetic moments, are doped into otherwise nonmagnetic semiconductors. The dopand element is typically a $3d$-metal such as Mn, Fe or Co and the semiconductor is either of the III-V or II-VI class. The amount of dopand element that can be dissolved into the host material before chemical segregation and structural deformation occurs is dependent on the chemical properties of the dopand and host elements. The difference between II-VI and III-V semiconductors is large in this regard. In a II-VI semiconductor such as ZnTe it was possible to dissolve up to 50% of Mn [159]. In experiments the magnetic properties of a DMS often show a clear dependence on the concentration of the magnetic dopand. The blue spheres in Fig. 1.1 show how 5% of the Ga atoms are randomly substituted by Mn atoms in Mn-doped GaAs.

The sample preparation technique named Molecular Beam Epitaxy (MBE) allow III-V semiconductors to be doped with concentrations up to 10% without segregation. Other techniques have failed to achieve this as segregation occured for even lower concentrations. With higher concentrations of magnetic atoms these DMS materials showed FM at low temperatures. The quest for a dilute magnetic semiconductor that would remain FM at room temperatures intensified [160] in the 90s. The driving force is the potential use of DMS in spintronics [161] where spin and charge are information carriers. This is an extension of traditional semiconductor based electronics where information is carried only by the charge.

Theoretical efforts to calculate and simulate the properties of DMS is an example of the how calculations, from first principles but also from model Hamiltonians, play an important role in design of new materials. The importance of interplay between experiment and theory for succesful research in this field should however be emphasized. First-principles theory of dilute magnetic semiconductors is discussed in detail the recent review by Sato *et al.* [13]. The review of Jungwirth *et al.* [75] covers theoretical frameworks as the $k-d$ model, and effective tight-binding models.

The calculations presented in Paper II constitutes an ASD study of the magnetization dynamics of the III-V DMS GaAs doped with 5% Mn. The

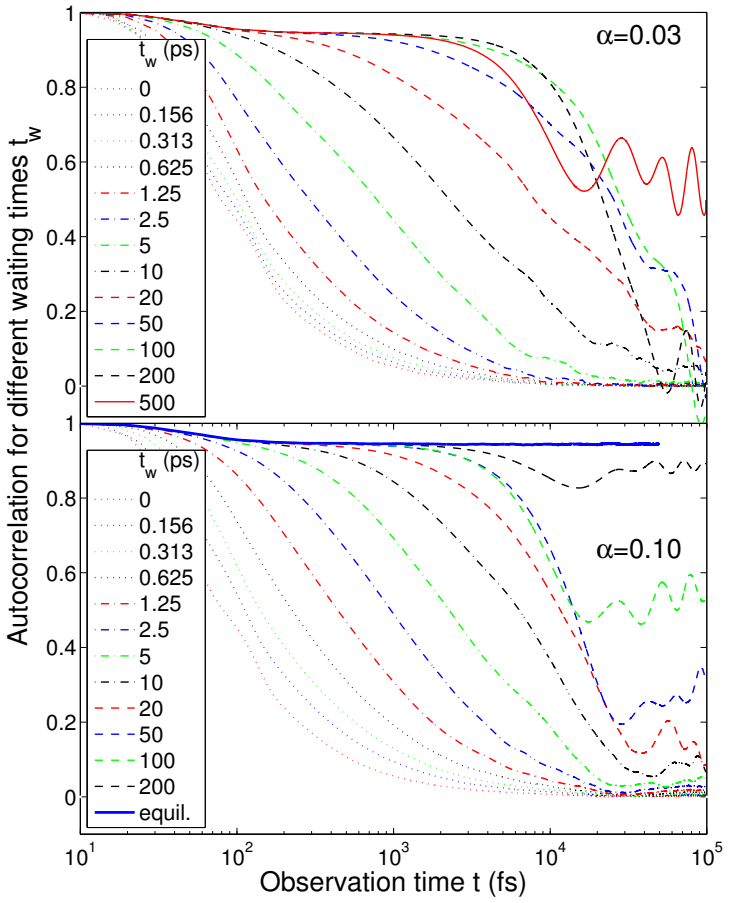

Figure 6.3: Autocorrelation $C_0(t_w+t,t_w)$ for 5 % Mn doped GaAs, with 0.25 % As antisite concentration. The simulation is following a quenching protocal where the initial magnetization configuration is random. At time $t_0 = 0$ the temperature is set to 10 K. Simulations were made with $\alpha = 0.03$ (top panel) and $\alpha = 0.10$ (bottom panel).

relaxation from DLM or FM states to thermally equilibrated magnetic configurations is investigated by sampling of the magnetic ordering function, the time evolution of pair correlation functions and the autocorrelation. Figure 6.2 shows that the pair correlation reaches thermally equilibrated values faster when a simulation is started from a FM configuration than when it is started from a DLM configuration, for the As antisite concentration $y = 0.25$ % and a temperature $T = 100$ K. The dynamics between nearest neighbour Mn atoms is, as revealed by the pair correlation function, considerably faster than the more long ranged interaction. In simulations at the same temperature for higher As antisite concentrations, it was found that short ranged order exists up to and even above the ordering temperature. Starting from random configurations the pair correlation function, for distances up to $4a$ ($a =$ lattice parameter), reaches equilibrium on a time scale of 10-20 ps.

As discussed in Chapter 5 the autocorrelation is a suitable quantity for analysis of the dynamical response and possible spin glass behaviour. Sampling of the autocorrelation shows that Mn doped GaAs does not display spin glass behaviour, for moderate ($y = 0\% - 1.75\%$) concentrations of As antisites. Comparisons are made with the relaxation behaviour of the archetypical ferromagnetic bcc Fe. For the highest defect concentration, $y = 2.00\%$, the nature of the phase transition (ferromagnetic or spin glass) of the simulation cell cannot be accurately determined from the data. The autocorrelation function for antisite concentration $y = 0.25$ % at temperature $T = 10$ K is shown in Fig. 6.3.

6.1.2 The spin glass alloy CuMn

That CuMn is a spin glass is well established. In Paper III comparisons are done between a Hamiltonian with parameters for CuMn calculated in density functional theory electronic structure programs, and the Heisenberg generalisation of the Edwards-Anderson model. It is investigated how the aging is affected by the size of the damping parameter α.

6.2 Dynamics of FM and AFM

This section introduces Papers V and VI.

For a large set of problems within micromagnetism, it is possible to describe small domains or nanoparticles with one large effective magnetic moment. This macrospin approximation is one of the techniques that makes it possible to investigate some switching and relaxation phenomena without unduly computational effort. Antiferromagnets and ferrimagnets can be described with one lattice spin representing the magnetization of all magnetic moments residing on one sublattice. This construction is similar to, but clearly not identical to the macrospin approximation. The chief difference is that antiferromagnets

and ferrimagnets have more degrees of freedom that allows for complicated spin wave modes, typically more complex than the modes of ferromagnets.

6.2.1 Spin wave instabilities

Thermally stable magnetic domains with well defined spatial extensions are the building blocks for information in magnetic storage media. Magnetocrystalline anisotropies and shape anisotropy for thin films causes the magnetic domains either to lie along an easy axis in the plane of the film or to be perpendicular to the film. Switching of a magnetization domain (i.e. changing the bit stored from 0 to 1 or vice versa) can be initiated by external magnetic fields from a permanent magnet or a current coil, by magneto-optical mechanisms with a laser pulse or with spinpolarized currents. After the external excitation, the magnetization relaxes in the presence of anisotropies to eventually lay to rest in the new direction. Relaxation processes of magnetization dynamics involve transfer of energy and angular momentum, either to the lattice, the electrons or within the magnons (the low energy magnetic excitations). Phenomenological models such as Gilbert damping and Bloch-Bloembergen damping have been used to describe relaxation on the macroscopic level (see Fig. 6.4). In the micromagnetic approach magnetization is treated as a continuum $\mathbf{m}(\mathbf{r},t)$. The concept of macrospin arises by coarse graining the magnetization over distances on which the magnetization is reasonably collinear. The macrospin, $\mathbf{M}$, represents the direction and magnitude of the magnetization in an element of e.g. a thin film. The initial rotation of the magnetization of a ferromagnet in an external field can be seen as an excitation of a large number of uniform k=0 magnons. During the relaxation process these magnons interact, dissipating energy and angular momentum. Relaxation can occur via two processes, one where both energy and angular momentum are transfered out of the magnetic system and the second where energy is transfered within the magnetic system, to other non-uniform $k \neq 0$ magnons. The first process, which describes a dissipative damping in the equations of motion for magnetization dynamics, results in a Gilbert like relaxation,

$$\frac{\partial \mathbf{M}}{\partial t} = -\gamma \mathbf{M} \times \mathbf{H} + \frac{\alpha}{M} \mathbf{M} \times \frac{\partial \mathbf{M}}{\partial t}, \tag{6.1}$$

where $\mathbf{M}$ is the macro moment, $\mathbf{H}$ the effective field and α a damping parameter. The second process, which is described by the precessional term in the equations of motion, results in a special case ($|M_z|$ constant) of the Bloch-Bloembergen damping,

$$\frac{\partial \mathbf{M}}{\partial t} = -\gamma \mathbf{M} \times \mathbf{H} - \frac{M_x}{R} \hat{\mathbf{e}}_x - \frac{M_y}{R} \hat{\mathbf{e}}_y, \tag{6.2}$$

where the effective field is assumed to lie in the z-direction and R is a relaxation parameter. This second process is the focus of Paper VI. Here a

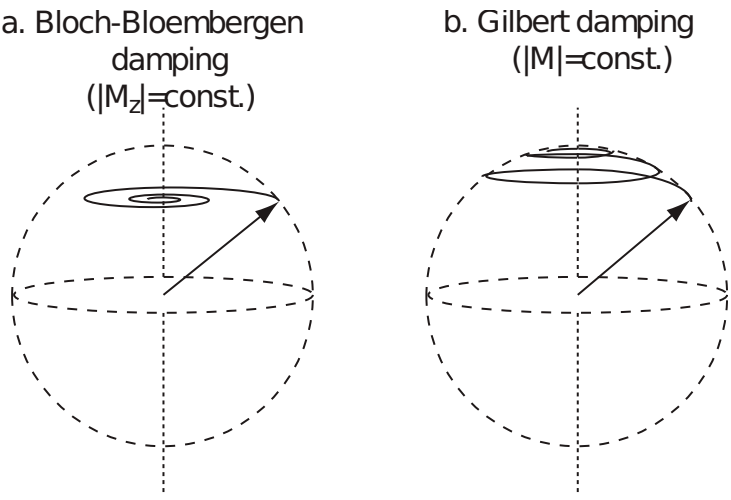

Figure 6.4: The figures illustrate the Bloch-Bloembergen (a) damping and the Gilbert (b) damping for a macro moment precessing in an effective magnetic field along the z-axis. In the former (a) case the x- and y-components of the macrospin vanish whereas the z-component is preserved. For the latter (b) the macrospin magnitude is preserved.

macrospin, constructed as the average of the atomic magnetic moments in a $20 \times 20 \times 20$ bcc Fe simulation cell, is relaxed in the presence of an external magnetic field or a magnetocrystalline anisotropy. The main result is that the macrospin, even in the absence of Gilbert like damping (i.e. $\alpha = 0$ in the ASD equation of motion Eq. 4.1) can shrink to very small values or even disappear. This process was investigated for longer length scales of the magnetization within the micromagnetic approach by Kashuba [162] and is refered to as a spin wave instability (SWI). That this phenomena is present also on shorter length scales is demonstrated in a series of ASD simulations. The conditions for a SWI to occur are shown to be: A finite temperature to initiate the deviations from $k = 0$ magnons, and the presence of magnetocrystalline anisotropy. Figure 6.5 shows how the distribution of atomic magnetic moments is changed under influence of an external magnetic field and an anisotropy axis. Further details on the simulations and the results are found in Paper V.

6.2.2 Switching of an artificial antiferromagnet

In Paper VI it is investigated how fast the magnetization direction can be switched in an artificial antiferromagnet. Through a favourable cooperation of the torques from the external magnetic field, and the torque that act from one sublattice to the other, a very rapid switching is demonstrated. The time scale of the switching is investigated for different damping parameters and at different temperatures.

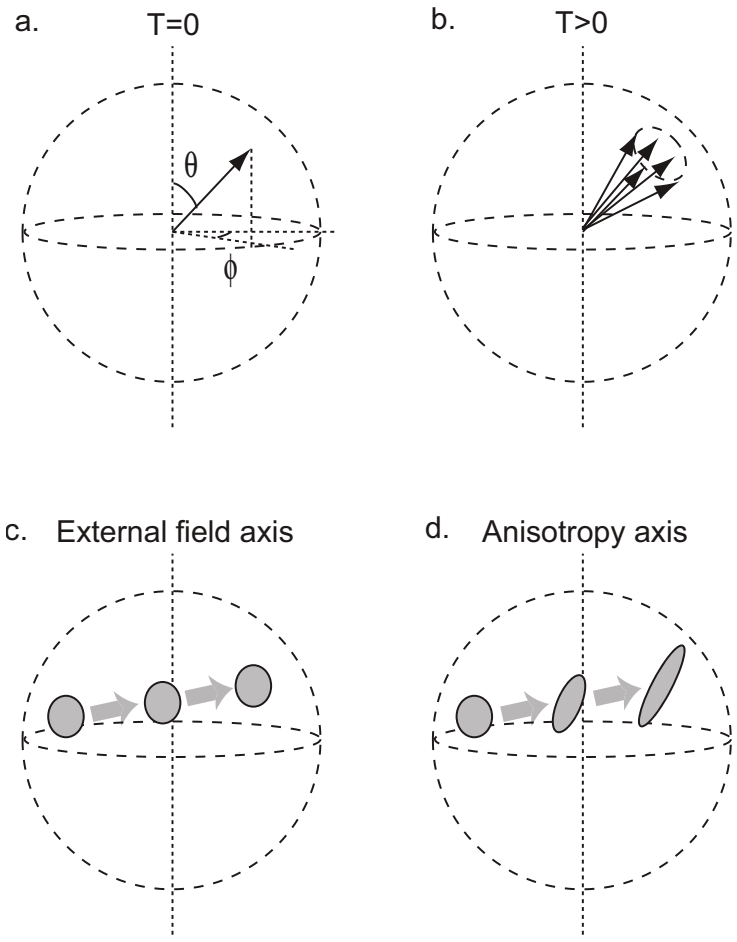

Figure 6.5: Figures (a) and (b) show the distribution of atomic moments of the spin dynamics simulations. At finite temperature the orientations of the atomic spins are distributed around a common axis (b). Figures (c) and (d) show the evolution of the spin distribution, as given by the evolution of the circular grey disc representing the distribution of magnetic moments defined in (b). The system is at finite temperature in an external field (c) and in a uniaxial anisotropy (d).

6.3 Dynamics of 1D and 2D magnetic systems

This section introduces Papers VII and VIII.

Dimensionality plays a determining role in all kinds of physics, so also in the physics of magnetism. The magnetic properties of a solid are changed drastically in the transition from extension in three dimensions to extension in two or only in one extension. One consequence of the lower dimensionality is that the coordination numbers for neighbouring atoms get lower. Due to this, the total coupling strength, of interatomic exchange interactions but also of other interactions, will be lower per atom in a thin film compared to bulk. This is a purely geometric effect and is present even in the case that the chemistry remains the same. In reality, the chemical and structural properties of a thin film on a substrate can differ substantially from the bulk properties of the same material. The film can be strained in the plane of the substrate, due to missmatch of lattice constants, it can also relax in the direction perpendicular to the substrate. In Paper VII investigations are done for an Fe monolayer on a W(110) substrate. Here two different electronic structure methods are used. The first program can handle the relaxation of the structure, the second program then uses these relaxed coordinates for calculations on the magnetic properties. The study aims to investigate how the magnon modes softens, i.e. get reduced in energy for a given wavevector. Often the energies obtained in frozen magnon calculations correspond very well to experiment. It turns out that in the case of Fe/W(110) also the effect of temperature is important. This is not automatically captured by the frozen magnon approach. Temperature can enter in form of the heatbath used in the atomistic spin dynamics method. But, the effects of temperature can also be come in at an earlier stage by using a partial disordered local moments configuration for the electronic structure calculation. More details can be found in Paper VII.

In Paper VIII the magnetization of nanothreads of Pt is investigated. Anisotropy energies are usually stronger, per atom, in reduced dimensions compared to bulk. It has recently been suggested that the local magnetic moment can collapse alltogether if the magnetic moments are forced into a hard direction. It is investigated in spin dynamics simulations how this so called colossal magnetic anisotropi compares with regular uniaxial anisotropy. Magnetic order is not stable in one-dimensional magnets, as already insignificant fluctuations can break up the ferromagnetic order. In the simulations are investigated how an enforced ferromagnetic start-configuration decays with time. It turns out that presence of colossal magnetic anisotropy makes this decay even faster than in the case of regular anisotropy.

6.4 Comments on my contributions to the papers

I This paper describes the method for, and implementation of, a scheme for atomistic spin dynamics. I did some of the simulations, contributed to the interpretatation of results and came with comments on the paper. For comments on the program package UppASD, see Appendix A

II I suggested some of the questions for the project. I did all the ASD simulations, analysed the results, did literature search, and wrote the paper.

III I took part in the interpretation of results and in writing of the paper.

IV Conference proceedings paper, complementary to papers II and III. I did all the ASD simulations, the analyses and wrote the paper.

V I took part in the formulation of the problem and contributed to the interpretation of the first results. I did a second set of simulations and wrote the second version of the paper.

VI I assisted in some of the ASD simulations, took part in the interpretation of results and came with comments on the paper.

VII I assisted in some of the ASD simulations, took part in the interpretation of results, and took part in writing of the paper

VIII I took part in the interpretation of results and came with coments on the manuscript.

7. Conclusions and outlook

The method for atomistic spin dynamics simulations is a general technique with various applications. The method has here been used in a number of studies that in the previous Chapter 6 were grouped into three parts. This closing section will briefly comment on what could be possible future developments for these categories. At first some comments should be made on the method itself. The different bits and pieces for the method are all well established in general solid state theory, statistical physics, and first principles density functional theory. In that regard, the main achievement in the pursuit of the research that has lead to this Thesis, has been to obtain and compile the necessary skills and knowledge necessary from different fields of physics and mathematics. More or less all the results in the Papers rely on numerical simulations. The implementation of, and continuous development of, a software package to enable these simulations is an ambitious task that requires the combined efforts of younger and senior scientists.

Among the chemically disordered systems that were the subject of Papers II-IV, the III-V diluted magnetic semiconductor GaMnAs stands out for one reaon. It is a candidate material for applications in spintronics and therefore attracts large interest from the scientific community and also from industry. One of the challenges, for GaMnAs but also for related compounds, is to arrive to compositions that with some margin remain ferromagnetic at room temperature. The frustrated, chemically disordered spin glass materials on the other hand, are an example of materials where research is driven not so much by the quest for possible applications but by scientific curiosity. The statistical physics aspects of spin glasses are intriguing, but also often very complicated. If Langevin dynamics with material specific parameters for exchange interactions, possibly with anisotropic contributions, and optional inclusion of magnetostatic interactions, is a fruitful way to go, or more of a parenthesis, in the research on spin glasses remains to see.

Papers V and VI have in common that they investigate mechanisms for fast switching. In Paper V simulations are performed to investigate spin wave instabilities. The anisotropy values used are as such unrealistic, but the mechanism for the instabilities can be relevant also for smaller, realistic values of the parameters.

The reduced dimensions of thin films and nanowires renders their magnetic properties drastically different than for bulk materials. In Paper VIII are investigated the very fast relaxation mechanisms for the magnetic order in one-

dimensional wires of Pt. For an experimental technique to be able to address such wires, it requires extraordinary spatial and temporal resolution. There are a number of experimental techniques that are suitable particularly for thin films. The calculations and simulations in Paper VII aimed to reproduce the results in recent experiments on magnon softening in Fe monolayers on W substrates [163]. The outcome of the simulations were that they indeed could do so. Among the already published Papers included in this Thesis, the results in Paper VII stands out for their immediate relevance to a recent experiment.

8. Acknowledgments

To write the present thesis would not have been possible without the great environment for research that the Materials Theory Division, Department of Physics and Astronomy, of Uppsala University provides. I would first of all like to thank my supervisor Olle for introducing me to the topic of spin dynamics. Your expertise and experience in solid state physics, combined with an optimistic stance and good support when research projects go into grid lock are very much appreciated. My assistant supervisor Lars N for all discussions and your answers on often difficult questions. I am truly astonished of your talent to explain quantum mechanics fundamentals and technicalities, so that it all seems not that difficult.

I would like to give a special thanks to the colleagueas with whom I have been interacting closely in research on spin dynamics. Björn, it was very stimulating to work with you and we had a really good time in California when we visited SLAC. Anders, your drive and positive attitude has meant a lot to me. In addition to the physics research that we have been involved in together, I also really appreciate the way that we have worked together in maintaining the main branches of the UppASD program. Andrea, with your background in statistical physics, you have brought in fresh ideas and different viewpoints to the Materials Theory Division. It is always a good conversation around the table when you are around, be it in physics or on some other topic. Johan M, starting with your first visit to Uppsala, it has been a pleasure to collaborate with you. Oleg, the study on spin glass alloys that Björn and you started, and I joined into, was a very good collaboration. Lars B, your skills, in an uncountable number of electronic structure programs, and in table-top ice hockey, are impressive. I would also like to greet welcome those colleagues, Sumanta, Peter L, and Satadeep, who more recently have joined in to the research on spin dynamics. I hope you find it an interesting branch of solid state physics.

Lars B and Diana, for your tireless efforts in calculations on the electronic structure of some difficult compounds. Josef, for your expertise and patience in teaching me Green functions TB-LMTO, and your hospitality during my visits to Prague, often together with Diana. Peter O, for the authorative lectures series you have given on magnetooptics, and for discussions on magnetization dynamics. Biplab and Jonas, for hosting journal clubs and for showing interest into my work. Biplab, also thanks for the collaboration on diluted magnetic semiconductors and for introducing me to cricket. Pooja and Younsuk, for all dinners and sport activities. Ola, Fredrik, and Duck Young for

being good travel company to the Jülich Spring school. My roommates Patrik, Oscar, and Igor for letting me overhear your discussions on dynamical mean field theory. The Czechoslovak trio Dominik, Karel, and Jan for proving that man can live on meat and liquid bread alone. Peter L and Nina for the computer support, Elisabeth for accepting all my expense reports on Glögg and ginger bread houses. Francesco, Marco, Igor, Guiseppe, and Andrea, for your frantic arguments on serie A and world cup football. Martin for letting me practice mein Schwäbisch. Micke, Anden, and Cecilia, for the courses that we attended together, Petros and Fredrik for strange music, Torbjörn and Sergiu for endless discussions on just about anything.

Life is not only physics, and I would like to thank my good friends, many of whom, I during the last years have unfortunately not been meeting up with as often as I would have liked to. Greger and Märta, and all you good friends from my undergraduate years in engineering physics at KTH. Friends from scouting and choir singing, Ralph and Liza from Tübingen, and my friends from early childhood years, Daniel, Carl, Martin, Rikard and Carl-Gustav.

Warm thanks for all support goes to my parents Inga and Lars, my sister Kristina and my brother in law Claes, and to my uncle Per and aunt Ann. After the defence I look forward to spend more time also with my extended family through marriage, Angela, Aurel and Roxana. And, most of all I long to meet up abroad with my dear wife Diana, who has already started her postdoc.

9. Sammanfattning på svenska

Ämnet för denna avhandling är magnetiseringsdynamik på atomära längdskalor. Metoden är semiklassisk så tillvida att parametrar extraheras från kvantmekaniska beräkningar och används for att formulera en klassisk Hamiltonian. Rörelsekvationerna för Hamiltonianen är ickelinjära och kopplade differentialekvationer. Exakta analytiska lösningar är möjliga endast för en högst begränsad mängd problem. Det finns ett antal metoder för att lösa rörelsekvationerna approximativt. Detta inbegriper ofta linjärisering av tidsberoende fält och begränsning till små vinklar mot symmetriaxlar. Numeriska beräkningar och simuleringar utgör i praktiken den mest framkomliga metoden för att undersöka magnetiseringsdynamik. Resultaten som presenteras i denna avhandling baseras huvudsakligen på data från numeriska simuleringar.

Att fasta material kan vara magnetiserade går endast att förklara genom att inbegripa kvantmekanik. Att en rent klassisk teori inte kan förklara förekomsten av magnetisering är en konsekvens av Bohr-van Leuven-satsen. I denna bevisas att susceptibiliteten χ alltid kommer att vara noll då elektronernas laddning inte är en tillräcklig egenskap för att ge ett nettomässigt bidrag till χ. Därmed kan vare sig förekomst av para- eller ferromagnetism förklaras. Det är endast genom att introducera spinnfrihetsgrader som en mekanism för magnetism i fasta material är möjlig. Elektroner bär på ett inneboende spinrörelsemängdsmoment $\mathbf{s}$ och ett banrörelsemängdsmoment $\mathbf{l}$. En elektrons magnetiska moment är relaterat till dess rörelsemängdsmoment genom den gyromagnetiska faktorn $\gamma_l = g_l \frac{\mu_B}{\hbar}$. Elektronens g-faktor är $g_s \approx 2$ för spinnrörelsemängdsmoment och $g_l = 1$ för banrörelsemängdsmoment. Det totala magnetiska momentet för en elektron kan uttryckas som

$$\mu = -(\gamma_s \mathbf{s} + \gamma_l \mathbf{l}) \tag{9.1}$$

$$= -\frac{\mu_B}{\hbar}(2\mathbf{s} + \mathbf{l}). \tag{9.2}$$

Även kärnpartiklarna bär på rörelsemängdsmoment och magnetiskt moment. Dessa behöver oftast inte betraktas i teorin för magnetism i fasta material. Till en följd av de kvantmekaniska postulaten kommer elektronernas spinn att precessera runt ett effektivt magnetiskt fält. Detta fält kan utgöras av dels magnetiska fält, från de magnetiska momenten i materialet och från ett externt magnetfält, och dels av interna effektiva bidrag från kvantmekanisk utbytesväxelverkan och magnetoskristallin anisotropienergi. Rörelsekvationen

fås fram genom att ställa upp Heisenbergs rörelseekvation $\frac{d\hat{A}}{dt} = \frac{i}{\hbar}[\hat{A}, \mathscr{H}]$. för spinnrörelsmängdsoperatorn och Hamiltonianen. Detta görs i Kapitel 3 för den en-partikel Kohn-Sham Hamiltonian som används inom täthetsfunktionalteori. Genom att integrera magnetiseringstätheten över de atomära volymerna erhålls en rörelsekvation för de atomära magnetiska momenten, av samma form som de mikromagnetiska Landau-Lifshitz-ekvationerna.

Den metod som i denna Avhandling har använts för beräkningar på spinndynamik är en två-stegs-procedur. Materialspecifika värden på atomära magnetiska moment och kvantmekaniska utbytesväxelverkningar har beräknats med elektronstrukturprogram baserade på täthetsfunktionalteori. Dessa värden har använts för att ställa upp en parametriserad magnetisk Hamiltonian. Det andra steget består av numeriska simuleringar av spinndynamiken genom integrering över tid av den stokastiska Landau-Lifshitz-ekvationen. Inverkan av ändlig temperatur modelleras genom Langevin-dynamik. I några simuleringar har även magnetokristallin anisotropi och relativistiska Dzyaloshinskii-Moriya växelverkningar ingått. I de föreliggande resultaten har dessa varit värden som uppskattats från kännedom av typiska värden från experimentella mätningar. Men, det går att beräkna även dessa värden i elektronstrukturberäkningar. De numeriska simuleringarna har utförts med programpaketet UppASD, Uppsala Atomistic Spin Dynamics, ett programpaket som utvecklas inom Avdelningen för Materialteori, Institutionen för Fysik och Astronomi, Uppsala Universitet alltsedan år 2005.

De artiklar som ingår i avhandlingen kan grupperas efter olika teman. Artikel I beskriver metoden och innehåller exempel på beräkningar av magnetiseringsdynamik till följd av starka magnetiska fält, beräkning av spinnvågsspektra och hur en två-temperatur-modell kan användas för att modellera hur energi överförs från magnetiska frihetsgrader till fononer i kristallen. I Artiklarna II-IV studeras dynamiken hos kemiskt oordnade material. I Artiklarna V och VI studeras dynamiken hos en vanlig ferromagnet och för en artificiell antiferromagnet. I Artiklarna VII och VIII studeras dynamiken hos magneter med rumslig utsträckning i två eller endast i en dimension.

I antiferromagneter är de lokal magnetiska momenten kopplade med växelverkningar vars energier minimeras om momenten är antiparallella till de grannar som de växelverkar med. För vissa material kan det hända att det, till följd av kristallstrukturen, inte går att samtidigt minimera energin för samtliga utbytesväxelverkningar. Detta fenomen benämns frustration, och magneter av det slaget benämns sålunda frustrerade magneter. Antalet degenererade energiminima för en frustrerad magnet tilltar exponentiellt med antalet atomer vilket medför besynnerliga termodynamiska egenskaper. När frustration förekommer tillsammans med oordning, antingen som nod- eller bindningssoordning, hävs degenereringen i energilandskapet. Experimentellt sett befinner sig ett sådant system aldrig i termodynamisk jämnvikt, det kan åldras över geologiska tidsskalor. Denna klass av

material benämns spinnglas och har, som namnet antyder, flera egenskaper gemensamma med vanligt glas. I en simulering av en ändlig cell går det i princip alltid att utforska fasrymden för att i stickprov mäta de degenererade grundtillstånden. Detta är tidskrävande beräkningar för vilka särskilda algoritmer, såsom värmebads-algoritmen och parallel-temporering, kommer till god användning. I de simuleringar som rapporteras i Artiklarna II-IV eftersträvas inte en utforskning av grundtillstånden. Istället utforskas hur materialen åldras över ett kontinuum av tidsskalor genom mätning av autokorrelationsfunktionen. Direkta jämnförelser med experiment är svårt då den del av den logaritmiska tidsaxeln som utforskas i numerisk simulering är i intervallet $10^{-14} - 10^{-9}$ s. Detta kan jämföras med tidsskalor på $10^{-5} - 10^{5}$ för experimentella protokoll, som exempelvis termoremanent magnetisering och susceptibilitetsmätningar. Att CuMn är ett spinnglas är väl känt. I Artikel III görs jämförelser mellan en Hamiltonian med parametrar för CuMn erhållna från första-princips-beräkningar och Heisenbergvarianten av Edwards-Anderson-modellen. Det undersöks även hur åldringen påverkas av värdet på den mikroskopiska dämpningsparametern α. I Kapitel 5 rapporteras preliminära resultat för den frustrerade magnetiska halvledaren ZnMnSe. Till följd av alltmer kraftfulla datorer och vidareutveckling av UppASD kommer avsevärt större simuleringar att kunna genomföras för ZnMnSe och CdMnTe än vad som var fallet i studien på CuMn. Detta öppnar upp för en mer avancerad analys av simulerade rådata med tekniker från teorin för dynamisk kritisk skalning och renormaliseringsgruppen.

Den utspädda magnetiska halvledaren GaMnAs är ett högintressant material då det ses som en kandidat för att ingå i spinntroniska konstruktioner. På tillämpningssidan är spinntroniken, med några undantag, ännu i sin linda. En av förhoppningarna är att kunna utveckla en ny sorts komponenter där en kombination av traditionell halvledarteknologi kombineras med de möjligheter som öppnas då även spinnfrihetsgraden kan användas för att representera information inom logiska kretsar eller minneskretsar. I Artikel II presenteras simuleringar på GaMaAs med 5% dopningsgrad, olika halter av As-orenheter på Ga-positioner i kristallen, och vid olika temperaturer. I simuleringar från ett helt ordnat lågtemperaturtillstånd, alternativt från ett oordnat högtemperaturtillstånd, till temperaturer strax under eller ovanför Curietemperaturen framgår att de atomära magnetiska momenten är korrelerade över korta avstånd även i det paramagnetiska tillståndet. Med ökande koncentration av As-orenheter introduceras allteftersom antiferromagnetiska växelverkningar i materialet. Detta ger sig tillkänna som frustration, dock inte i tillnärmelsevis lika stor omfattning som för de ovan nämnda spinnglasen. Effekten är dock tillräcklig för att ge sig tillkänna i autokorrelationsfunktionen, från vilken det framgår att relaxeringstiden tilltar med ökande halt av As-orenheter.

För en stor mängd problem inom klassisk magnetiseringsdynamik går det att beskriva små domäner eller nanopartiklar med ett enda stort magnetiskt

moment. Denna makrospinn-metodologi är en de förenklingar som kan möjliggöra studier av switchnings- och relaxeringförlopp utan att tyngre beräkningar behöver utföras. För de fall då kortvågiga excitationer gör att det lokala magnetiska momentet minskar är makrospinnmetoden inte användbar. I Artikel V studeras hur makrospinnmodellen bryter samman i simulering av precession av en ferromagnet runt en magnetokristallin anisotropiaxel. Att effekten kan uppstå till följd av geometriberoende magnetostatisk anisotropi är känt sedan länge. I Artikel V används ett starkt anisotropifält för att demonstrera att effekten mycket väl kan uppkomma till följd av magnetokristallin anisotropi. En direkt jämförelse med experiment är dock inte möjligt på grund av att det ansatta värdet på anisotropin är storleksordningar större än de som kan förekomma ens i de hårdaste av magnetiska material.

De tidsskalor över vilka magnetiseringsriktningen kan ändras i en ferromagnet begränsas nedifrån av vilka styrkor hos pålagda magnetfält och strömtätheter som går att använda utan att det material som ska magnetiseras tar skada. Det kan även vara svårt att uppnå erforderliga fältstyrkor och strömtätheter även om det magnetiska materialet i sig skulle kunna klara av det. Med sikte på att under kontrollerade former kunna ändra magnetiseringsriktningen på pikosekundnivå har mycket intresse ägnats mekanismer för ultrasnabb magnetisering i antiferromagneter och ferrimagneter. I Artikel VI undersöks i simuleringar hur snabbt det går att ändra magnetiseringsriktningen hos en syntetisk antiferromagnet. Genom gynnsam samverkan av kraftmomentet från det pålagda magnetfältet och de kraftmoment som verkar från det ena magnetiska delgittret på det andra delgittret går mycket snabba ändringar av magnetiseringsriktningen att uppnå. Simuleringarna genomförs med olika värden på dämpningsparameter och vid olika temperaturer.

I nyligen utförda experiment har för första gången demonstrerats hur magnetiseringsriktningen kan fås att vända hundraåttio grader till följd av en ultrasnabb puls av cirkulärpolariserat ljus. Detta möjliggörs genom att som magnetiskt material välja en ferrimagnetisk legering. Ferrimagnetisk ordning liknar kollinjär antiferromagnetisk ordning men skiljer sig åt såtillvida att de atomära momenten inte kompenserar varandra fullt ut, resulterande i nettomässig magnetisering. I Kapitel 5 redovisas de första resultaten från ett pågående projekt om ferrimagneter. Här undersöks dynamiken hos en enkel ferrimagnet vid precession i en uniaxiell anistropi-axel. Vid låga temperaturer beter sig magneten likt en vanlig ferromagnet. I ett känsligt temperaturintervall runt den magnetiska kompensationspunkten respektive rörelsemängdsmoments-kompensationspunkten ger sig den distinkta karaktären hos en ferrimagnet tillkänna. I simuleringar undersöks hur precessionsrörelsen påverkas runt kompensationspunkterna. Den kvalitativa överensstämmelsen med experiment på ferrimagneter är god. Likt studien i Artikel V visar det sig att makrospinnmetoder kan komma till korta och att

modellering med en ändlig simuleringscell kan vara avgörande för att kunna reproducera de beteenden som kan observeras i experiment.

Dimensionalitet spelar en avgörande roll inom all slags fysik, så även inom magnetismens fysik. De magnetiska egenskaperna hos ett fast material ändras drastiskt vid övergången från att ett objekt har utsträckning i tre dimensioner till att ha utsträckning i två, eller endast i en dimension. En minskning av rumslig dimension har som konsekvens att koordinationstalen för antalet närliggande atomer blir lägre. Därmed blir de totala kopplingarna per atom, lägre än i fallet för bulk. Detta är en rent geometrisk effekt och kan studeras med modell-Hamiltonianer. I Artikeln VII beräknas de interatomära utbytesväxelverkningarna för ett monolager av järn på ett wolframsubstrat, Fe/(110), i elektronstrukturberäkningar. Till följd av skillnaden i kemiska egenskaper hos järnatomer i ytlager och i bulk skiljer sig utbytesväxelverkningarna för monolagret åt från de för järn i bulkfas. Med kännedom om dessa materialspecifika parametrar möjliggörs beräkningar av spinnvågsspektrat i vilka det går att åtskilja effekter av geometri, kemi och även temperatur. Resultaten från simuleringarna jämförs med nyligen utförda experiment utförda med spinpolariserad elektronemissions-spektroskopi. I Artikel VIII studeras magnetiseringen hos nanotrådar av platina. Anisotropienergier är i regel starkare per atom i reducerade dimensioner är för bulk. Det har dessutom nyligen föreslagits att de lokala magnetiska momenten kan kollapsa helt om de tvingas att ligga i en hård anisotropiriktning. I spinndynamiksimuleringar jämförs effekten av denna så kallade kolossala magnetisk anisotropi med vanlig uniaxiell anisotropi. I endimensionella magneter är spontan magnetisk ordning inte stabil då redan obetydliga termiska fluktuationer bryter upp ordningen till att endast vara korrelerad över korta avstånd. I simuleringarna studeras hur, utgående från ett påtvingat ferromagnetiskt grundtillstånd, den långräckviddiga magnetiska ordningen avtar. Det visar sig att förekomst av kolossal magnetisk anisotropi får denna process att gå än snabbare än i fallet med vanlig uniaxiell anisotropi.

A. History of development of UppASD

The atomistic spin dynamics simulations presented in this thesis have been performed with UppASD [164], a software developed in the Materials Theory Division, Department of Physics and Astronomy, Uppsala University. The name UppASD is an acronym for Uppsala Atomistic Spin Dynamics. Research on atomistic spin dynamics in the Materials Theory Division was initiated in 2005 by Prof. Olle Eriksson and Associate Prof. Lars Nordström. The PhD students Björn Skubic and Johan Hellsvik were involved from the start.

The following developers have been and are contributing to the program:
- Björn Skubic (UU) 2005-2007
- Johan Hellsvik (UU) 2005-
- Anders Bergman (UU) 2008-
- Johan Mentink (Radboud U. Nijmegen) 2009-
- Andrea Taroni (UU) 2009-

The first versions of the program were written in close collaboration between BS and JH, with BS contributing more lines of source code than JH. Shared memory parallelization, optimizations, inclusion of Dzyaloshinskii-Moriya interactions and magnetostatic interactions was done by AB. The new semi-implicit differential equation solver SIB for the stochastic LL equation was recently developed by JM *et al* [138]). JM has implemented this solver as a subroutine in UppASD. The solver allows for a larger time step in the evolution of the magnetic moments and thus enables larger and longer simulations. The functionality for chemically disordered magnets has been improved and extended by JH. Revisions of subroutines for Monte Carlo was done by AT and AB. Since 2008, JH and AB have shared the responsibility as main developers, including program design, documentation and distribution to users other than the developers. With the aim to improve source code quality in general, AB has during the third quarter of 2010 performed a complete overhaul of the code. Data structures and subroutines are now more transparent, accessable and better documented.

With the exception of the inclusion of standard random number generators, all lines of source code has been written by the developers. The program is written in Fortran 90. No specific libraries are necessary in order to run the program. The program has successfully been compiled and used on a large

number of different hardware and operative systems. As of Oct 2010 there are, in addition to the developers, around ten users of the program.

In revisions into the year 2009 the implementation of the Heun differential equation solver was found to be expedient. The effective magnetic field was not recalculated between the calculation of the predictor and the calculation of the corrector. This scheme has less good properties than the Heun scheme. As a consequence, the time step used in simulations was kept very short ($10^{-18} - 10^{-17}$ s) to ensure numerical stability. The results in Papers I-V were calculated with this solver. A sample of these simulations have been recalculated with the Heun scheme where the effective field is recalculated between the calculation of the predictor and the corrector. The conclusion of the tests is that the results of Papers I-V hold. The comments on necessary size of the time step in Fig. 8 of Paper I refers to the less efficient scheme where the effective field was not updated inbetween the predictor and the corrector step.

From the start of 2010 the program contains two carefully tested differential equation solvers, the explicit Heun [132], and the semi-implicit SIB solver [138]. Depending on the strength and range of the exchange interactions, the SIB solver can be used with a time step in the range $10^{-15} - 10^{-16}$ s.

As mentioned in Chapter 5, the program is designed to be able to cope with arbitrary geometry and chemical disorder. Output files from the electronic structure programs, The Prague TB-LMTO-CPA code [62], The Linköping/Stockholm KKR Bulk Greens Function Method code (BGFM) [63] and The Stockholm/Uppsala exact muffin tin orbital (EMTO) program [165] can easily be transfered into the input files needed for UppASD. These three programs have all implemented the coherent potential approximation, used to calculate the exchange parameters in Papers II-IV and VII. Values for the interatomic exchange interaction tensor $\mathscr{J}_{ij}$ can be read from calculations performed with The Budapest/Vienna SKKR program [91, 92].

B. The Fokker-Planck equation

B.1 Dimensionless SLL equation on Langevin form

Starting from the dimensionless form of the SLL equation,

$$\frac{\partial \hat{\mathbf{e}}_i}{\partial \tau} = -\hat{\mathbf{e}}_i \times [\mathbf{b}_i + \mathbf{b}_i^{\mathrm{fl}}] - \alpha \hat{\mathbf{e}}_i \times (\hat{\mathbf{e}}_i \times [\mathbf{b}_i + \mathbf{b}_i^{\mathrm{fl}}]), \tag{B.1}$$

with,

$$\langle b_{i,\mu}^{\mathrm{fl}}(t) \rangle = 0, \quad \langle b_{i,\mu}^{\mathrm{fl}}(t) b_{j,\nu}^{\mathrm{fl}}(s) \rangle = 2\tilde{D}\delta_{\mu\nu}\delta_{ij}\delta(t-s). \tag{B.2}$$

it can be recasted in the general form of a multidimensional Langevin equation,

$$\begin{aligned}
\frac{\partial \hat{\mathbf{e}}_i}{\partial \tau} &= -\hat{\mathbf{e}}_i \times \mathbf{b}_i - \alpha \hat{\mathbf{e}}_i \times (\hat{\mathbf{e}}_i \times \mathbf{b}_i) \\
&\quad -\hat{\mathbf{e}}_i \times \mathbf{b}_i^{\mathrm{fl}} - \alpha \hat{\mathbf{e}}_i \times (\hat{\mathbf{e}}_i \times \mathbf{b}_i^{\mathrm{fl}}) \\
&= -\hat{\mathbf{e}}_i \times \mathbf{b}_i - \alpha \hat{\mathbf{e}}_i (\hat{\mathbf{e}}_i \cdot \mathbf{b}_i) + \alpha \mathbf{b}_i (\hat{\mathbf{e}}_i \cdot \hat{\mathbf{e}}_i) \\
&\quad -\hat{\mathbf{e}}_i \times \mathbf{b}_i^{\mathrm{fl}} - \alpha \hat{\mathbf{e}}_i (\hat{\mathbf{e}}_i \cdot \mathbf{b}_i^{\mathrm{fl}}) + \alpha \mathbf{b}_i^{\mathrm{fl}} (\hat{\mathbf{e}}_i \cdot \hat{\mathbf{e}}_i) \\
&= -\sum_k [(\sum_j \varepsilon_{ijk} e_j) b_k - \alpha (e_i e_k b_k - \delta_{ik} e^2 b_k)] \\
&\quad -\sum_k [(\sum_j \varepsilon_{ijk} e_j) b_k^{\mathrm{fl}} - \alpha (e_i e_k b_k^{\mathrm{fl}} - \delta_{ik} e^2 b_k^{\mathrm{fl}})].
\end{aligned} \tag{B.3}$$

The scalar products $\hat{\mathbf{e}}_i \cdot \hat{\mathbf{e}}_i$ were kept as e^2. The $A_i(\hat{\mathbf{e}}, \tau)$ and $B_{ik}(\hat{\mathbf{e}}, \tau)$ are then identified as,

$$A_i(\hat{\mathbf{e}}, \tau) = \sum_k [(\sum_j -\varepsilon_{ijk} e_j) - \alpha e_i e_k + \alpha \delta_{ik} e^2] b_k, \tag{B.4}$$

$$B_{ik}(\hat{\mathbf{e}}, \tau) = (\sum_j -\varepsilon_{ijk} e_j) - \alpha e_i e_k + \alpha \delta_{ik} e^2. \tag{B.5}$$

B.2 The Fokker-Planck equation

The following discussion on how to calculate the terms of the Fokker-Planck equation for the SLL closely follow Garcia *et al.* [115]. The purpose of the present appendix is to provide the intermediate expressions that were not included in Appendix B of Ref. [115]. The starting point is the Fokker-Planck

equation on the form of a conservation equation for the probability distribution,

$$\begin{aligned}
&\frac{\partial P}{\partial t} \\
&= -\sum_i \frac{\partial}{\partial y_i}\left[\left(A_i + D\sum_{jk} B_{jk}\frac{\partial B_{ik}}{\partial y_j}\right)P\right] + \sum_{ij}\frac{\partial^2}{\partial y_i \partial y_j}\left[\left(D\sum_k B_{ik}B_{jk}\right)P\right] \\
&= -\sum_i \frac{\partial}{\partial y_i}\left\{\left[A_i - D\sum_k B_{ik}\left(\frac{\partial B_{jk}}{\partial y_j}\right) - D\sum_{jk} B_{ik}B_{jk}\frac{\partial}{\partial y_j}\right]P\right\}. \qquad \text{(B.6)}
\end{aligned}$$

The three parts of the right hand side of the Fokker-Planck equation are calculated one by on. The first term A_i trivially carries over, but can preferably be written on the original LL form,

$$\frac{\partial \hat{\mathbf{e}}_i}{\partial \tau} = -\hat{\mathbf{e}}_i \times \mathbf{b}_i - \alpha \hat{\mathbf{e}}_i \times (\hat{\mathbf{e}}_i \times \mathbf{b}_i). \qquad \text{(B.7)}$$

For the second term, by first evaluating the derivative

$$\begin{aligned}
\frac{\partial B_{ik}}{\partial e_j} &= \frac{\partial[(\sum_j -\varepsilon_{ijk}e_j) - \alpha e_i e_k + \alpha\delta_{ik}e^2]}{\partial e_j} \\
&= -\varepsilon_{ijk} - \alpha\delta_{ij}e_k - \alpha e_i\delta_{jk} + \alpha\delta_{ik}e_j + \alpha\delta_{ik}e_j \qquad \text{(B.8)} \\
&= -\varepsilon_{ijk} + \alpha(2\delta_{ik}e_j - \delta_{ij}e_k - \delta_{jk}e_i), \qquad \text{(B.9)}
\end{aligned}$$

and specifically,

$$\begin{aligned}
\sum_j \frac{\partial B_{jk}}{\partial e_j} &= \sum_j \left[-\varepsilon_{jjk} + \alpha(2\delta_{jk}e_j - \delta_{jj}e_k - \delta_{jk}e_j)\right] \\
&= \sum_j [\alpha(2e_k - 3e_k - e_k)] \\
&= -2\alpha e_k, \qquad \text{(B.10)}
\end{aligned}$$

and,

$$\begin{aligned}
&\sum_k B_{ik}\left(\sum_j \frac{\partial B_{jk}}{\partial e_j}\right)\\
&= \sum_k\{[(\sum_j -\varepsilon_{ijk}e_j) - \alpha e_i e_k + \alpha\delta_{ik}e^2](-2\alpha e_k)\}\\
&= 2\alpha\sum_k[(\sum_j -\varepsilon_{ijk}e_j)e_k - \alpha e_i e_k e_k + \alpha\delta_{ik}e^2 e_k]\\
&= 2\alpha\hat{\mathbf{e}}\times\hat{\mathbf{e}} + 2\alpha^2\sum_k[-e_i e_k e_k + \delta_{ik}e^2 e_k]\\
&= 0. \qquad\qquad (B.11)
\end{aligned}$$

The last part contains double cross products. After expanding the cross products, the terms are sorted in powers of α,

$$\begin{aligned}
&-D\sum_{jk} B_{ik}B_{jk}\frac{\partial P}{\partial\hat{\mathbf{e}}}\\
&= -D\sum_{jk}\left\{\left[\left(-\sum_m \varepsilon_{imk}e_m\right) - \alpha e_i e_k + \alpha\delta_{ik}\right]\left[\left(-\sum_n \varepsilon_{jnk}e_n\right) - \alpha e_j e_k + \alpha\delta_{jk}\right]\right\}\frac{\partial P}{\partial\hat{\mathbf{e}}}\\
&= -D\sum_{jk}\left\{\left(\sum_{mn}\varepsilon_{imk}\varepsilon_{jnk}e_m e_n\right)\right\}\frac{\partial P}{\partial\hat{\mathbf{e}}}\\
&\quad +\alpha D\sum_{jk}\left\{(\sum_m \varepsilon_{imk}e_m)(e_i e_k - \delta_{ik}) - \alpha(\sum_n \varepsilon_{jnk}e_n)(e_i e_k - \delta_{ik})\right\}\frac{\partial P}{\partial\hat{\mathbf{e}}}\\
&\quad -\alpha^2 D\sum_{jk}\left\{e_i e_j - e_i e_k\delta_{jk} - e_j e_k\delta_{ik} + e_k e_k\delta_{ik}\delta_{jk}\right\}\frac{\partial P}{\partial\hat{\mathbf{e}}}\\
&= -D\sum_{jk}\left\{\left(\sum_{mn}\varepsilon_{imk}\varepsilon_{jnk}e_m e_n\right)\right\}\frac{\partial P}{\partial\hat{\mathbf{e}}}\\
&\quad +\alpha D\left\{\sum_{jm}\varepsilon_{imk}e_m(e_i e_k - e_k e_i) - \sum_{jn}\varepsilon_{jnk}e_n(e_i e_k - e_k e_i)\right\}\frac{\partial P}{\partial\hat{\mathbf{e}}}\\
&\quad -\alpha^2 D\sum_j\left\{e_i e_j - e_i e_j - e_j e_i + e_j e_j\delta_{ij}\right\}\frac{\partial P}{\partial\hat{\mathbf{e}}}\\
&= D\left[\hat{\mathbf{e}}\times\left((\hat{\mathbf{e}}\times\frac{\partial P}{\partial\hat{\mathbf{e}}}\right)\right]_i - \alpha^2 D\sum_j\left\{-e_i e_j + e_j e_j\delta_{ij}\right\}\frac{\partial P}{\partial\hat{\mathbf{e}}}. \qquad (B.12)\\
&\qquad\qquad (B.13)
\end{aligned}$$

where terms that contains α have canceled. Terms with α^0 and α^2 remain,

$$\begin{aligned} &= D\sum_j \left\{e_i e_j - e_j e_j \delta_{ij}\right\} \frac{\partial P}{\partial \hat{\mathbf{e}}} + \alpha^2 D \sum_j \left\{e_i e_j - e_j e_j \delta_{ij}\right\} \frac{\partial P}{\partial \hat{\mathbf{e}}} \\ &= (1+\alpha^2) D \sum_j \left\{e_i e_j - e_j e_j \delta_{ij}\right\} \frac{\partial P}{\partial \hat{\mathbf{e}}} \\ &= (1+\alpha^2) D \left[\hat{\mathbf{e}} \times \left((\hat{\mathbf{e}} \times \frac{\partial P}{\partial \hat{\mathbf{e}}} \right) \right]_i . \end{aligned} \tag{B.14}$$

The result for the third part can be written on compact form,

$$-D\sum_{jk} B_{ik} B_{jk} \frac{\partial P}{\partial e_j} = (1+\alpha^2) D \left[\hat{\mathbf{e}} \times \left(\hat{\mathbf{e}} \times \frac{\partial P}{\partial \hat{\mathbf{e}}} \right) \right]_i . \tag{B.15}$$

Collecting the first and third part, the final equation for the Fokker-Planck equation for the SLL equation is

$$\frac{\partial P}{\partial \tau} = -\frac{\partial}{\partial \hat{\mathbf{e}}} \left\{ \left[-\hat{\mathbf{e}} \times \mathbf{b} - \alpha \hat{\mathbf{e}} \times (\hat{\mathbf{e}} \times \mathbf{b}) + D(1+\alpha^2) \hat{\mathbf{e}} \times \left(\hat{\mathbf{e}} \times \frac{\partial}{\partial \hat{\mathbf{e}}} \right) \right] P \right\} . \tag{B.16}$$

Bibliography

[1] John David Jackson. *Classical electrodynamics*. Wiley, New York, 3. ed. edition, 1999.

[2] Amikam Aharoni. *Introduction to the theory of ferromagnetism*. Clarendon, Oxford, 1996.

[3] L. D. Landau and E. M. Lifshitz. Theory of the dispersion of magnetic permeability in ferromagnetic bodies. *Physikalische Zeitschrift Sowietunion*, 8:153, 1935.

[4] Burkard Hillebrands and André. Thiaville. *Spin dynamics in confined magnetic structures Vol 1, 2 and 3*. Springer, Berlin, 2002, 2003, 2006.

[5] Charles Kittel. *Introduction to solid state physics*. Wiley, New York, 7. ed. edition, 1996.

[6] Neil W. Ashcroft and N. David Mermin. *Solid state physics*. Saunders College, Philadelphia, 1976.

[7] Michael Plischke and Birger Bergersen. *Equilibrium statistical physics*. World Scientific, Singapore, 2. ed. edition, 1994.

[8] Richard M. Martin. *Electronic structure : basic theory and practical methods*. Cambridge Univ. Press, Cambridge, 2004.

[9] P. W. Anderson. More is different. *Science*, 177(4047):393, 1972.

[10] Piers Coleman. Many body physics: Unfinished revolution. arXiv:cond-mat/0307004v2 [cond-mat.str-el], 2003.

[11] L. Bergqvist, O. Eriksson, J. Kudrnovský, V. Drchal, P. Korzhavyi, and I. Turek. Magnetic percolation in diluted magnetic semiconductors. *Physical Review Letters*, 93(13):137202, 2004.

[12] Diana Iuşan, Biplab Sanyal, and Olle Eriksson. Theoretical study of the magnetism of mn-doped zno with and without defects. *Physical Review B*, 74(23):235208, 2006.

[13] K. Sato, J. Kudrnovský, P. H. Dederichs, O. Eriksson, I. Turek, B. Sanyal, G. Bouzerar, H. Katayama-Yoshida, V. A. Dinh, T. Fukushima, H. Kizaki, and R. Zeller. First-principles theory of dilute magnetic semiconductors. *Reviews of Modern Physics*, 82(2):1633, 2010.

[14] Nicola A. Hill. Why are there so few magnetic ferroelectrics? *The Journal of Physical Chemistry B*, 104(29):6694, 2000.

[15] Bas B Van Aken, Thomas T M Palstra, Alessio Filippetti, and Nicola A Spaldin. The origin of ferroelectricity in magnetoelectric ymno3. *Nature materials*, 3(3):164–70, 2004.

[16] S. Picozzi, K. Yamauchi, B. Sanyal, I. A. Sergienko, and E. Dagotto. Dual nature of improper ferroelectricity in a magnetoelectric multiferroic. *Phys. Rev. Lett.*, 99(22):227201, Nov 2007.

[17] Soshin Chikazumi and C. D. Graham. *Physics of ferromagnetism*. Clarendon Press, Oxford, 2. ed. edition, 1997.

[18] Francesco Cricchio, Oscar Grånäs, and Lars Nordström. . in manuscript.

[19] Kei Yosida. *Theory of magnetism*. Springer, Berlin, 1996.

[20] Jürgen Kübler. *Theory of itinerant electron magnetism*. Clarendon Press, Oxford, 2000.

[21] Sang-Wook Cheong and Maxim Mostovoy. Multiferroics: a magnetic twist for ferroelectricity. *Nat Mater*, 6(1):13–20, 2007.

[22] I Dzyaloshinsky. A thermodynamic theory of "weak" ferromagnetism of antiferromagnetics. *Journal of Physics and Chemistry of Solids*, 4(4):241, 1958.

[23] Tôru Moriya. Anisotropic superexchange interaction and weak ferromagnetism. *Physical Review*, 120(1):91, 1960.

[24] N. A. Spaldin and M. Fiebig. The renaissance of magnetoelectric multiferroics. *Science*, 309:391, 2005.

[25] A. G. Gurevihvc* and G. A. Melkov. *Magnetization oscillations and waves*. CRC, Boca Raton, 1996.

[26] F. Keffer and C. Kittel. Theory of antiferromagnetic resonance. *Physical Review*, 85(2):329, 1952.

[27] Roald K. Wangsness. Magnetic resonance in ferrimagnetics. *Physical Review*, 93(1):68, 1954.

[28] David P. Landau and Kurt Binder. *A guide to Monte Carlo simulations in statistical physics*. Cambridge University Press, Cambridge, 2. ed. edition, 2005.

[29] G. Binasch, P. Grünberg, F. Saurenbach, and W. Zinn. Enhanced magnetoresistance in layered magnetic structures with antiferromagnetic interlayer exchange. *Phys. Rev. B*, 39(7):4828–4830, Mar 1989.

[30] M. N. Baibich, J. M. Broto, A. Fert, F. Nguyen Van Dau, F. Petroff, P. Etienne, G. Creuzet, A. Friederich, and J. Chazelas. Giant magnetoresistance of (001)fe/(001)cr magnetic superlattices. *Phys. Rev. Lett.*, 61(21):2472–2475, Nov 1988.

[31] M. Julliere. Tunneling between ferromagnetic films. *Physics Letters A*, 54(3):225–226, 1975.

[32] Peter M. Oppeneer. *Magneto-optical Kerr spectra. in, Handbook of magnetic materials. Vol. 13; Editor, Buschow, K. H. J.* Elsevier, Amsterdam, 2001.

[33] C. Kittel. On the theory of ferromagnetic resonance absorption. *Physical Review*, 73:155, 1948.

[34] W. E. Bailey, L. Cheng, D. J. Keavney, C.-C. Kao, E. Vescovo, and D. A. Arena. Precessional dynamics of elemental moments in a ferromagnetic alloy. *Physical Review B*, 70(17):172403, 2004.

[35] C. D. Stanciu, A. V. Kimel, F. Hansteen, A. Tsukamoto, A. Itoh, A. Kirilyuk, and Th. Rasing. Ultrafast spin dynamics across compensation points in ferrimagnetic gdfeco: The role of angular momentum compensation. *Physical Review B*, 73(22):220402, 2006.

[36] Tapan Chatterji, editor. *Neutron scattering from magnetic materials*. Elsevier, 2005.

[37] J. Kübler, K. Höck, J. Sticht, and A. R. Williams. Local spin-density functional theory of noncollinear magnetism (invited). *Journal of Applied Physics*, 63(8):3482–3486, 1988. Cited By (since 1996): 29.

[38] L. M. Sandratskii. Noncollinear magnetism in itinerant-electron systems: theory and applications. *Advances in Physics*, 47:91, 1998.

[39] B. L. Györffy, A. J. Pindor, J. Staunton, G. M. Stocks, and H. Winter. A first-principles theory of ferromagnetic phase transitions in metals. *Journal of Physics F: Metal Physics*, 15:1337, 1985.

[40] V. P. Antropov, M. I. Katsnelson, M. van Schilfgaarde, and B. N. Harmon. Ab initio spin dynamics in magnets. *Physical Review Letters*, 75:729, 1995.

[41] V. P. Antropov, M. I. Katsnelson, B. N. Harmon, M. van Schilfgaarde, and D. Kusnezov. Spin dynamics in magnets: Equation of motion and finite temperature effects. *Physical Review B*, 54:1019, 1996.

[42] G. M. Stocks, B. Ujfalussy, X. Wang, D. M. C. Nicholson, W. A. Shelton, Y. Wang, A. Canning, and B. L. Györffy. Towards a constrained local moment model for first principles spin dynamics. *Philoscophical Magazine B*, 78:665, 1998.

[43] B. Ujfalussy, B. Lazarovits, L. Szunyogh, G. M. Stocks, and P. Weinberger. Ab initio spin dynamics applied to nanoparticles: Canted magnetism of a finite co chain along a pt(111) surface step edge. *Physical Review B*, 70(10):100404, 2004.

[44] W. F. Brown. Thermal fluctuations of a single-domain particle. *Physical Review*, 130:1677, 1963.

[45] R. Kubo and N. Hashitsume. Brownian motion of spins. *Supplement of the Progress of Theoretical Physics*, 46:210, 1970.

[46] Vladimir Antropov. Time-dependent density-functional spin dynamics and its application for fe and ni. *Journal of Applied Physics*, 97(10):10A704, 2005.

[47] M. Fähnle, R. Drautz, R. Singer, D. Seiauf, and D. Berkov. A fast ab initio approach to the simulation of spin dynamics. *Computational Materials Science*, 32(1):118, 2005.

[48] J. M. Sanchez, F. Ducastelle, and D. Gratias. Generalized cluster description of multicomponent systems. *Physica A*, 128:334, 1984.

[49] X. Tao, D. P. Landau, T. C. Schulthess, and G. M. Stocks. Spin waves in paramagnetic bcc iron: Spin dynamics simulations. *Physical Review Letters*, 95(8):087207, 2005.

[50] S. V Halilov, A. Y Perlov, P. M Oppeneer, and H Eschrig. Magnon spectrum and related finite-temperature magnetic properties: A first-principle approach. *Europhysics Letters (EPL)*, 39(1):91, 1997.

[51] S. Halilov, H. Eschrig, A. Perlov, and P. Oppeneer. Adiabatic spin dynamics from spin-density-functional theory: Application to fe, co, and ni. *Physical Review B*, 58(1):293, 1998.

[52] Qian Niu and Leonard Kleinman. Spin-wave dynamics in real crystals. *Physical Review Letters*, 80(10):2205, 1998.

[53] Q. Niu, Xindong Wang, L. Kleinman, Wu-Ming Liu, D. Nicholson, and G. Stocks. Adiabatic dynamics of local spin moments in itinerant magnets. *Physical Review Letters*, 83(1):207, 1999.

[54] S. Savrasov. Linear response calculations of spin fluctuations. *Physical Review Letters*, 81(12):2570, 1998.

[55] Paweł Buczek, Arthur Ernst, Patrick Bruno, and Leonid Sandratskii. Energies and lifetimes of magnons in complex ferromagnets: A first-principle study of heusler alloys. *Physical Review Letters*, 102(24):247206, 2009.

[56] S. Diallo, V. Antropov, T. Perring, C. Broholm, J. Pulikkotil, N. Ni, S. Bud'ko, P. Canfield, A. Kreyssig, A. Goldman, and R. McQueeney. Itinerant magnetic excitations in antiferromagnetic $cafe_2as_2$. *Physical Review Letters*, 102(18):187206, 2009.

[57] Takashi Hotta, Seiji Yunoki, Matthias Mayr, and Elbio Dagotto. A-type antiferromagnetic and c-type orbital-ordered states in lamno$_3$ using cooperative jahn-teller phonons. *Physical Review B*, 60:R15009, 1999.

[58] P. W. Anderson. Localized magnetic states in metals. *Phys. Rev.*, 124(1):41–53, Oct 1961.

[59] P. Hohenberg and W. Kohn. Inhomogeneous electron gas. *Physical Review*, 136:B864, 1964.

[60] W. Kohn and L. J. Sham. Self-consistent equations including exchange and correlations effects. *Physical Review*, 140:A1133, 1965.

[61] O. K. Andersen and O. Jepsen. Explicit, first-principles tight-binding theory. *Physical Review Letters*, 53(27):2571, 1984.

[62] I. Turek, V. Drchal, V. Kudrnovský, M. Šob, and P. Weinberger. *Electronic structure of disordered alloys, surfaces and interfaces*. Kluwer Academic, Boston, 1997.

[63] I. A. Abrikosov and H. L. Skriver. Self-consistent linear-muffin-tin-orbitals coherent-potential technique for bulk and surface calculations: Cu-ni, ag-pd, and au-pt random alloys. *Physical Review B*, 47:16532, 1993.

[64] R. Oppenheimer M. Born. Zur quantentheorie der molekeln. *Annalen der Physik*, 389(20):457, 1927.

[65] K. Capelle, G. Vignale, and B. L. Györffy. Spin currents and spin dynamics in time-dependent density-functional theory. *Physical Review Letters*, 87(20):206403, 2001.

[66] D. C. Ralph and M. D. Stiles. Spin transfer torques. *Journal of Magnetism and Magnetic Materials*, 320:1190, 2008.

[67] J. C. Slonczewski. Current-driven excitation of magnetic multilayers. *Journal of Magnetism and Magnetic Materials*, 159:1996, 1996.

[68] L. Berger. Emission of spin waves by a magnetic multilayer traversed by a current. *Physical Review B*, 54:9353, 1996.

[69] P. H. Dederichs, S. Blügel, R. Zeller, and H. Akai. Ground states of constrained systems: Application to cerium impurities. *Physical Review Letters*, 53:2512, 1984.

[70] L. Udvardi, L. Szunyogh, K. Palotás, and P. Weinberger. First-principles relativistic study of spin waves in thin magnetic films. *Physical Review B*, 68(10):104436, 2003.

[71] L. Udvardi and L. Szunyogh. Chiral asymmetry of the spin-wave spectra in ultrathin magnetic films. *Physical Review Letters*, 102(20):207204, 2009.

[72] A. V. Kimel, A Kirilyuk, P. A. Usachev, R. V. Pisarev, A. M. Balbashov, and Th. Rasing. Ultrafast non-thermal control of magnetization by instantaneous photomagnetic pulses. *Nature*, 435(7042):655–7, 2005.

[73] A. L. Liechtenstein, M. I. Katsnelson, V. P. Antropov, and V. A. Gubanov. Local spin density functional approach to the theory of exchange interactions in ferromagnetic metals and alloys. *J. Magn. Magn. Mater.*, 67:65, 1987.

[74] Jens Jensen and Allan R. Mackintosh. *Rare earth magnetism*. Clarendon Press, Oxford, 1991.

[75] T. Jungwirth, J. Sinova, J. Masek, J. Kucera, and A. H. MacDonald. Theory of ferromagnetic (iii,mn)v semiconductors. *Reviews of Modern Physics*, 78(3):809, 2006.

[76] A. V. Ruban, S. Shallcross, S. I. Simak, and H. L. Skriver. Atomic and magnetic configurational energetics by the generalized perturbation method. *Physical Review B*, 70(12):125115, 2004.

[77] O. Grotheer, C. Ederer, and M. Fähnle. Fast ab initio methods for the calculation of adiabatic spin wave spectra in complex systems. *Physical Review B*, 63(10):100401, 2001.

[78] David J. Singh and Lars Nordström. *Planewaves, pseudopotentials and the LAPW method*. Springer Science+Business Media, Inc., Boston, MA, 2. ed. edition, 2006.

[79] The wien2k program. http://www.wien2k.at/.

[80] Fleur: The jülich flapw code family. http://www.flapw.de.

[81] The elk fp-lapw code. http://elk.sourceforge.net/.

[82] The exciting code. http://exciting-code.org/.

[83] M. Heide, G. Bihlmayer, and S. Blügel. Describing dzyaloshinskii-moriya spirals from first principles. *Physica B: Condensed Matter*, 404(18):2678–2683, 2009. Proceedings of the Workshop "AttheFrontiersofCondensedMatterIV" - Current Trends and Novel Materials.

[84] S. Heinze, M. Bode, A. Kubetzka, O. Pietzsch, X. Nie, S. Blügel, and R. Wiesendanger. Real-space imaging of two-dimensional antiferromagnetism on the atomic scale. *Science*, 288(5472):1805, 2000.

[85] M Bode, M Heide, K von Bergmann, P Ferriani, S Heinze, G Bihlmayer, A Kubetzka, O Pietzsch, S Blügel, and R Wiesendanger. Chiral magnetic order at surfaces driven by inversion asymmetry. *Nature*, 447(7141):190–3, 2007.

[86] J.M. Wills, O. Eriksson, P. Andersson, A. Delin, O. Grechnyev, and M. Alouani. *Full-Potential Electronic Structure Method*. Springer Series in Solid-State Sciences, Vol. 167. Springer, 2011.

[87] Hugues Dreyssé. *Electronic structure and physical properties of solids : the uses of the LMTO method : lectures of a workshop held at Mont Saint Odile, France, October 2-5, ...* Springer, Berlin, 2000.

[88] The rspt fp-lmto program. http://www.rspt.net/.

[89] Till Burkert, Lars Nordström, Olle Eriksson, and Olle Heinonen. Giant magnetic anisotropy in tetragonal feco alloys. *Physical Review Letters*, 93(2):027203, 2004.

[90] Till Burkert, Olle Eriksson, Peter James, Sergei I. Simak, Börje Johansson, and Nordström. Calculation of uniaxial magnetic anisotropy energy of tetragonal and trigonal fe, co, and ni. *Physical Review B*, 69(10):104426, 2004.

[91] L. Szunyogh, B. Újfalussy, P. Weinberger, and J. Kollár. Self-consistent localized kkr scheme for surfaces and interfaces. *Phys. Rev. B*, 49(4):2721–2729, Jan 1994.

[92] R. Zeller, P. H. Dederichs, B. Újfalussy, L. Szunyogh, and P. Weinberger. Theory and convergence properties of the screened korringa-kohn-rostoker method. *Phys. Rev. B*, 52(12):8807–8812, Sep 1995.

[93] A. Antal, B. Lazarovits, L. Udvardi, L. Szunyogh, B. Újfalussy, and P. Weinberger. First-principles calculations of spin interactions and the magnetic ground states of cr trimers on au(111). *Physical Review B*, 77(17):174429, 2008.

[94] Herbert Goldstein, Charles P. Poole, and John Safko. *Classical mechanics*. Pearson education, Upper Saddle River, 3. ed. edition, 2002.

[95] T. L. Gilbert. A phenomenological theory of damping in ferromagnetic materials. *Magnetics, IEEE Transactions on*, 40(6):3443, 2004.

[96] T. Holstein and H. Primakoff. Field dependence of the intrinsic domain magnetization of a ferromagnet. *Physical Review*, 58:1098, 1940.

[97] H. Suhl. Theory of the magnetic damping constant. *IEEE transactions on magnetics*, 34:1834, 1998.

[98] K. Lenz, H. Wende, W. Kuch, K. Baberschke, K. Nagy, and A. Jánossy. Two-magnon scattering and viscous gilbert damping in ultrathin ferromagnets. *Physical Review B*, 73(14):144424, 2006.

[99] Kh. Zakeri, J. Lindner, I. Barsukov, R. Meckenstock, M. Farle, U. von Hörsten, H. Wende, W. Keune, J. Rocker, S. Kalarickal, K. Lenz, W. Kuch, K. Baberschke, and Z. Frait. Spin dynamics in ferromagnets: Gilbert damping and two-magnon scattering. *Physical Review B*, 76(10):104416, 2007.

[100] V. Kamberský. On the landau–lifshitz relaxation in ferromagnetic metals. *Canadian Journal of Physics*, 48:2906, 1970.

[101] J. Kuneš and Kamberský. First-principles investigation of the damping of fast magnetization precession in ferromagnetic 3d metals. *Physical Review B*, 65(21):212411, 2002.

[102] D. Steiauf, J. Seib, and M. Fähnle. Unified theory of near-adiabatic magnetization dynamics for collinear and noncollinear magnetization. *Physical Review B*, 78(2):020410, 2008.

[103] V. Kamberský. On ferromagnetic resonance damping in metals. *Czechoslovak Journal of Physics*, 26(12):1366, 1976.

[104] Y. U. Gilmore, K. Idzerda and M. D. Stiles. Identification of the dominant precession-damping mechanism in fe, co, and ni by first-principles calculations. *Physical Review Letters*, 99(2):027204, 2007.

[105] Jeongwon Ho, F. C. Khanna, and B. C. Choi. Radiation-spin interaction, gilbert damping, and spin torque. *Physical Review Letters*, 92(9):097601, 2004.

[106] Arne Brataas, Yaroslav Tserkovnyak, and Gerrit E. W. Bauer. Scattering theory of gilbert damping. *Physical Review Letters*, 101(3):037207, 2008.

[107] Yaroslav Tserkovnyak, Arne Brataas, and Gerrit E. W. Bauer. Enhanced gilbert damping in thin ferromagnetic films. *Physical Review Letters*, 88(11):117601, 2002.

[108] S. Zhang. Roles of nonequilibrium conduction electrons on the magnetization dynamics of ferromagnets. *Physical Review Letters*, 93(12):127204, 2004.

[109] K. Capelle and B. L. Györffy. Exploring dynamical magnetism with time-dependent density-functional theory: From spin fluctuations to gilbert damping. *Europhysics Letters*, 61:354, 2003.

[110] E. Beaurepaire, J.-C. Merle, A. Daunois, and J.-Y. Bigot. Ultrafast spin dynamics in ferromagnetic nickel. *Physical Review Letters*, 76:4250, 1996.

[111] C Stamm, T Kachel, N Pontius, R Mitzner, T Quast, K Holldack, S Khan, C Lupulescu, EF Aziz, M Wietstruk, HA Dürr, and W Eberhardt. Femtosecond modification of electron localization and transfer of angular momentum in nickel. *Nature materials*, 6(10):740–3, 2007.

[112] K. Carva, D. Legut, and P. M. Oppeneer. Influence of laser-excited electron distributions on the x-ray magnetic circular dichroism spectra: Implications for femtosecond demagnetization in ni. *EPL (Europhysics Letters)*, 86(5):57002, 2009.

[113] M. Battiato, K. Carva, and P. Oppeneer. Superdiffusive spin transport as a mechanism of ultrafast demagnetization. *Physical Review Letters*, 105(2):027203, 2010.

[114] Andrei Kirilyuk, Alexey V. Kimel, and Theo Rasing. Ultrafast optical manipulation of magnetic order. *Rev. Mod. Phys.*, 82(3):2731–2784, Sep 2010.

[115] J. L. García-Palacios and F. J. Lázaro. Langevin-dynamics study of the dynamical properties of small magnetic particles. *Physical Review B*, 58:14937, 1998.

[116] Giorgio Bertotti, I. D. Mayergoyz, and Claudio. Serpico. *Nonlinear magnetization dynamics in nanosystems*. Elsevier, Oxford, 2009.

[117] M. E. Fisher. The theory of equilibrium critical phenomena. *Review of Modern Physics*, 30:615, 1967.

[118] M. E. Fisher. The renormalization group in the theory of critical behavior. *Review of Modern Physics*, 46:597, 1974.

[119] John L. Cardy. *Scaling and renormalization in statistical physics*. Cambridge Univ. Press, Cambridge, 1996.

[120] H. Eugene Stanley. Scaling, universality, and renormalization: Three pillars of modern critical phenomena. *Rev. Mod. Phys.*, 71(2):S358, Mar 1999.

[121] Bertrand Delamotte. A hint of renormalization. *American Journal of Physics*, 72(2):170, 2004.

[122] P. C. Hohenberg and B. I. Halperin. Theory of dynamic critical phenomena. *Review of Modern Physics*, 49:435, 1977.

[123] K. Chen and D. P. Landau. Spin-dynamics study of the dynamic critical behavior of the three-dimensional classical heisenberg ferromagnet. *Physical Review B*, 49:3266, 1994.

[124] A. Peter Young, editor. *Spin glasses and random fields*. World Scientific, Singapore, 1998.

[125] Herbert Callen and Theodore Welton. Irreversibility and generalized noise. *Physical Review*, 83(1):34, 1951.

[126] R Kubo. The fluctuation-dissipation theorem. *Reports on Progress in Physics*, 29(1):255, 1966.

[127] Hannes Risken. *The Fokker-Planck equation : methods of solution and applications*. Springer-Vlg, Berlin, 2. ed. edition, 1989.

[128] A. Einstein. Über die von der molekularkinetischen theorie der wärme geforderte bewegung von in ruhenden flüssigkeiten suspendierten teilchen. *Annalen der Physik*, 322(8):549, 1905.

[129] N. G. van Kampen. *Stochastic processes in physics and chemistry*. Elsevier, Amsterdam, 3. ed. edition, 2007.

[130] G. N. Milshtein and M. V. Tret'yakov. Numerical solution of differential equations with colored noise. *Journal of Statistical Physics*, 77(3-4):691, 1994.

[131] Peter E. Kloeden and Eckhard Platen. *Numerical solution of stochastic differential equations*. Springer-Vlg, Berlin, 1992.

[132] W. Rümelin. Numerical treatment of stochastic differential equations. *SIAM Journal of Numerical Analysis*, 19:604, 1982.

[133] Edward James McShane. *Stochastic calculus and stochastic models*. Academic Press, New York, 1974.

[134] D. Steiauf and M. Fähnle. Damping of spin dynamics in nanostructures: An ab initio study. *Physical Review B*, 72(6):064450, 2005.

[135] N. David Mermin. Time-dependent correlations in a solvable ferromagnetic model. *Physical Review*, 134:A112, 1964.

[136] Vladimir L. Safonov and H. Neal Bertram. Spin-wave dynamic magnetization reversal in a quasi-single-domain magnetic grain. *Physical Review B*, 63(9):094419, 2001.

[137] Massimiliano d'Aquino, Claudio Serpico, and Giovanni Miano. Geometrical integration of landau-lifshitz-gilbert equation based on the mid-point rule. *Journal of Computational Physics*, 209(2):730–753, 2005.

[138] J H Mentink, M V Tretyakov, A Fasolino, M I Katsnelson, and Th Rasing. Stable and fast semi-implicit integration of the stochastic landau–lifshitz equation. *Journal of Physics: Condensed Matter*, 22(17):176001, 2010.

[139] M. d'Aquino, C. Serpico, G. Coppola, I. D. Mayergoyz, and G. Bertotti. Midpoint numerical technique for stochastic landau-lifshitz-gilbert dynamics. *Journal of Applied Physics*, 99(8):08B905, 2006.

[140] J. Stöhr and H.-C. Siegmann. *Magnetism: From fundamentals to nanoscale dynamics*. Springer Verlag, Berlin, 2006.

[141] Pui-Wai Ma, S. L. Dudarev, A. A. Semenov, and C. H. Woo. Temperature for a dynamic spin ensemble. *Physical Review E*, 82(3):031111, 2010.

[142] U. Atxitia, O. Chubykalo-Fesenko, R. W. Chantrell, U. Nowak, and A. Rebei. Ultrafast spin dynamics: The effect of colored noise. *Phys. Rev. Lett.*, 102(5):057203, Feb 2009.

[143] D. A. Garanin, V. V. Ishchenko, and L. V. Panina. Dynamics of an ensemble of single-domain magnetic particles. *Theoretical Mathematical Physics*, 82:169, 1990.

[144] D. A. Garanin. Fokker-planck and landau-lifshitz-bloch equations for classical ferrogmagnets. *Physical Review B*, 55:3050, 1997.

[145] N. Kazantseva, D. Hinzke, U. Nowak, R. Chantrell, U. Atxitia, and O. Chubykalo-Fesenko. Towards multiscale modeling of magnetic materials: Simulations of fept. *Physical Review B*, 77(18):184428, 2008.

[146] K. Vahaplar, A. M. Kalashnikova, A. V. Kimel, D. Hinzke, U. Nowak, R. Chantrell, A. Tsukamoto, A. Itoh, A. Kirilyuk, and Th. Rasing. Ultrafast path for optical magnetization reversal via a strongly nonequilibrium state. *Physical Review Letters*, 103(11):117201, 2009.

[147] C. D. Stanciu, F. Hansteen, A. V. Kimel, A. Kirilyuk, A. Tsukamoto, A. Itoh, and Th. Rasing. All-optical magnetic recording with circularly polarized light. *Physical Review Letters*, 99(4):047601, 2007.

[148] Anders Bergman. *A theoretical study of magnetism in nanostructured materials*. PhD thesis, Uppsala University, 2006.

[149] A. Zunger, S.-H. Wei, L. G. Ferreira, and J. E. Bernhard. Special quasirandom structures. *Physical Review Letters*, 65:353, 1989.

[150] E. Holmström, N. Bock, T. Peery, E. Chisolm, R. Lizárraga, G. De Lorenzi-Venneri, and D. Wallace. Structure discovery for metallic glasses using stochastic quenching. *Phys. Rev. B*, 82(2):024203, Jul 2010.

[151] C. D. Stanciu, A. Tsukamoto, A. V. Kimel, F. Hansteen, A. Kirilyuk, A. Itoh, and Th. Rasing. Subpicosecond magnetization reversal across ferrimagnetic compensation points. *Physical Review Letters*, 99(21):217204, 2007.

[152] G Bouzerar. Magnetic spin excitations in diluted ferromagnetic systems: The case of ga_{1−x}mn_xas. *EPL (Europhysics Letters)*, 79(5):57007, 2007.

[153] Roderich Moessner and Arthur P. Ramirez. Geometrical frustration. *Physics Today*, 59(2):24–29, 2006.

[154] J. S. Gardner, G. Ehlers, S. T. Bramwell, and B. D. Gaulin. Spin dynamics in geometrically frustrated antiferromagnetic pyrochlores. *Journal of Physics Condensed Matter*, 16:S643, 2004.

[155] P. H. Conlon and J. T. Chalker. Spin dynamics in pyrochlore heisenberg antiferromagnets. *Phys. Rev. Lett.*, 102(23):237206, Jun 2009.

[156] K. Binder and A. P. Young. Spin glasses: Experimental facts, theoretical concepts and open questions. *Review of Modern Physics*, 58:801, 1986.

[157] Eric Vincent, Jacques Hammann, Miguel Ocio, Jean-Philippe Bouchaud, and Leticia F. Cugliandolo. Slow dynamics and aging in spin-glasses. arXiv:cond-mat/9607224v1, 1996.

[158] Oleg E. Peil. *Theory of Disordered Magnets*. PhD thesis, Uppsala University, 2009.

[159] P. M. Shand, A. D. Christianson, T. M. Pekarek, L. S. Martinson, J. W. Scheitzer, I. Miotkowski, and B. C. Crooker. Spin-glass ordering in the diluted magnetic semiconductor $Zn_{1-x}Mn_xTe$. *Physical Review B*, 58:12876, 1998.

[160] H. Ohno. Making nonmagnetic semiconductors ferromagnetic. *Science*, 281(5379):951, 1998.

[161] S. A. Wolf, D. D. Awschalom, R. A. Buhrman, J. M. Daughton, S. von Molnár, M. L. Roukes, A. Y. Chtchelkanova, and D. M. Treger. Spintronics: a spin-based electronics vision for the future. *Science*, 294(5546):1488–95, 2001.

[162] A. Kashuba. Domain instability during magnetization precession. *Physical Review Letters*, 96(4):047601, 2006.

[163] J. Prokop, W. X. Tang, Y. Zhang, I. Tudosa, T. R. F. Peixoto, Kh. Zakeri, and J. Kirschner. Magnons in a ferromagnetic monolayer. *Physical Review Letters*, 102(17):177206, 2009.

[164] Uppasd: The uppsala atomistic spin dynamics program. www.fysik.uu.se/cmt/asd/.

[165] L. Vitos. Total-energy method based on the exact muffin-tin orbitals theory. *Physical Review B*, 64(1):014107, 2001.

Acta Universitatis Upsaliensis

Digital Comprehensive Summaries of Uppsala Dissertations from the Faculty of Science and Technology 706

Editor: The Dean of the Faculty of Science and Technology

A doctoral dissertation from the Faculty of Science and Technology, Uppsala University, is usually a summary of a number of papers. A few copies of the complete dissertation are kept at major Swedish research libraries, while the summary alone is distributed internationally through the series Digital Comprehensive Summaries of Uppsala Dissertations from the Faculty of Science and Technology. (Prior to January, 2005, the series was published under the title "Comprehensive Summaries of Uppsala Dissertations from the Faculty of Science and Technology".)

Distribution: publications.uu.se
urn:nbn:se:uu:diva-120103

ACTA
UNIVERSITATIS
UPSALIENSIS
UPPSALA
2010